ELUCIDATION OF MECHANISMS OF SALINITY TOLERANCE IN *Zoysia matrella* CULTIVARS: A STUDY OF STRUCTURE AND FUNCTION OF SALT GLANDS

A Dissertation

by

SHEETAL SADANAND RAO

Submitted to the Office of Graduate Studies of
Texas A&M University
in partial fulfillment of the requirements for the degree of

DOCTOR OF PHILOSOPHY

May 2011

Major Subject: Molecular and Environmental Plant Sciences

ELUCIDATION OF MECHANISMS OF SALINITY TOLERANCE IN *Zoysia matrella* CULTIVARS: A STUDY OF STRUCTURE AND FUNCTION OF SALT GLANDS

A Dissertation

by

SHEETAL SADANAND RAO

Submitted to the Office of Graduate Studies of
Texas A&M University
in partial fulfillment of the requirements for the degree of

DOCTOR OF PHILOSOPHY

Approved by:

Chair of Committee,	Marla L. Binzel
Committee Members,	Carol A. Loopstra
	Leonardo Lombardini
	Andreas Holzenburg
Intercollegiate Faculty Chair,	Dirk B. Hays

May 2011

Major Subject: Molecular and Environmental Plant Sciences

ABSTRACT

Elucidation of Mechanisms of Salinity Tolerance in *Zoysia matrella* Cultivars:

A Study of Structure and Function of Salt Glands. (May 2011)

Sheetal Sadanand Rao, B. S., University of Mumbai; M. S., University of Mumbai

Chair of Advisory Committee: Dr. Marla L. Binzel

Salt glands are important structural adaptations in some plant and animal species that are involved in the excretion of excess salts. *Zoysia matrella* is a highly salt-tolerant turf grass that has salt glands. Two cultivars of *Z. matrella*, 'Diamond' and 'Cavalier', were examined in this study to look for salt gland-related factors responsible for the differences in their degree of salt tolerance. In addition to the adaxial salt gland density being higher in 'Diamond', the salt glands in salt treated (300 mM NaCl) plants of this cultivar were bigger than the ones in 'Cavalier'. 'Diamond', as well as some of the 'Diamond' x 'Cavalier' hybrid lines, showed a significant induction in salt gland density in response to salt treatment. Examination of salt gland density in 'Diamond' x 'Cavalier' hybrid lines showed that salt gland density was a highly heritable trait in the salt-treated population. Ultrastructural modifications in the salt glands observed with Transmission Electron Microscopy (TEM), coupled with Cl^- localization studies, suggested a preference for symplastic transport of saline ions in *Z. matrella*.

Salt glands have been studied in several plant species; however, no studies have tried to associate the role of ion transporters with the functioning of salt glands in plants.

RNA *in situ* studies with Na^+ transporters showed localization of *ZmatHKT1* transcripts in the adaxial salt glands, leaf mesophyll and bundle sheath cells for both cultivars. *ZmatSOS1* expression was observed in the xylem parenchyma cells for leaves from both cultivars, but the expression was markedly different around the cells bordering the vascular tissue. The strongest expression of *ZmatSOS1* for 'Diamond' was seen in the bundle sheath cells and the phloem, while for 'Cavalier' the signal was strongest in the mestome sheath cells and in cells surrounding the phloem. No expression of *ZmatSOS1* was seen in the salt glands for either cultivars. *ZmatNHX1* expression in both cultivars was very low, and observed in the salt glands and neighboring epidermal cells. Three alleles of *ZmatNHX1* were identified in *Z. matrella*, along with three alternatively-spliced forms of *ZmatNHX1*, the expression of which were cultivar and treatment specific.

Together, these results provide a model for salt transport in *Z. matrella* and signify potential roles of salt glands and select ion transporters in the salt tolerance of this species.

DEDICATION

This dissertation is dedicated to my loving husband, Atul Ganpatye, my advisor, Dr. Binzel, and my best friend, Claudia Aguillon. The three people who always believed in me, provided me with moral support on days that I almost gave up, and who actively supported me in achieving my goal.

ACKNOWLEDGEMENTS

I would like to thank my chair, Dr. Binzel, without whom it would have been almost impossible to write this dissertation. I would also like to thank my committee members, Dr. Lombardini, Dr. Holzenburg and Dr. Loopstra, for their guidance, support and encouragement throughout the duration of my research.

I owe my deepest gratitude to Dr. Kranthi Mandadi, Dr. Azucena Mendoza, and E. Ann Ellis for their valuable advice on my research projects. Their knowledge and guidance was extremely helpful. I would also like to thank Dr. McKnight, Dr. Versaw, Dr. Koiwa, and Dr. Lekvin at Texas A&M University for being kind enough to let me use the equipment in their laboratories and Dr. Krizek and Janaki Mudunkothge at the University of South Carolina for letting me spend time in their laboratory learning the RNA *in situ* hybridization technique. I would like to acknowledge Karl Gregory and Minkyung Oh from the Statistics department for helping me with the statistical analysis of my data.

I want to thank my friends Carol Johnson, Sonia Irigoyen, Dr. Sreenath Palle, Dr. Tesfamichael Kebrom, and Dr. Michelle Raisor, who provided me with support and motivation during the entire course of my graduate studies. My deepest gratitude to Jason Miller and Nolan Bentley, the undergraduate students who assisted me with the counting of salt glands. My heartfelt thanks to Otto, Dr. Binzel's cat, for entertaining me during my stay in Dallas while working on one part of this research project.

This study was supported by Texas AgriLife Research and the I4 project. I would also like to acknowledge the financial support provided by the Department of

DEDICATION

This dissertation is dedicated to my loving husband, Atul Ganpatye, my advisor, Dr. Binzel, and my best friend, Claudia Aguillon. The three people who always believed in me, provided me with moral support on days that I almost gave up, and who actively supported me in achieving my goal.

NOMENCLATURE

SEM	Scanning Electron Microscopy
TEM	Transmission Electron Microscopy
STEM	Scanning Transmission Electron Microscopy
EDS	Energy Dispersive Spectroscopy
NaCl	Sodium Chloride
LSD	Least Significant Difference
RACE	Random Amplification of cDNA Ends
PTA	Phospho-tungstic Acid

TABLE OF CONTENTS

Page

CHAPTER Page

LIST OF FIGURES

Page

Page

Page

LIST OF TABLES

Page

Page

CHAPTER I

INTRODUCTION - THE IMPORTANCE OF THIS RESEARCH

With the ever increasing population of the world, the demand for agricultural crops is growing. Salinity has long been known to pose a threat to agriculture (Sen and Kasera, 2002). Approximately 10% of the world's area is salt-affected and it has been noted that approximately 20% of all agricultural lands are becoming saline (Khan and Ungar, 1995; Ma et al., 2007). The population in Texas is projected to double by the year 2060 leading to an expected increase (~27%) in the demand for water (Water for Texas, 2011). According to the U.S. Geological Survey, of the 26 billion gallons of water consumed daily in the United States, approximately 30% is devoted to outdoor uses, mainly landscaping (Solley et al., 1998; Vickers 2001). It is estimated that a typical suburban lawn consumes ~10,000 gallons of fresh water each year (Vickers, 2001). Considering the limited amount of water resources and increasing area of land becoming non-arable due to salt contamination, growing crops under saline conditions might serve as a good strategy to conserve potable water. Efforts are underway to substitute the fresh water used for landscape irrigation with reclaimed water in states such as California, Colorado and Texas. For example, the San Antonio Water System (SAWS) in Texas is actively involved in producing and distributing to its customers millions of gallons of

---

This dissertation follows the style of The Plant Cell.

recycled water on a daily basis. One disadvantage of using recycled water is that it has a high concentration of salts. According to SAWS data, recycled water (from water recycling centers) has approximately ten times more sodium (90-102 ppm) and chloride (135-190 ppm) than SAWS potable water.

Under normal (non-saline) physiological conditions in a plant, a high potassium/sodium (K^+/Na^+) ratio is maintained in the cytosol with relatively high K^+ (100-200 mM) and low Na^+ (1-10 mM) concentrations (Taiz and Zeiger, 2010). For most plants Na^+ is not essential for plant growth; however, K^+ is essential for protein synthesis, enzyme activity, and osmoregulation, hence this nutrient is required in high concentrations (Schachtman and Liu, 1999). The ratio of K^+/Na^+ found under non-saline conditions is optimal for metabolic functions in the cell.

K^+ plays an important role in activating many enzymes and is also required during protein synthesis for binding of tRNA to the ribosomes (Tester and Davenport, 2003). Under saline conditions, Na^+ competes with K^+ for its intracellular binding sites as well as for uptake across plant plasma membranes via K^+-selective ion channels (Tester and Davenport, 2003). Thus, salinity can decrease the K^+/Na^+ ratio in the cell and alter the osmotic balance, as well as interfere with protein synthesis. When supplied in excess (>100 mM) to plants, salt (sodium chloride) can slow down plant growth either by having osmotic effects (water stress), ion specific effects (ion imbalance), or toxic effects due to excessive ion accumulation (Lessani and Marschner, 1978). The effect seen in a plant may depend on the species or cultivar, salt concentration and environmental conditions. Some of the responses seen in plants, following salt stress,

include inhibition of photosynthesis, inactivation of enzymes and inhibition of protein synthesis (Greenway and Munns, 1980; Munns and Teermat, 1986; Hasegawa et al., 2000; Tuteja, 2007). Dehydration and death of leaf cells can result from hyperosmotic stress caused by Na^+ accumulation. High concentrations of Na^+ can affect yield, and ultimately lead to plant death in case of highly salt sensitive species (Bennett and Khush, 2003).

Plants have evolved several mechanisms to deal with and overcome the harmful effects of exposure to excess salt. The mechanisms of salt tolerance in a plant may involve morphological (salt glands), physiological (ion exclusion, ion sequestration, ion extrusion), and biochemical processes (ion transporters). The difference in the amount of Na^+ and Cl^- translocated to the leaf blades is one of the key factors responsible for differences in salt sensitivity among species (Lessani and Marschner, 1978). Most plants that are sensitive to soil salinity (glycophytes) are affected by 100 mM NaCl (~ 20% sea water); however, a smaller group of plants, known as halophytes, are salt-tolerant even at concentrations exceeding 250 mM NaCl, ~ 49% sea water (Tuteja, 2007). Salt-sensitive species tend to minimize salt uptake by the roots. Salt-tolerant species have developed mechanisms to avoid salt damage once the salt has entered the shoot system. These include sequestration of excess salt in the cellular vacuole of the leaves, thus preventing salt accumulation in the cytoplasm; transport of leaf Na^+ into the phloem for recirculation back to the roots; or compartmentation of excess Na^+ in the older leaves (Tester and Davenport, 2003). In some salt-tolerant plants, the salt sequestered in the

vacuole is eventually excreted onto the leaf surface via specialized epidermal cells (salt glands).

Work done towards this dissertation focused on the contribution of salt glands towards salinity tolerance of *Zoysia matrella*, a grass used for turf. *Zoysia matrella*, a highly salt-tolerant turf grass, is capable of tolerating high levels of salt (~ 300 mM = 58% sea water). Functional salt glands have been observed in *Z. matrella* but the mechanisms by which this grass tolerates high amounts of salt has not yet been determined. Advanced breeding lines of *Zoysia* have been developed at the Texas AgriLife Research Center at Dallas. These lines include, but are not limited to, two cultivars of *Z. matrella*, 'Diamond' and 'Cavalier', differing in their degrees of salt and drought tolerance, as well as resistance to insects and disease (Engelke et al., 2002a; Engelke et al., 2002b). 'Diamond' has excellent salt tolerance while 'Cavalier' has moderate salt tolerance (Engelke et al., 2002a; Engelke et al., 2002b). The difference in salt-tolerance of these two cultivars could be due to factors such as the density of the salt glands, or the efficiency of salt transported to the glands by the ion transporters, in addition to other factors. Elucidation of the functional role of salt glands in *Z. matrella* is crucial for an in-depth understanding of salt tolerance in this highly salt-tolerant species. The objective of this dissertation research project was to focus on three aspects of the role of the salt glands in the salinity tolerance of *Z. matrella*: the ultrastructure of salt glands, the density of salt glands, and the expression of key Na^+ transporters (*HKT*, *SOS* and *NHX*).

CHAPTER II

SALT GLANDS IN *Zoysia matrella*

INTRODUCTION

Salt glands are found in some plant and animal species. In the animal kingdom, salt glands are seen in marine birds and iguanas, crocodiles, and sea turtles, where they function in the secretion of excess salt (mostly Na^+ and Cl^-). In the plant kingdom, salt glands are commonly found in the leaves of grasses such as *Spartina foliosa* (Levering and Thomson, 1971), *Cynodon dactylon* (Oross and Thomson, 1982a; Oross and Thomson, 1982b; Oross and Thomson, 1984) and *Distichlis stricta* (Oross and Thomson, 1982b). Salt glands are specialized leaf epidermal structures found in several dicotyledonous plant families but restricted to the subfamilies of Chloridoideae and Panicoideae in the Monocotyledonae (Marcum, 1999). These salt glands facilitate the secretion of excess salt arriving from the transpiration stream; thus, plants with salt glands are capable of tolerating higher concentrations of salt in the xylem as compared to the plants lacking salt glands (Flowers, 1985). In a plant with active salt glands, the secreted salt can be observed in the form of salt crystals on the leaf surface. Apart from Na^+ and Cl^-, the other ions secreted by salt glands include K^+, Mg^{2+}, Ca^{2+}, SO_4^{2-}, PO_4^{3-} and CO_3^{2-} (Haberlandt, 1914). During secretion, ionic preference can vary with species. For *Aeluropus littoralis*, the preference is $Na^+ > K^+ > Ca^{2+}$ (Pollack and Waisel, 1970; Thomson, 1975) but in *Spartina anglica* the salt glands are more selective for Na^+ secretion than the other cations, although both *Aeluropus* and *Spartina* are

monocotyledonous plants (Rozema and Gude, 1981). For *Tamarix* (a dicotyledonous plant) the preference is $Na^+ > Ca^{2+} > K^+$ (Waisel, 1961; Thomson, 1975) while *in vitro* experiments with *Limonium* (also a dicotyledonous plant) have showed that leaf discs that were placed on a salt solution could actively secrete Na^+, K^+, Cs^+, Rb^+, Cl^-, Br^-, and I^- (Hill, 1967a; Hill, 1967b; Larkum and Hill, 1970; Shachar-Hill and Hill, 1970; Hill, 1970a; Hill, 1970b; Thomson, 1975). These observations suggest that even within the classes Monocotyledonae and Dicotyledonae, the ionic preference for salt gland secretions may vary between closely related species.

Salt glands exist in different forms and the form depends on which family a given species belongs to. On the basis of their structure, salt glands have been classified into three major types: the two-celled salt glands characteristic of the family Poaceae (also known as Gramineae), the bladder cells unique to the Chenopodiaceae family, and the more complex multicellular salt glands seen in several dicotyledonous plant families (Thomson, 1975). Salt glands have been studied in several members of the Poaceae and have been reported to have a bicellular structure. These bicellular structures are referred to as bicellular trichomes, microhairs, or salt glands (Naidoo and Naidoo, 1998). An outer cap cell and a mesophyll-embedded basal cell constitute a bicellular salt gland.

Based on morphology, the two-celled salt glands characteristic of family Poaceae can either be sunken (e.g. *Sporobolus sp*), semi-sunken (*A. littoralis*), or trichome-like as seen in *Bouteloua* sp. (Liphschitz and Waisel, 1974). Salt glands in monocotyledonous plants consist of a basal cell embedded in the leaf mesophyll and an external cap cell (Sutherland and Eastwood, 1916; Skelding and Winterbotham, 1939; Oross and

Thomson, 1982a; Oross and Thomson, 1982b). The sunken glands have a cap cell that is large and oval, a form that has the capacity to secrete more salt than other salt gland forms. Although the trichome-like glands have an elongated cap cell, the basal cell is narrower which is potentially why their salt secretion capacity is less than what is seen in the sunken glands. Species with semi-sunken glands are intermediate between the other two forms as in the case of *Tetrapogon* (Liphschitz and Waisel, 1974).

A large central vacuole, characteristic of most plant cells, is not found in gland cells (Waisel, 1972). The cap cell has a large nucleus, mitochondria, several small vacuoles, and a thick cuticle with a cuticular space (cavity) at the tip of the cell serving as a collecting chamber for the salt that is eventually secreted from the gland (Oross and Thomson, 1984). The salt accumulated in the cuticular space is secreted to the outside by minute pores in the cuticle (Campbell and Thomson, 1975). Characteristic features of the basal cell include, but are not limited to, a large nucleus, small vacuoles, and numerous mitochondria needed to provide energy for the salt excretion process. A distinguishing feature of the basal cell is the presence of partitioning membranes which are formed by extensive infoldings of the plasma membrane into the cytoplasm of the basal cell (Luttge, 1971; Gunning, 1977; Oross and Thomson, 1982a). These infoldings have been found to originate from the common wall between the basal cell and the cap cell, and have been reported in several grass species including *S. foliosa* (cordgrass), *C. dactylon* (bermudagrass), *D. stricta* (saltgrass), *S. virginicus*, and *A. littoralis* (Levering and Thomson, 1971; Oross and Thomson, 1982a; Oross and Thomson, 1982b; Naidoo and Naidoo, 1998; Barhoumi et al., 2007; Barhoumi et al., 2008). As the plasma membrane

extends into the cytoplasm of the basal cell, the space between the membrane infoldings serves as an extracytoplasmic channel for solute transport and is in continuum with the apoplastic space between the two gland cells (Levering and Thomson, 1971; Oross and Thomson, 1982b).

Zoysia matrella is a warm-season, salt-tolerant turf grass belonging to the sub-family Chloridoideae. A previous study of salt glands in *Z. japonica* and *Z. matrella* suggested that, even though salt glands were located on both leaf surfaces of these species, only the salt glands on the adaxial surface were functional, as indicated by the appearance of salt (NaCl) crystals following salt treatment (Marcum and Murdoch, 1990). The salt glands present on the abaxial leaf surface of *Z. matrella* were reported to be smaller than the ones on the adaxial side and were inactive for salt secretion as demonstrated by Scanning Electron Microscopy (SEM) studies (Marcum and Murdoch, 1990). *Zoysia matrella* was confirmed to be the more salt-tolerant species in their comparative study because it secreted more Na^+ than *Z. japonica* as demonstrated by tissue washing experiments. This study showed a good comparison of salt tolerance between species, however there were no studies pertaining to the comparison of cultivars within each of the two species that differed in salt tolerance.

No Transmission Electron Microscope (TEM) studies have been done with *Z. matrella* to date. SEM studies are essential for examination and comparison of the external features of salt glands, between the different cultivars, as well as to determine if the salt glands in *Z. matrella* are involved in salt secretion. At the same time, TEM studies are crucial for understanding the anatomy of salt glands which may yield

information regarding how salt glands may be functioning in a highly salt-tolerant species like *Z. matrella*. TEM studies will also shed light on the mechanism of salt movement from the vasculature of the leaf to the leaf surface and will allow visualization of leaf cells located in the vicinity of the salt glands.

This part of the study aimed at comparing form and function of salt glands seen in two cultivars within the same species differing in their degree of salt tolerance. *Zoysia matrella*, a highly salt-tolerant turf grass, is capable of tolerating high levels of salt (~ 300 mM NaCl = 55 % sea water). Advanced breeding lines of *Zoysia* have been developed at the Texas AgriLife Research Center at Dallas. These lines include, but are not limited to, two cultivars of *Z. matrella*, 'Diamond' and 'Cavalier' (Engelke et al., 2002a; Engelke et al., 2002b). 'Diamond' has excellent salt tolerance while 'Cavalier' is moderately salt tolerant (Engelke et al., 2002a; Engelke et al., 2002b). In a previous study of 57 Zoysia grasses that included 'Diamond' and 'Cavalier', 'Diamond' was found to be the most salt-tolerant cultivar based upon percent leaf firing in response to salt treatment with 400 mM NaCl (Marcum et al., 1998).

Zoysia matrella was an ideal candidate for this study because within this species there were cultivars differing in their degree of salt tolerance. The factors governing this difference have not yet been determined. We hypothesized that the difference in salt tolerance of these two cultivars could be due to factors such as the anatomy of salt glands, salt gland density, or the efficiency of salt transported to the glands by the ion transporters, in addition to some other factors. This study focused on comparison of salt

gland anatomy in ‘Diamond’ and ‘Cavalier’ with an aim to find structural differences in salt glands that might be responsible for enhanced salt tolerance in ‘Diamond’.

METHODS

Plant material and salinity treatment

‘Diamond’ and ‘Cavalier’ lines were obtained from the Texas AgriLife Research Center at Dallas, Texas. Plants were grown in pots containing Metro Mix 200 (American Clay Works, Denver, CO). Three pots from each cultivar were supplied with a 50 mM NaCl solution, which was later increased to 300 mM in increments of 50 mM per consecutive day, to avoid the plants from experiencing an osmotic shock. The plants were then watered once a week with 300 mM NaCl (containing Peter’s 20-20-20 fertilizer) for at least four weeks before examining the leaves. Salt treatment was applied by using a sub-irrigation system, thus ensuring that the salt seen on the leaves after treatment was from excretion by the salt glands, and not a residue left behind after watering with the salt solution. These plants were used for most of the work involved in this project.

Salt gland dimensions

Epidermal imprints of leaves were used to measure salt glands dimensions (length and width). Each leaf was coated with clear nail enamel and allowed to dry for 1 h before peeling off the imprint with a forcep. The imprint was placed on a glass slide with a cover slip on top before examination under a microscope. Both leaf surfaces were observed under a compound microscope (Olympus IX81 spinning disk confocal

microscope, Center Valley, PA) at 200X magnification. Measurements were made on the second youngest leaf from each cultivar. One hundred salt glands were measured for 'Diamond' and 'Cavalier' leaves collected from control and salt-treated plants. The length of a salt gland and the width of its cap cell were measured by comparison with a stage micrometer using a digital image editing software (Photoshop CS3, Adobe, San Jose, CA).

Salt gland ultrastructure

SEM Studies - A JEOL JSM-6400 (Peabody, MA) SEM was used to observe the spatial location of the salt glands on the leaf surface. A protocol was developed to fix the leaves while preserving the salt crystals on its surface (Rao et al., 2008). The second youngest leaves were excised from 'Diamond' and 'Cavalier', before and after salt treatment. For salt-treated cultivars, leaves were collected after salt crystals started becoming clearly visible on the leaf surface. Leaves were fixed by exposure to 100% acrolein vapors (Electron Microscopy Sciences, Hatfield, PA) for 1 h under a fume hood, followed by exposure to ruthenium vapors (Electron Microscopy Sciences, Hatfield, PA) for 10 min (0.02 g of ruthenium chloride was placed in a plastic bottle cap next to the leaves and 1 mL of sodium hypochlorite was added to it).

Each leaf was then picked up with a locking forcep and plunged into liquid nitrogen for 1 min, followed by a 30 s wash in methanol, and finally dipped in hexamethyl disilazane (Electron Microscopy Sciences, Hatfield, PA) for 1 min. Leaves were allowed to dry for 1-2 min, after which they were mounted on SEM stubs using double-sided carbon tape. Some leaves were oriented with their adaxial surface facing up

and others with their abaxial side up. The mounted leaves were then coated with 30 nm of carbon and examined in a JEOL 6400-SEM at an accelerating voltage of 15 kV. Energy dispersive spectroscopy (EDS) was used for qualitative elemental analysis of the leaf surface.

TEM Studies – Our preliminary studies with *Z. matrella* revealed that this grass poses a challenge to fixation for TEM studies; hence a protocol was first developed for fixation of *Z. matrella* leaves. The second youngest yet fully mature leaves of *Z. matrella* were first dipped in chloroform for 30 s under a fume hood to dissolve the cuticle. The leaves were then cut into small segments and fixed in 0.1 M HEPES (Electron Microscopy Sciences, Hatfield, PA) containing 2.5% (v/v) glutaraldehyde and 2% (w/v) paraformaldehyde. The leaves were then post-fixed with osmium tetroxide (Electron Microscopy Sciences, Hatfield, PA), dehydrated in an acetone series, and embedded in a modified Spurr's epoxy resin (Spurr, 1969). Sections were cut on a Reichert-Jung Ultracut E microtome (C. Reichert Optische Werke AG, Austria) using a Diamond knife. Semi-thin sections stained with toluidene blue were used for visualization under a light microscope while ultra-thin (100 nm) sections post-stained with uranyl acetate (Electron Microscopy Sciences, Hatfield, PA) and lead citrate (Reynolds, 1963) were used for TEM studies.

For enhanced visualization of the plasma membrane, ultra-thin sections were picked up on a nickel grid. The sections were oxidized by placing in 1% (w/v) periodic acid for 30 min at room temperature, followed by five washes in deionized water (10 min per wash). The grids containing sections were allowed to stay in the last wash

overnight. The next day the grids were washed once in deionized water and then stained with 1% (w/v) phosphotungstic acid (PTA) in 10% (w/v) chromic acid. This was followed by five washes in deionized water (10 min per wash). The grids were then picked up with locking forceps and allowed to dry on a slide warmer before proceeding with observation under a JEOL 1200 EX TEM at an accelerating voltage of 100 kV. LUXFilm™ TEM supports (nickel and copper) from Tedpella, Inc. (Redding, CA) were used for all TEM studies.

For Cl^- localization, a branch of salt-treated plants that had three to four leaf blades was dipped in a 0.01 M (w/v) $AgNO_3$ (silver nitrate) solution for 30 min. The leaves were then dipped in chloroform for 30 s and fixed in 0.1 M HEPES containing 2.5% (v/v) glutaraldehyde and 2% (v/v) acrolein. After post-fixation with osmium tetroxide and dehydration in a methanol series, the leaves were embedded in a modified Spurr's epoxy resin (Spurr, 1969). Ultrathin sections were later examined by STEM using a FEI Tecnai G2 F20 microscope (Hillsboro, OR).

All SEM, TEM and STEM studies were performed at the Microscopy and Imaging Center (MIC) at Texas A&M University, College Station, TX.

Statistical analysis

Measurements involved three replicates each of plants treated with 0 mM NaCl and 300 mM NaCl. Five leaves were randomly chosen and 100 glands were counted from plants belonging to each treatment group. The means of salt gland dimensions were compared using ANOVA. Since the means between treatments were significantly

different, Fisher's LSD was used for pairwise comparisons between the different treatments to determine the means that were significantly different.

RESULTS

Z. matrella leaf surface

The leaves of *Z. matrella* had an uneven surface, ridged by the presence of parallely arranged veins. These ridges had grooves in between which were more pronounced on the adaxial leaf surface. Alongside the ridges lay the salt glands, alternating with stomata. In both cultivars, one row of salt glands was arranged between two rows of stomata, on both the leaf surfaces (Figures 2.1 & 2.2). Glands of *Z. matrella* appeared to be of the semi-sunken kind. The salt glands protruded from the epidermis and laid flat on one of their sides. The orientation of all the glands on a given leaf surface was the same.

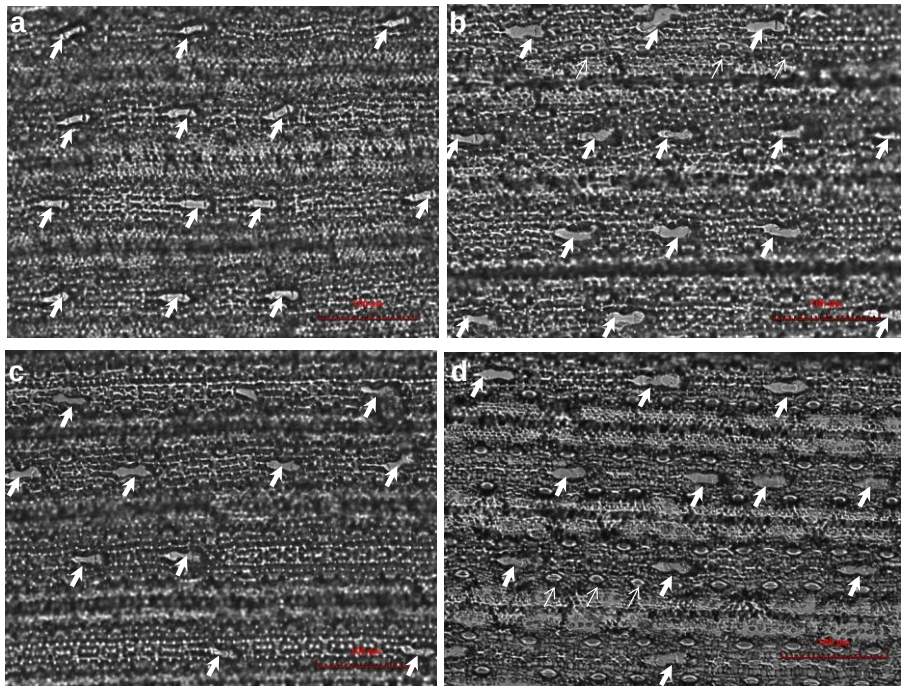

Figure 2.1 - Epidermal peels from adaxial leaf surface of *Z. matrella* cultivars.

(a) Adaxial leaf surface of 'Diamond' treated with 0 mM NaCl.

(b) Adaxial leaf surface of 'Diamond' treated with 300 mM NaCl.

(c) Adaxial leaf surface of 'Cavalier' treated with 0 mM NaCl.

(d) Adaxial leaf surface of 'Cavalier' treated with 300 mM NaCl.

Bold arrows, salt glands; thin arrows, stomata. Scale bar = 100 μm.

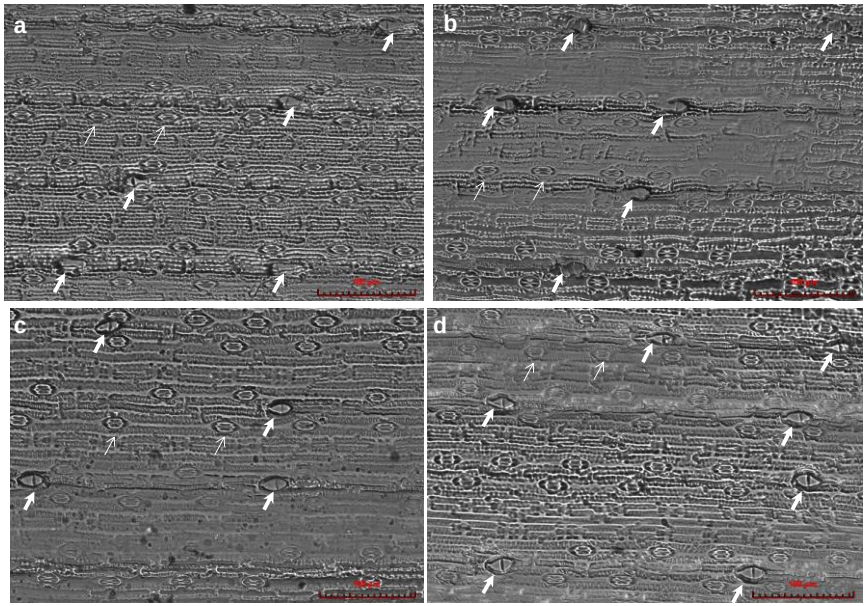

Figure 2.2 - Epidermal peels from abaxial leaf surface of *Z. matrella* cultivars.

(a) Abaxial leaf surface of 'Diamond' treated with 0 mM NaCl.

(b) Abaxial leaf surface of 'Diamond' treated with 300 mM NaCl.

(c) Abaxial leaf surface of 'Cavalier' treated with 0 mM NaCl.

(d) Abaxial leaf surface of 'Cavalier' treated with 300 mM NaCl.

Bold arrows, salt glands; thin arrows, stomata. Scale bar = 100 µm.

Apart from salt glands and stomata, other epidermal structures observed on *Z. matrella* leaves were prickles and papillae. Prickles are unicellular trichomes with an expanded base and a pointed tip (Amarasinghe and Watson, 1988; McWhorter et al., 1993); while papillae are short, sphere-like projections of the epidermal cells covered with wax (Aist, 1976).

Prickles were found in both cultivars although they were visually more abundant in 'Cavalier' (Figures 2.3 & 2.4). Although salt glands were found on both leaf surfaces of *Z. matrella*, papillate epidermal cells were seen only on the adaxial side (Figures 2.5 & 2.6).

Salt gland morphology

The salt glands on the adaxial side were morphologically different from the ones on the abaxial side for both *Z. matrella* cultivars (Figures 2.5-2.7). SEM studies showed that the adaxial glands were longer and swollen in appearance (Figures 2.5-2.6) while the ones on the abaxial side appeared smaller and sunken (Figure 2.7). Salt glands in *Z. matrella* can be easily visualized using epidermal imprints hence this approach was used for measuring the salt gland dimensions for both cultivars, in order to determine if the size of these glands contributed towards the difference in salt tolerance between 'Diamond' and 'Cavalier'.

Figure 2.3 - SEM of adaxial leaf surface of 'Diamond' treated with 300 mM NaCl.

Arrows, salt glands; S, salt crystals; p, prickles. Scale bar = 100 µm.

Figure 2.4 - SEM of adaxial leaf surface of 'Cavalier' treated with 300 mM NaCl.

Arrows, salt glands; S, salt crystals; p, prickles. Scale bar = 200 µm.

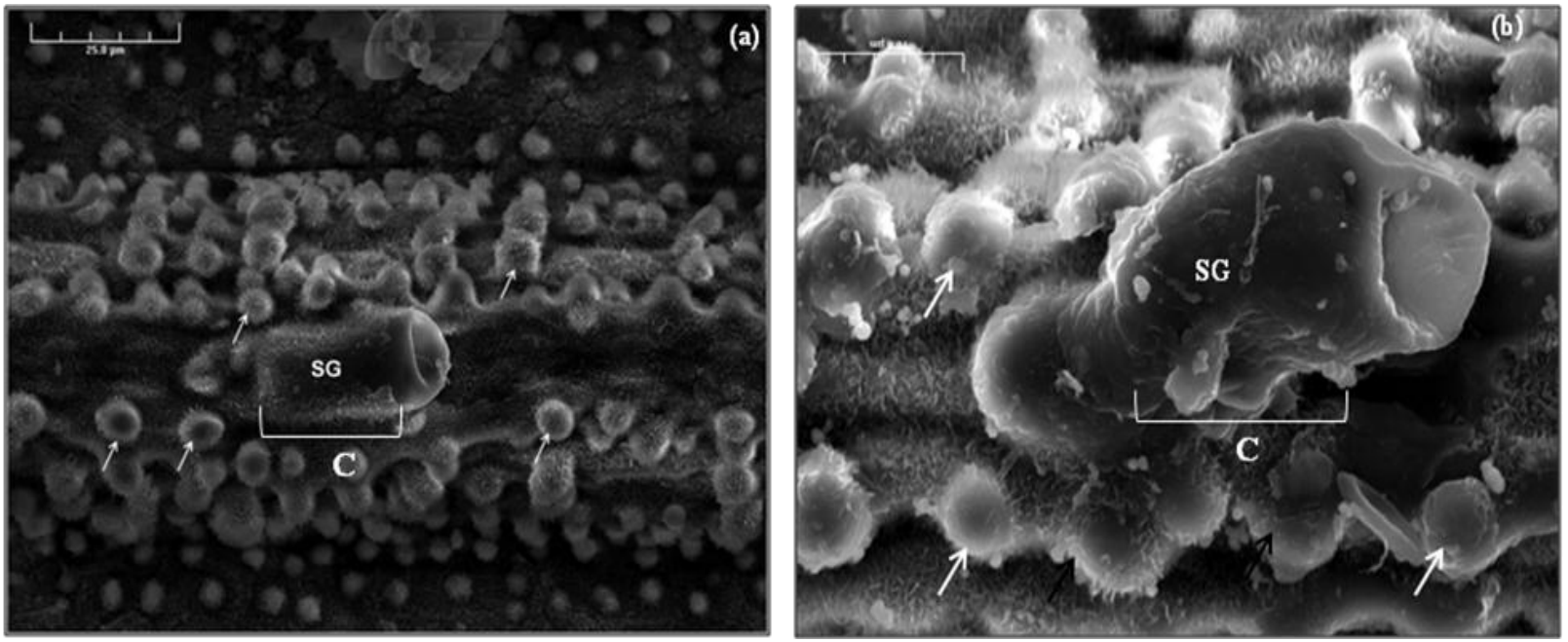

Figure 2.5 – SEM of salt glands on the adaxial leaf surface of plants treated with 0 mM NaCl.

(a) Adaxial leaf surface of 'Diamond' treated with 0 mM NaCl.

(b) Adaxial leaf surface of 'Cavalier' treated with 0 mM NaCl.

SG, salt gland; arrows, papillae; C, cuticle. Scale bar = 25 µm (a), 10 µm (b).

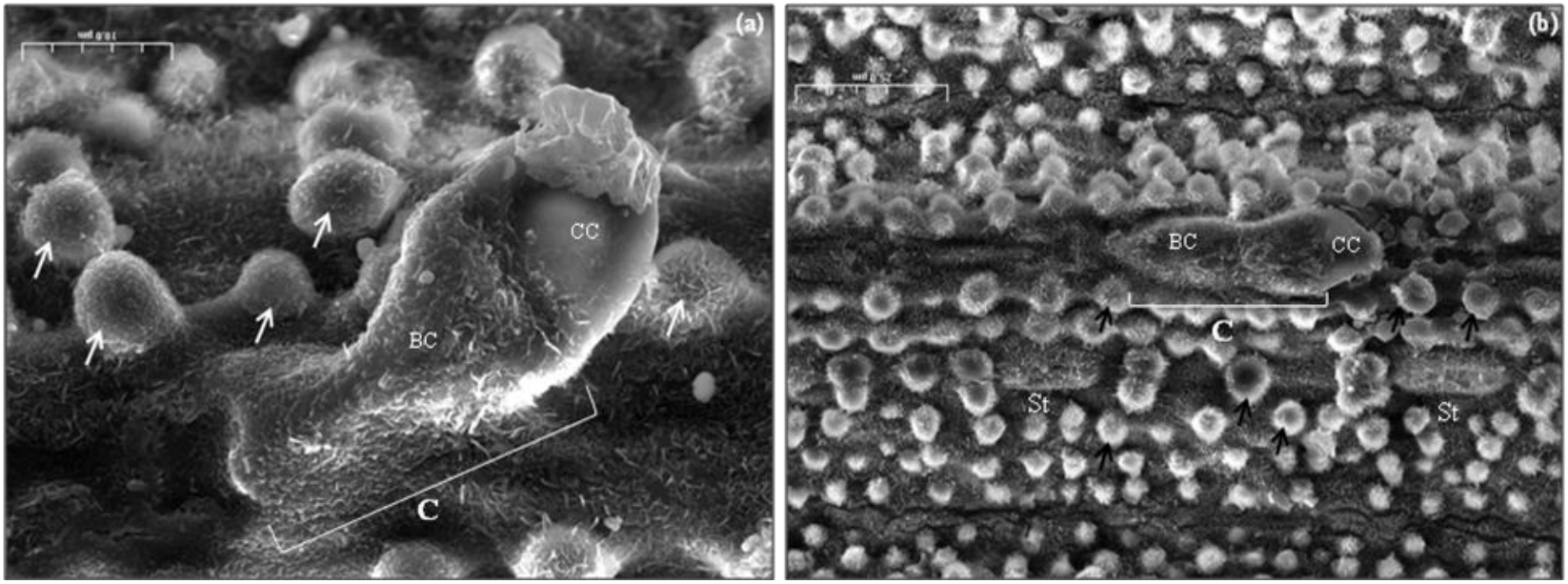

Figure 2.6 – SEM of salt glands on the adaxial leaf surface of plants treated with 300 mM NaCl.

(a) Adaxial leaf surface of 'Diamond' showing heavily cuticularized salt gland.

(b) Adaxial leaf surface of 'Cavalier' showing heavily cuticularized salt gland.

SG, salt gland; CC, cap cell of the salt gland; BC, basal cell of the salt gland; St, stomata; C, cuticle; arrows, papillae.

Scale bar = 25 μm (a); 10 μm (b).

Results obtained from the epidermal imprint study confirmed that the glands on the adaxial side were longer than the ones on the abaxial side for both the cultivars (Table 2.1). Salt glands of 'Cavalier' were longer and wider than the ones in 'Diamond' in untreated plants (0 mM NaCl). For 'Diamond', there was a positive correlation between the salt gland dimensions and salt treatment (300 mM NaCl); whereas, for 'Cavalier' this correlation was negative. To determine if salt treatment had any effect on the abaxial salt glands, the same parameters were measured for abaxial glands as well. In untreated plants, abaxial salt glands were longer and wider in 'Diamond', and were unaffected by salt treatment (Table 2.1). In 'Cavalier', although the salt glands in salt treated plants were longer, the width was not significantly affected.

To summarize, salt glands on both leaf surfaces of salt-treated 'Diamond' were longer, with a wider cap cell, than those observed in salt-treated 'Cavalier'.

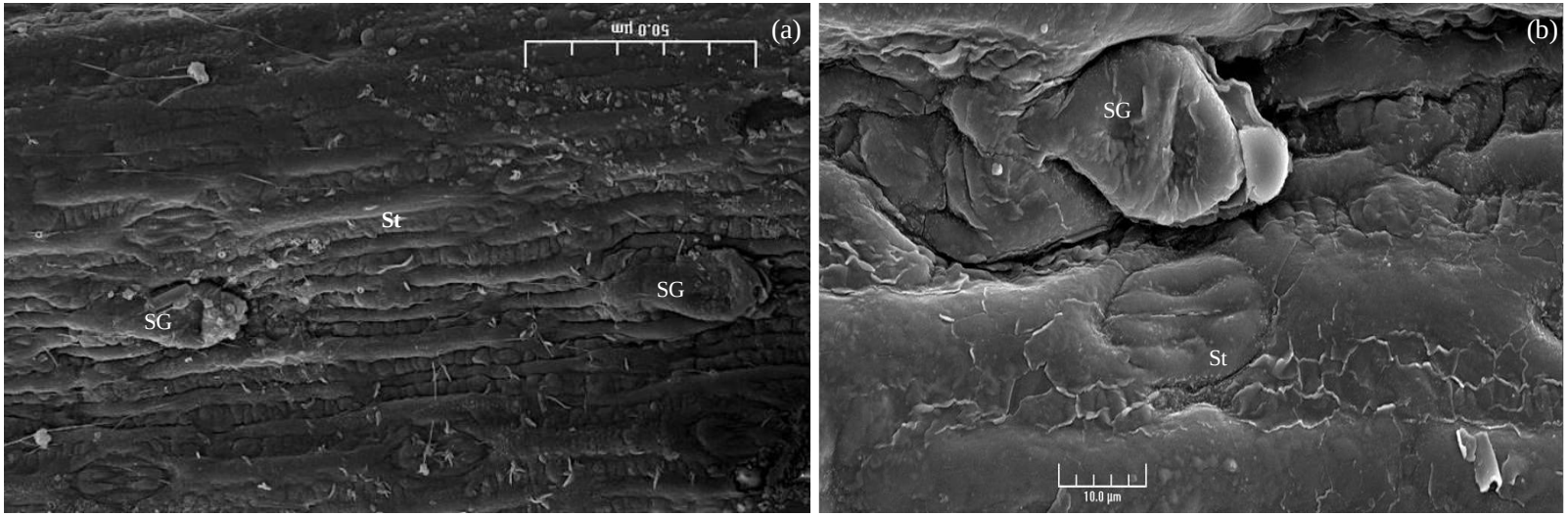

Figure 2.7 – SEM of abaxial salt glands in plants treated with 300 mM NaCl.

(a) Abaxial salt gland in ‘Diamond’.

(b) Abaxial salt gland in ‘Cavalier’.

SG, salt gland; St, stomata. Scale bar = 50 µm (a); 10 µm (b).

Table 2.1 - Salt gland dimensions for 'Diamond' and 'Cavalier'.

Cultivar	ADAXIAL Salt Glands[1]		ABAXIAL Salt Glands[1]	
	Length (µm)	Width (µm)	Length (µm)	Width (µm)
'Diamond' Control (0 mM NaCl)	38.71^{C}	10.00^{C}	33.18^{A}	12.61^{A}
'Diamond' Salt (300mM NaCl)	41.73^{A}	11.57^{A}	32.43^{AB}	12.69^{A}
'Cavalier' Control (0 mM NaCl)	42.03^{A}	10.96^{B}	29.80^{B}	11.68^{B}
'Cavalier' Salt (300mM NaCl)	39.99^{B}	9.67^{C}	31.92^{C}	12.04^{B}
$LSD_{0.05}$	1.24	0.55	1.26	0.53

[1] The data represents a mean of measurements from 100 glands per treatment.

[1] Means followed by the same letter within a column are not significantly different according to Fisher's LSD.

Scanning Electron Microscope (SEM) studies for visualizing salt secretion by salt glands

For further examination of salt gland morphology, cryo-fixed leaf specimens were examined under an SEM. The two parts of a salt gland – a cap cell and a basal cell (characteristic of salt glands in grasses), could be distinguished by SEM. Salt glands in salt-treated plants of both cultivars were heavily cuticularized (Figures 2.6). On the other hand, glands from control plants appeared to be less cuticularized, especially towards the tip of the salt gland (Figure 2.5). Salt treatment also had an effect on the overall shape of the salt glands. The glands from control plants were somewhat cylindrical in shape and there was no clear distinction between the cap cell and the basal cell (Figures 2.5). However, the glands from salt-treated plants were bulbous, shaped like a dumbbell (Figures 2.6).

Salt crystals were seen only on the leaves of salt treated plants. Salt secretion was distinctly visible on the leaf surface after four weeks of salt treatment (300 mM NaCl) and continued thereafter (Figure 2.8). Salt crystals were observed on the adaxial side for both 'Diamond' and 'Cavalier'. No salt crystals were observed in the leaves from control plants or on the abaxial side of salt-treated plants, indicating that salt secretion in these *Z. matrella* cultivars occurs only on the adaxial side (Figure 2.8).

SEM studies indicated that the salt crystals on the adaxial side were strictly localized around the salt glands of salt treated plants (Figures 2.8 & 2.9). This confirmed that the salt observed on the leaves was due to secretion by the adaxial salt glands. To verify if the excreted salt was predominantly Na^+ and Cl^-, an EDS map of the area

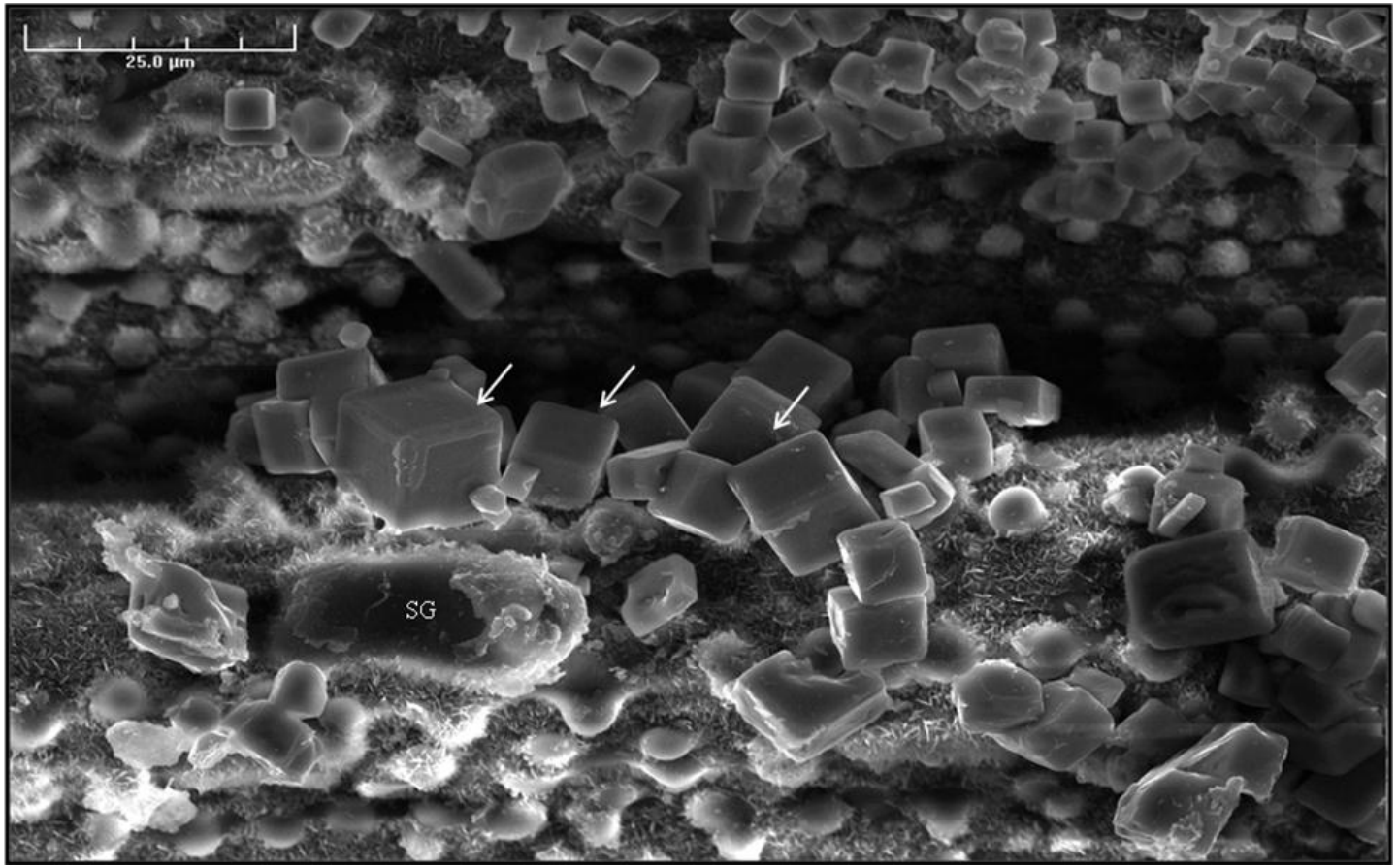

Figure 2.8 – SEM of adaxial leaf surface of 'Diamond' treated with 300 mM NaCl.

Note that salt crystals are localized around the salt gland. SG, salt gland; arrows, salt crystals. Scale bar = 25 µm.

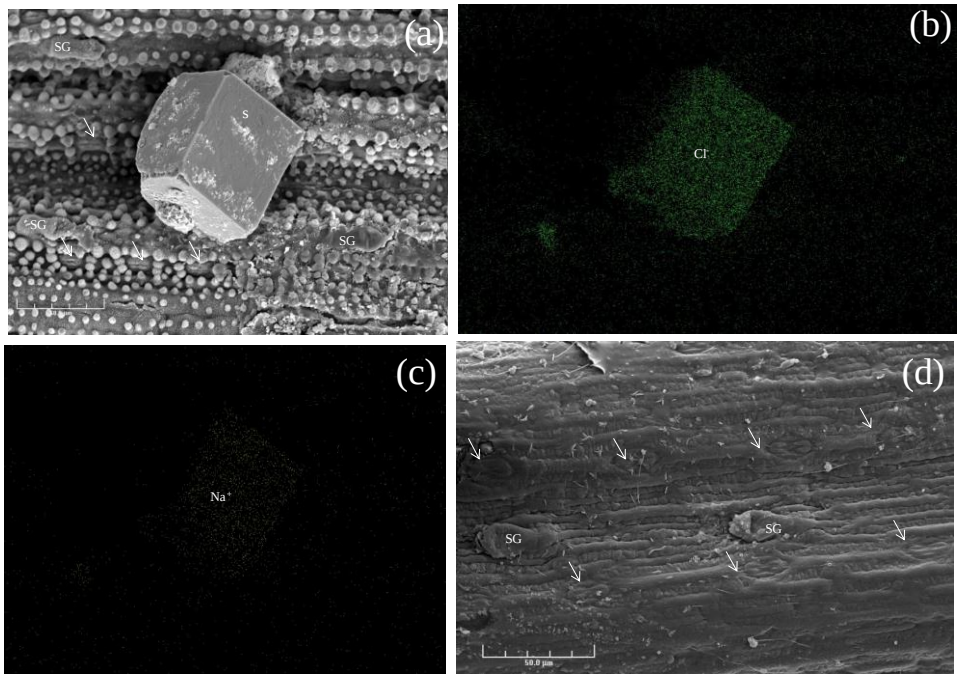

Figure 2.9 – SEM and EDS of leaves from 'Diamond' treated with 300 mM NaCl.

(a) SEM of adaxial leaf surface of 'Diamond' showing salt crystals (s), localized around a salt gland (SG).

(b) Cl^- map of the area in **(a)** showing the presence of Cl^- in the salt crystal.

(c) Na^+ map of the area in **(a)** showing the presence of Na^+ in the salt crystal.

(d) SEM of abaxial leaf surface of 'Diamond' showing salt glands (SG) and stomata (arrows), but no salt crystals.

Scale bar = 50 μm.

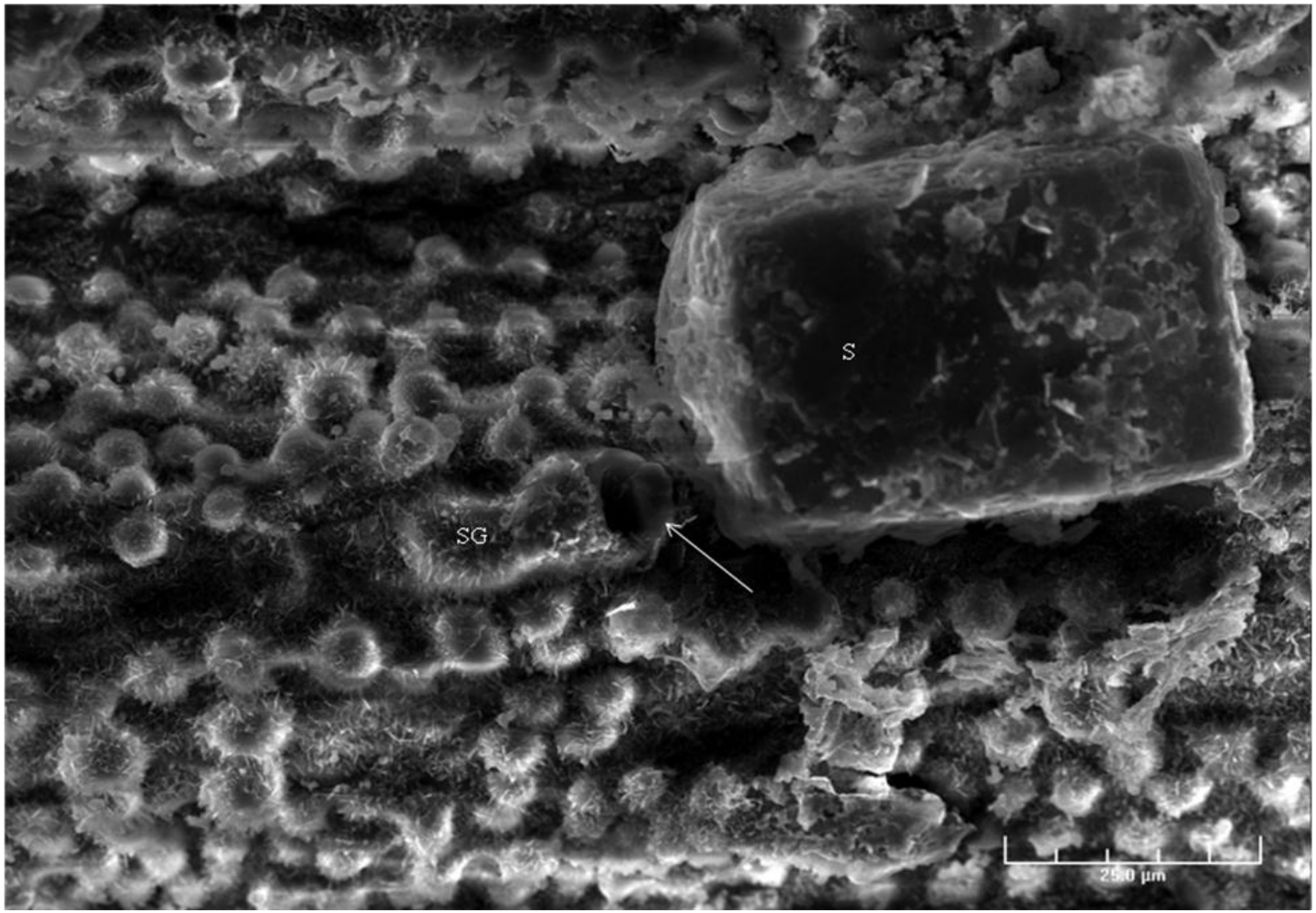

Figure 2.10 - SEM of adaxial leaf surface of 'Diamond' treated with 300 mM NaCl showing a salt gland pore.

Arrow, salt gland pore; SG, salt gland; S, salt crystal. Scale bar = 25 µm.

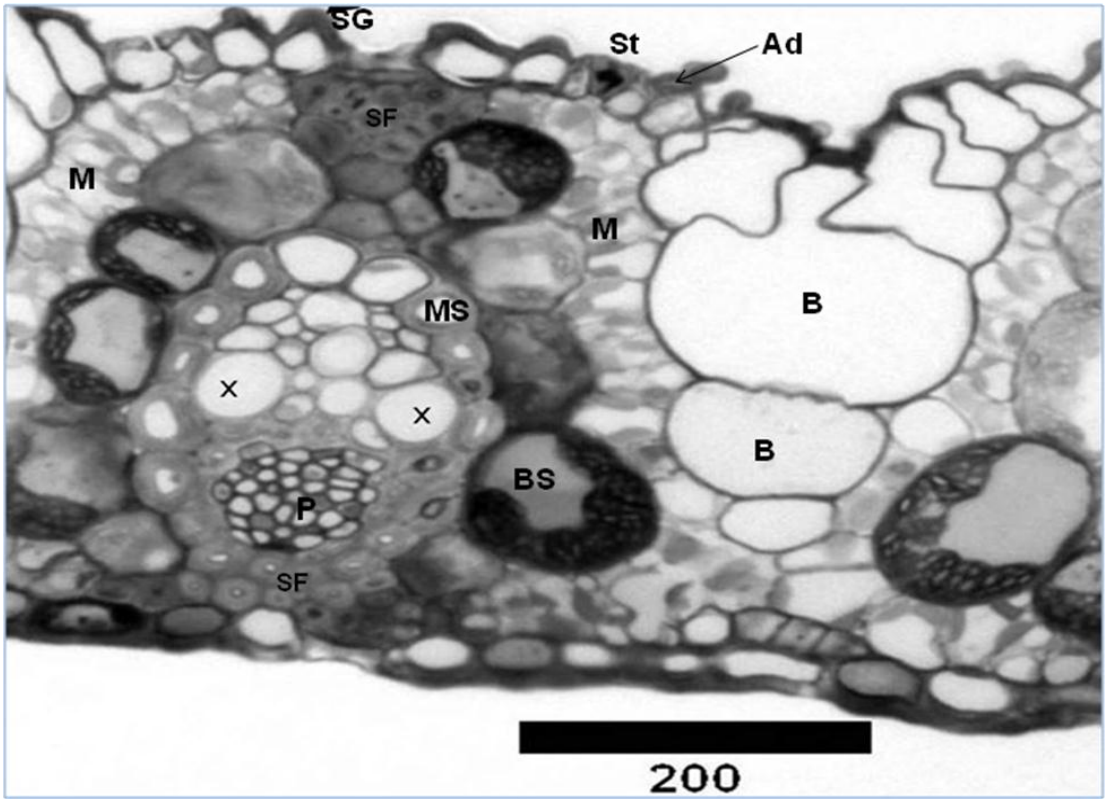

Figure 2.11 – Semi-thin cross-section of a 'Diamond' leaf.

Ad, adaxial epidermis; SG, salt glands; St, stomata; X, xylem vessels; P, phloem; SF, sclerenchyma fibers; BS, bundle sheath; MS, mestome sheath; B, bulliform cells; M, mesophyll. Scale bar = 200 μm.

comparable to Figure 2.9 was obtained. EDS confirmed that the excreted salt was mainly Na^+ and Cl^- (Figure 2.9). EDS analysis did not detect any Na^+ and Cl^- on the abaxial side where secretion was absent (Figures 2.7 & 2.9).

When viewed at higher magnification, a salt gland pore was seen at the tip of the adaxial salt glands through which Na^+ and Cl^- is excreted onto the leaf surface (Figure 2.10). The excreted saline ions later form salt crystals on the leaf surface as water evaporates.

Ultrastructure of *Z. matrella* salt glands

Examination of semi-thin leaf sections of 'Diamond' showed that the salt glands were located next to a pair of stomata (Figure 2.11). TEM studies were performed to examine salt gland ultrastructure and to look for anatomical differences induced by salt in 'Diamond' versus 'Cavalier' that could contribute towards differences in their salt tolerance.

Figure 2.12 - TEM of an adaxial salt gland from 'Diamond' treated with 0 mM NaCl.

CC, cap cell; BC, basal cell; EC, epidermal cell, MC, mesophyll; C, cuticle; CW, cell wall; PM, plasma membrane; V, vacuole; Cu, cuticular cavity. Scale bar = 10 µm.

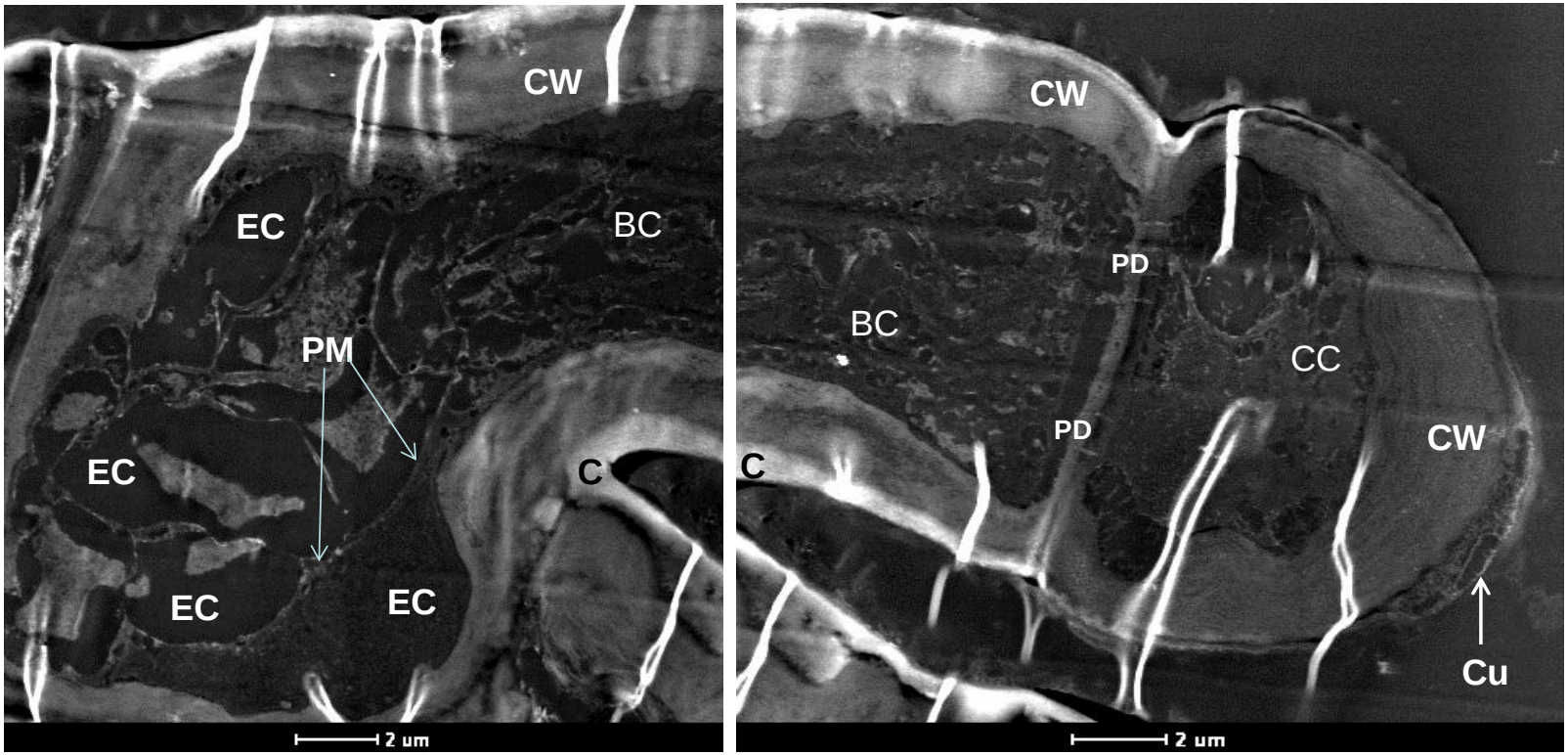

Figure 2.13 - STEM of an adaxial salt gland from 'Diamond' treated with 300 mM NaCl.

CC, cap cell; BC, basal cell; MC, mesophyll; EC, extracytoplasmic channel; C, cuticle; CW, cell wall; PM, plasma membrane; PD, plasmodesmata; V, vesicle; Cu, cuticular cavity. Scale bar = 2 µm.

Salt glands in both ‘Diamond’ and ‘Cavalier’ were bicellular with an upper cap cell and a lower basal cell (Figures 2.12-2.15). The basal cell lay embedded in the leaf epidermis while the cap cell protruded out from the epidermis and lay flat on the leaf surface. A cuticle surrounded both cells forming a continuous layer extending from the epidermis and over the salt gland.

The cap cell from control as well as treated plants contained numerous small vacuoles (Figures 2.12, 2.13 & 2.15). At the tip of the cap cell, a cuticular cavity (also referred to as the collecting chamber) was present. This cavity serves as a reservoir for salts that have been excreted from the salt gland. The cuticular cavity was seen in control (Figure 2.12) as well as salt-treated plants (Figures 2.13 & 2.14). However, only the cavity of salt-treated plants was filled with electron dense material.

In the basal cell of salt-treated cultivars, a dense network of partitioning membranes was observed (Figure 2.14). I determined that these membranes were plasma membrane derived using PTA-chromic acid (Mayo and Cocking, 1969; Hodges et al., 1972; Roland et al., 1972; Van Der Woude et al., 1974; Koehler et al., 1976; Leonard and Van Der Woude, 1976; Sundberg and Lembi, 1976; Nagahashi et al., 1978; Oross and Thomson, 1982a). Because only the plasma membrane is stained with PTA-chromic acid, I could distinguish the plasma membrane from the other endomembranes in the salt glands. The pattern of these membranes was different between the control and salt-treated plants. In the control plants, these membranes lacked organization and appeared as irregularly folded structures (Figure 2.12); whereas, in the salt-treated cultivars, these membranes were highly organized (Figures 2.13 & 2.14). These membranes formed a

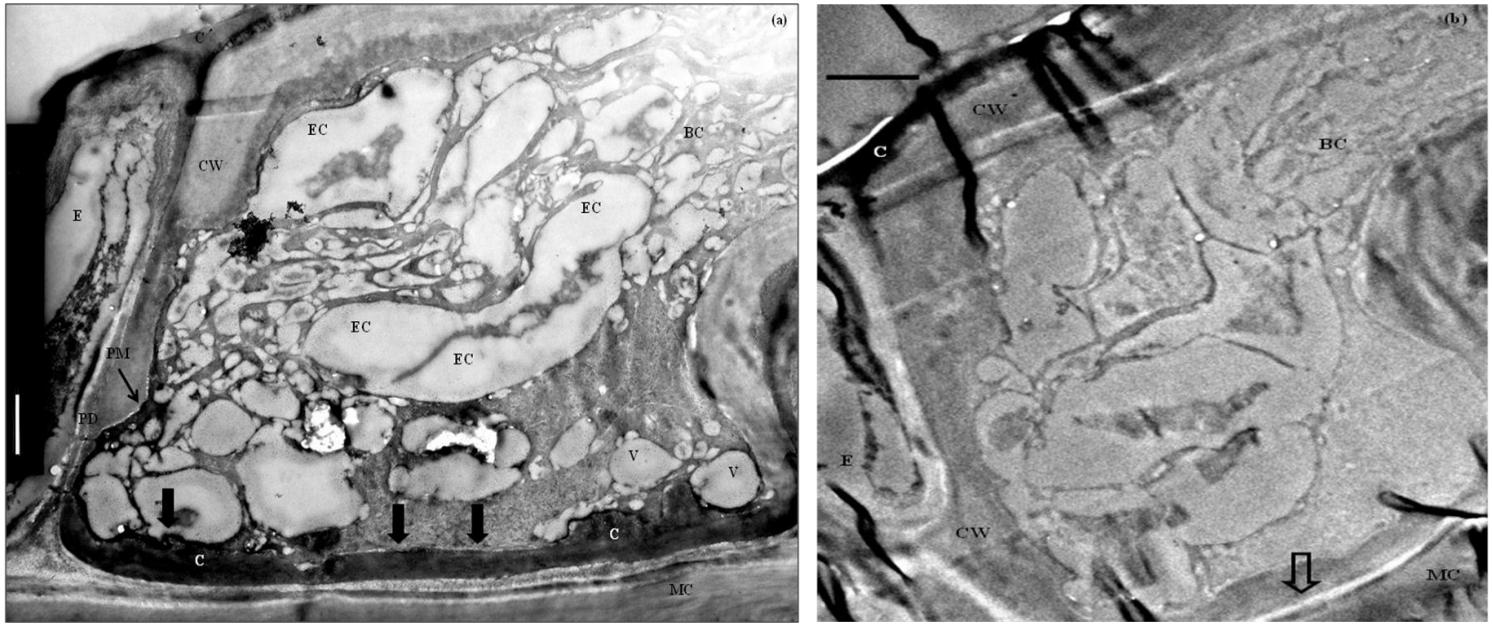

Figure 2.14 – TEM of basal cells from 'Diamond' and 'Cavalier' treated with 300 mM NaCl.

(a) Part of a basal cell of an adaxial salt gland from 'Cavalier' showing the presence of cuticle (filled block arrows) between the basal cell and mesophyll cell. (b) Part of a basal cell of an adaxial salt gland from 'Diamond' showing the absence of cuticle (block arrow) between the basal cell and mesophyll cell. BC, basal cell; E, epidermal cell, MC, mesophyll cell; C, cuticle; CW, cell wall; PM, plasma membrane; V, vacuoles; EC, extracytoplasmic channels. Scale bar = 2 μm.

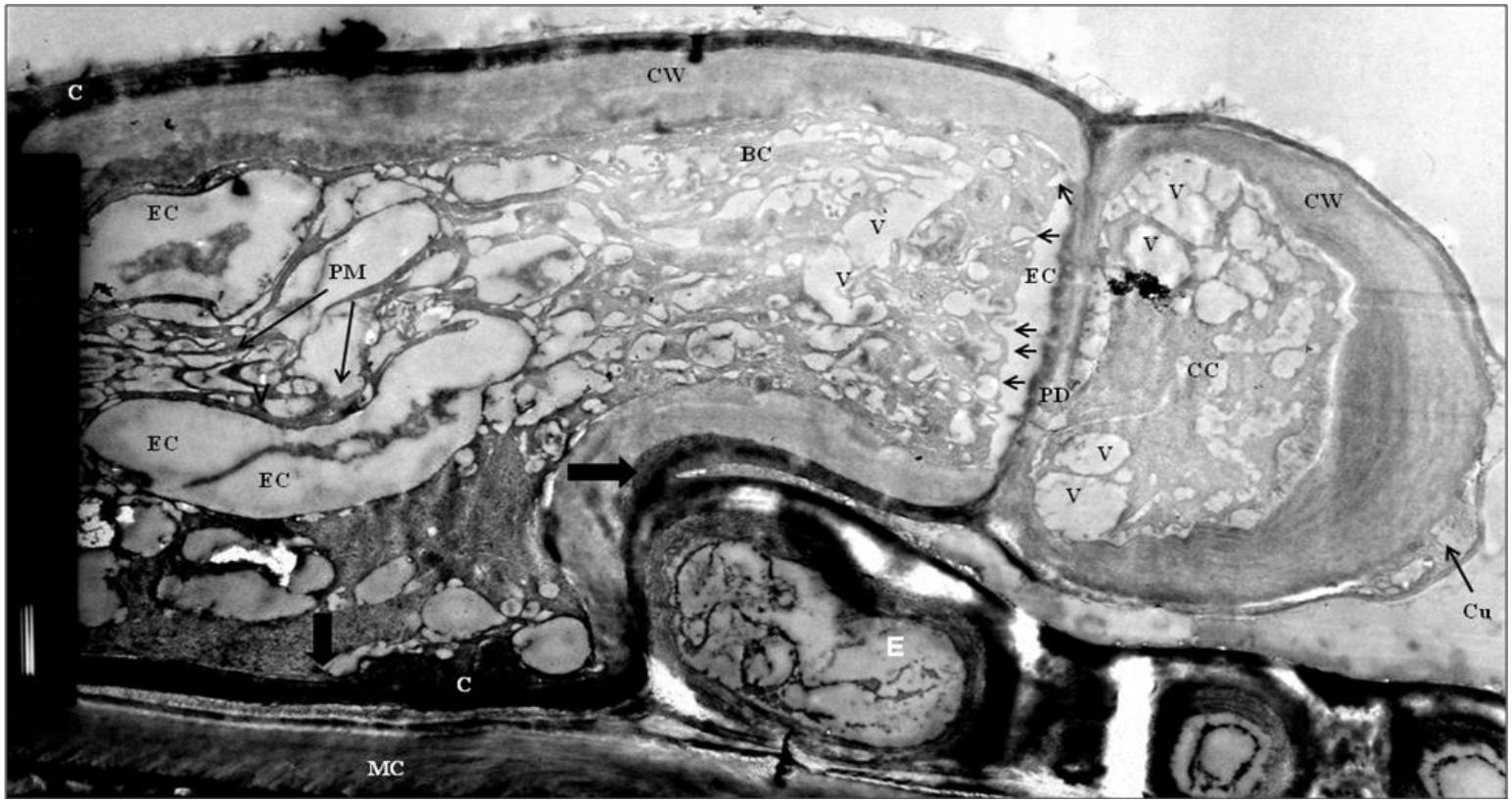

Figure 2.15 - TEM of an adaxial salt gland from 'Cavalier' treated with 300 mM NaCl.

CC, cap cell; BC, basal cell; E, epidermal cell; MC, mesophyll; C, cuticle; CW, cell wall; PM, plasma membrane; V, vacuoles; Cu, cuticular cavity; PD, plasmodesmata; EC, extracytoplasmic channel; arrows, microvacuoles. Scale bar = 2 μm.

distinct pattern of folds that were more pronounced towards the end of the basal cell that was closer to the epidermis. At this end of the basal cell, plasmodesmata were seen connecting the basal cell to an adjacent epidermal cell only in 'Cavalier' (Figure 2.14). Such a symplastic connection was not seen in 'Diamond' (Figure 2.14). The partitioning membranes in the basal cell of 'Cavalier' seemed to originate from this area where the above-mentioned plasmodesmata were located (Figure 2.14).

Plasmodesmatal connections between the basal cell and cap cell were seen for both cultivars following salt treatment (Figures 2.13 & 2.15); whereas, plasmodesmata between the basal cell and its adjacent epidermal cell were observed only for salt-treated 'Cavalier' (Figure 2.14a). The cuticle on the adaxial side covering the salt glands and the epidermal cells was electron dense, thus the distinction between the cell wall and the cuticle could be readily made (Figures 2.12 & 2.13). In salt-treated 'Cavalier' (Figure 2.14a), the cuticle around the salt gland was observed as a layer encapsulating the entire salt gland (cap cell and basal cell) such that there was a layer of cuticle between the basal cell and the underlying mesophyll cells. However, in salt-treated 'Diamond' (Figures 2.14b and 2.16), the cuticle was observed to be a continuous layer over the salt gland and the adjacent epidermal cells with no cuticle between the salt gland and its underlying mesophyll cells.

Also seen in the basal cells of salt-treated cultivars were several mitochondria and small vacuoles (Figure 2.17). The mitochondria were present in the vicinity of the partitioning membranes. Vacuoles observed in the basal cell varied in sizes and seemed

to fuse at the plasma membrane near the common wall of the cap cell and the basal cell (Figures 2.13 & 2.15).

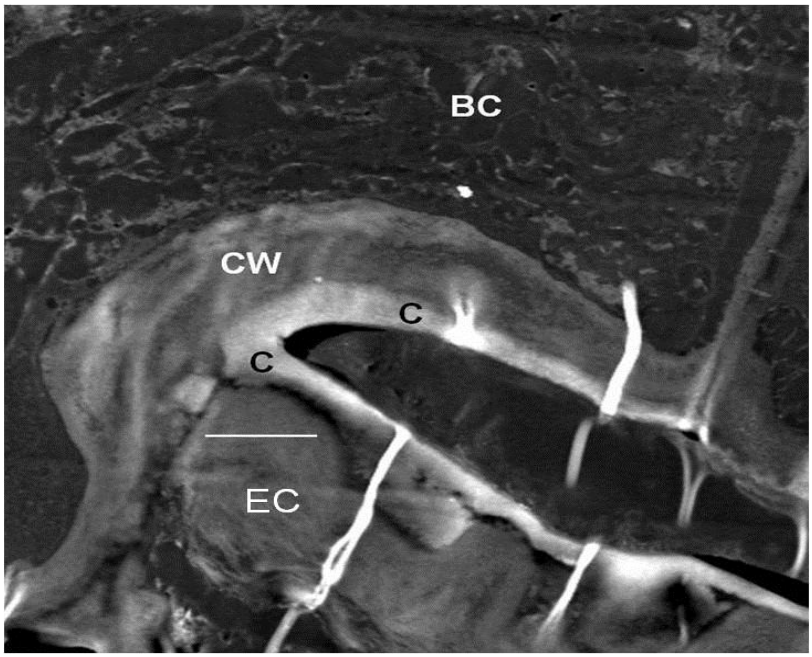

Figure 2.16 – STEM of a part of a basal cell of an adaxial salt gland and part of an adjacent epidermal cell from 'Diamond' treated with 300 mM NaCl.

BC, basal cell; EC, epidermal cell; C, cuticle; CW, cell wall. Scale bar = 2 μm.

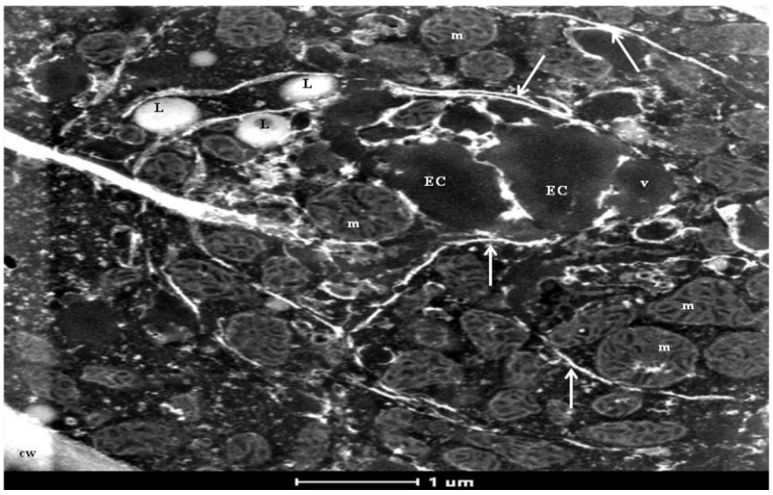

Figure 2.17 – STEM of a part of the basal cell of an adaxial salt gland from 'Diamond' treated with 300 mM NaCl.

Mitochondria (m) are located in the vicinity of the extracytoplasmic channels (EC) suggesting the occurrence of active transport along these membranes.

L, lipid bodies; cw, cell wall; v, vacuoles.

Localization of chloride ions (Cl^-) in the salt glands

Branches of salt-treated cultivars were treated with $AgNO_3$ to precipitate the Cl^- ions *in situ* as AgCl, which could then be visualized via Scanning Transmission Electron Microscopy (STEM). Electron dense precipitates were seen inside the cap cell of the salt gland as well as in the cell wall near the tip of the cap cell in salt-treated plants (Figures 2.18 & 2.19). STEM coupled with EDS indicated that the electron dense precipitates consisted of AgCl. EDS also indicated the presence of Na^+ as is evident by the energy

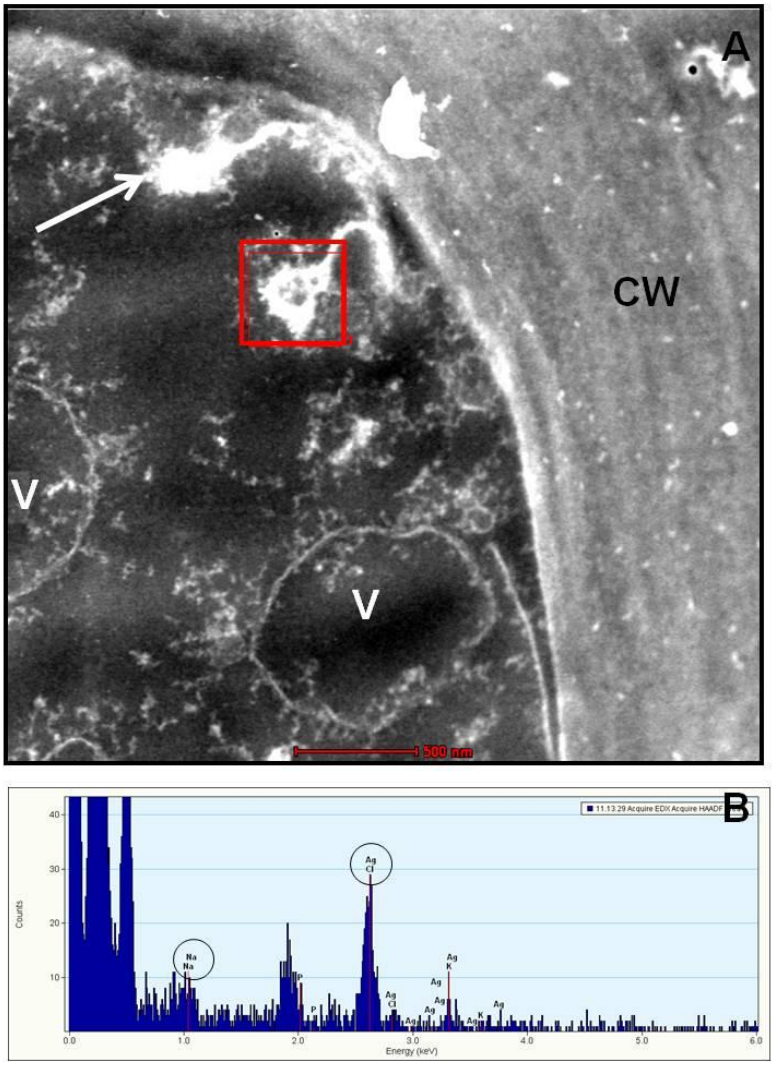

Figure 2.18 – Cl^- localization in the salt gland of 'Diamond' treated with 300 mM NaCl.

(A) Part of the cap cell of a salt gland from 'Diamond' after treatment with $AgNO_3$.

(B) STEM-EDS box analysis of the area marked in **(A)** indicating that the electron dense precipitate inside the cap cell is AgCl.

CW, cell wall; arrow, plasma membrane; v, vacuole; AgCl, silver chloride; $AgNO_3$, silver nitrate. Scale bar = 500 nm.

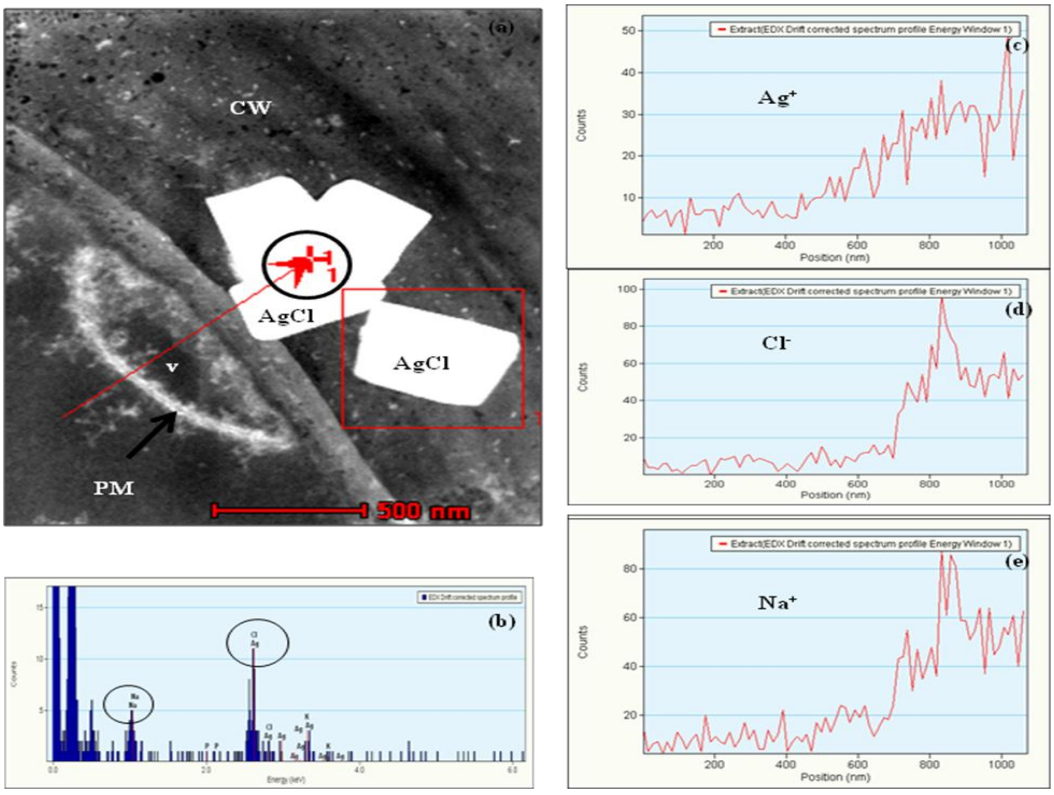

Figure 2.19 – Cl^- localization in the cell wall of cap cell from 'Diamond' treated with 300 mM NaCl.

(a) Part of the cap cell of a salt gland from 'Diamond' after treatment with $AgNO_3$.

(b) STEM-EDS analysis of the area circled in **(a)** indicating that the electron dense precipitate in the cap cell wall is AgCl.

(c) EDS line spectrum showing the presence of Ag^+ along the red line in **(a)**.

(d) EDS line spectrum showing the presence of Cl^- along the red line in **(a)**.

(e) EDS line spectrum showing the presence of Na^+ along the red line in **(a)**.

CW, cell wall; PM, plasma membrane; AgCl, silver chloride; $AgNO_3$, silver nitrate. Scale bar = 500 nm.

spectrum (Figures 2.18 & 2.19). Inside the cap cell, the precipitation was seen in the cytoplasm and around the plasma membrane, but not inside any of the vacuoles (Figure 2.18). Electron dense precipitates were detected by STEM in the cell wall of the cap cell. EDS line analysis across the cap cell showed that the intensity of the EDS signal increased in the direction of the cell wall (Figure 2.19). Similar electron dense precipitates of AgCl were also detected in the chloroplasts of mesophyll cells and in the plasmodesmata of mesophyll cells (Figures 2.20 and 2.21), but none were evident in the walls of the mesophyll cells.

DISCUSSION

Different aspects of salt gland morphology and structure in *Z. matrella* were examined to determine if structural differences in salt glands contributed towards the difference in the degree of salt tolerance between the two *Z. matrella* cultivars used in this study. Salt glands are modified epidermal cells with structural and functional adaptations for facilitating the secretion of salt. 'Diamond' and 'Cavalier' had salt glands on both leaf surfaces, although they had distinctive morphologies. The salt glands on the adaxial leaf surface were significantly longer than the ones on the abaxial side, and salt crystals indicative of salt secretion were seen only on the adaxial side for both cultivars in response to salt treatment.

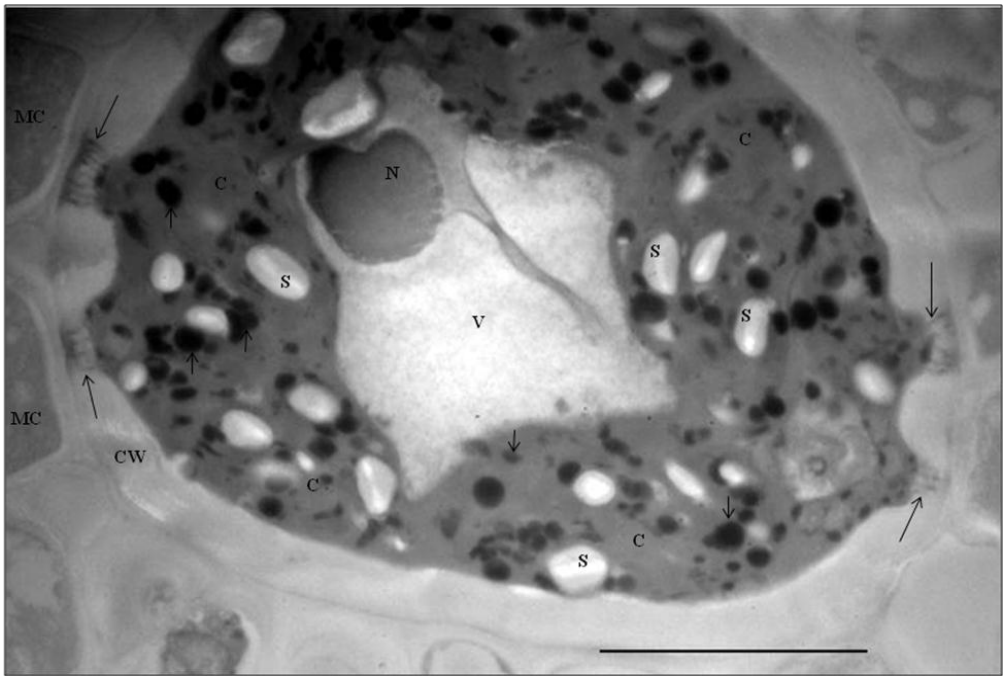

Figure 2.20 - TEM of a bundle sheath cell from 'Diamond' treated with 300 mM NaCl.

The bundle sheath cell located close to the adaxial epidermis of 'Diamond' leaf post-treated with silver nitrate, showed electron dense plasmodesmata (long arrows), and electron dense precipitates (short arrows) inside the chloroplast (C).

CW, cell wall; MC, mesophyll cell; V, vacuole; N, nucleus; S, starch. Scale bar = 5 μm.

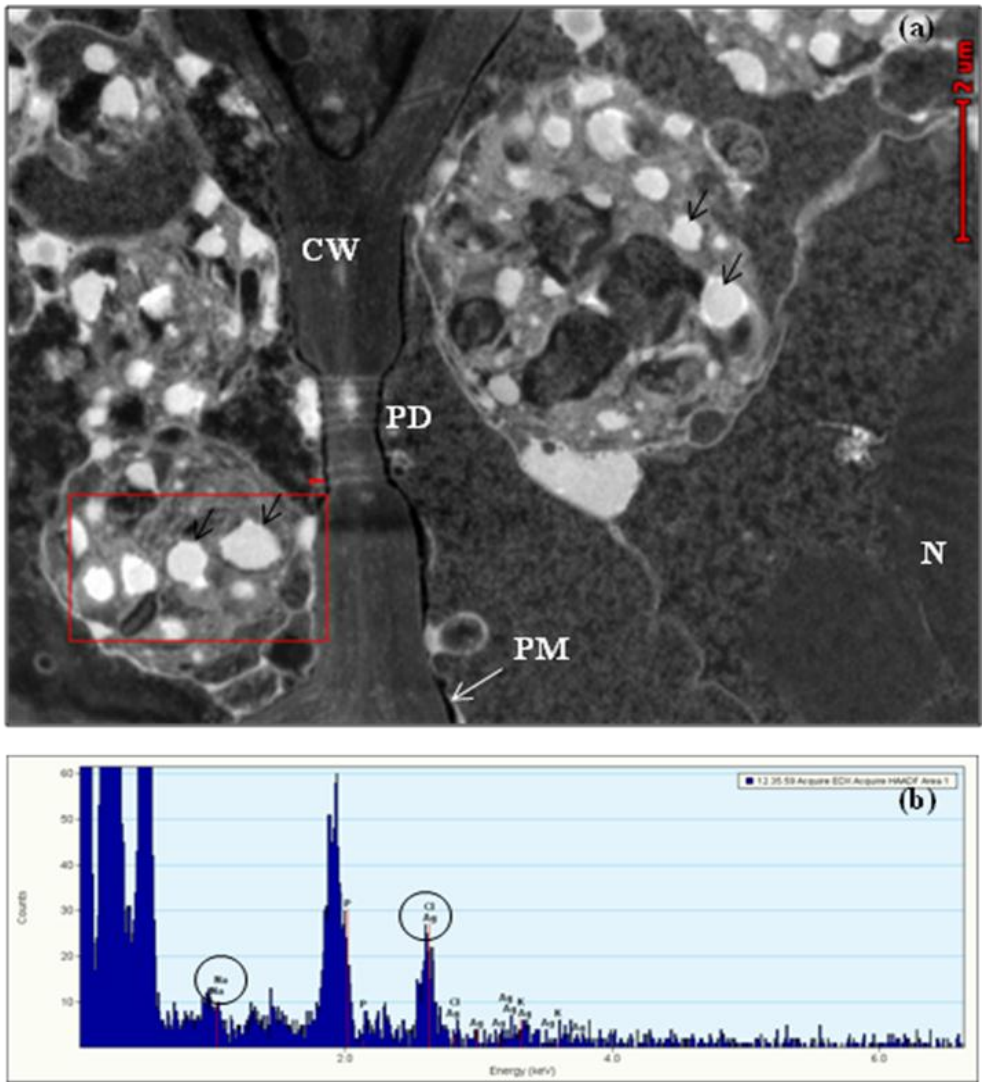

Figure 2.21 - STEM of two mesophyll cells from 'Diamond' treated with 300 mM NaCl and post-treated with silver nitrate.

(a) Electron-dense plasmodesmata between the two mesophyll cells.

(b) STEM-EDS box analysis of the area marked with a red box in **(a)** indicating that the electron dense precipitate (arrows) is AgCl.

CW, cell wall; PD, plasmodesmata; AgCl, silver chloride. Scale bar = 2 µm.

This suggests that only the glands present on the adaxial side of these cultivars are functional in salt secretion. However, in *Avicennia marina* (a dicotyledonous plant), salt secretion has been found to occur predominantly on the abaxial side, while in *S. virginicus*, *C. dactylon*, and *A. littoralis* (monocotyledonous plants), secretion can occur from glands on both leaf surfaces (Marcum and Murdoch, 1990; Fitzgerald et al., 1992; Naidoo and Naidoo, 1998; Barhoumi et al., 2008). The preference for the site of salt secretion thus seems to be species-specific.

The shape of the salt glands from salt-treated plants was observed to be dumbbell-like compared to the more cylindrical shape seen in control plants. The bulbous shape of the glands from salt-treated plants could be a result of salt accumulation inside the glands. Several papillae were observed on the adaxial side of both cultivars regardless of salt treatment, and are presumed to serve the function of protecting salt glands (Barhoumi et al., 2008) and stomata (Barhoumi et al., 2007). Since the papillae were seen only on the adaxial side of *Z. matrella* leaves, it can be hypothesized that these papillae are important for the protection of functional salt glands only. The abaxial side of both cultivars lacked papillae. Although their exact function has not been determined in other species with salt glands, in NaCl-treated *A. littoralis* a greater number of papillae were observed surrounding the adaxial salt glands (primary site of salt secretion) than the abaxial ones (Barhoumi et al., 2008).

From the data obtained from the comparison of salt gland dimensions between salt-treated cultivars, gland dimensions (length and width) increased following salt treatment in ‘Diamond’ while in salt-treated ‘Cavalier’ the glands were smaller

compared to the control plants. In a previous study (Marcum and Murdoch, 1990) involving two *Zoysia* species, it was reported that the species that was more salt tolerant had larger salt glands than the less salt tolerant species. A subsequent study involving five *Zoysia* grasses reported a positive correlation between salt gland Na^+ secretion rate and salt gland size (Marcum et al., 1998). The smaller size of salt glands in 'Cavalier' may account, in part, for lesser amount of Na^+ secreted by salt-treated 'Cavalier' than by salt-treated 'Diamond' (Binzel ML, unpublished data). The results seen from salt gland size comparison in this study suggest that the differences in salt gland size may be one of the factors responsible for enhanced salt tolerance of 'Diamond'.

TEM and STEM were used for the detailed examination of ultrastructural features of *Z. matrella* salt glands. The glands in *Z. matrella* were semi-sunken with a cap cell and a basal cell, similar to the bicellular glands reported for other grasses that have been studied. From previous studies, it is evident that the basal cell of a bicellular salt gland bears extensive infoldings of the plasma membrane that serve to provide increased surface area for salt secretion. Comparison of salt glands from control and salt-treated plants revealed that the glands from both groups of plants had plasma membrane infoldings in the basal cell of the salt gland. However, these infoldings were more well-defined in the basal cell of glands from salt-treated plants. The infoldings in the salt-treated plants from both cultivars extended into the basal cell from the end of the basal cell that was away from the cap cell (i.e. towards the epidermis) and formed large extracytoplasmic channels. This is contrasting to what has been reported for all other Chloridoid grasses studied to date, where the infoldings have been observed to extend

into the basal cell cytoplasm from the wall common to the cap cell and the basal cell of the salt gland.

Based on what is known for other grass species and our observations made with *Z. matrella*, we hypothesize that the pathway of saline ion transport from the vascular bundles to the salt glands in *Z. matrella* could be different from the other Chloridoid grasses studied until date. The epidermal cells located adjacent to the salt glands are presumed to play a role in channeling the salt from the mesophyll to the basal cell. It is hypothesized that the extracytoplasmic channels located at the common wall of the epidermal and basal cells serve to accommodate the saline ions arriving from the epidermal or mesophyll cells, in order to avoid overloading of these ions in the cytoplasm. Several mitochondria were observed in close association with these infoldings suggesting the occurrence of active transport along these membranes.

At the end of the basal cell closer to the cap cell, the channels became smaller, and several small vacuoles were seen that appeared to fuse with the plasma membrane near the common wall of the basal and the cap cells. The small vacuoles observed in both cultivars were plasma membrane-derived because they stained intensely with PTA-chromic acid. Plasmodesmatal connections were present between the basal cell and cap cell for both ‘Diamond’ and ‘Cavalier’, suggesting symplastic continuity between these two cells for movement of ions from the basal cell to the cap cell.

In addition to this symplastic connection seen between the two cells of the salt gland, plasmodesmata were also present between the basal cell and the adjacent epidermal cell in salt-treated ‘Cavalier’. This observation, in conjunction with the

presumed site of origin of the extracytoplasmic channels, supported the hypothesis of a role for epidermal cells in assisting the salt glands with salt transport to the glands in *Z. matrella*. Similar observations with symplastic continuity between the basal cell and epidermal cells have been made previously for some of the other Chloridoid grasses like *Cynodon* and *Distichlis*, and some dicotyledonous species like *Atriplex*. However, in case of 'Diamond', no plasmodesmata were observed between the basal cell and the adjacent epidermal cell, which has also been reported for Chloridoid grasses like *S. foliosa* and *A. littoralis* where symplastic connection between the salt gland and the adjacent epidermal cells was not observed (Levering and Thomson, 1971; Thomson, 1975).

The electron-dense cuticle, which was easily distinguishable from the cell wall, did not encapsulate either of the gland cells at their common wall suggesting that an apoplastic continuum also existed between the gland cells. However an interesting difference was observed between salt-treated 'Diamond' and 'Cavalier'. In the case of 'Diamond', the cuticle extended as a continuous layer from the top of the cap cell to the adjacent epidermal cell, whereas in 'Cavalier' the cuticle extended from the top of the salt gland to its base forming a apoplastic barrier between basal cell of the salt gland and its underlying mesophyll cell, which suggests a possible role for the cuticle to prevent the backflow of solutes from the salt gland to the mesophyll.

At the common wall between the two gland cells, several small vacuoles were observed. These vacuoles were plasma membrane derived and appeared to be fusing with the plasma membrane near the junction of the two cells, as well as at the tip of the

cap cell. We hypothesize that these vacuoles store the saline ions that have entered the cap cell and eventually fuse with the plasma membrane at the tip of the cap cell for unloading into the extracytoplasmic space near the cell wall. Our observations made with STEM and EDS studies in *Z. matrella* confirmed the presence of AgCl precipitate in this area. A similar mechanism of salt secretion via membrane-membrane fusion has been reported for the multicellular glands of *Tamarix aphylla* (Platt-Aloia et al., 1983).

Saline ions that have accumulated in the cap cell of salt glands are channeled into the cuticular cavity (collecting chamber) via diffusion through the cell wall of the cap cell. Cl^- localization studies revealed the presence of Cl^- (as an AgCl precipitate) and Na^+ in the cap cell wall. In *C. dactylon*, the salt glands from control plants had a smaller chamber than the ones from salt-treated plants (Oross and Thomson, 1982a), while in the case of *A. littoralis*, this chamber was not present in salt-treated plants (Barhoumi et al., 2007). For *Z. matrella*, the collecting chamber was seen in salt glands from control as well as salt-treated plants for both cultivars, with no significant differences. However, the chamber in the salt-treated plants contained electron dense material that was verified to be Cl^- and Na^+ by EDS. Upon their arrival in the cuticular chamber, saline ions can be excreted onto the leaf surface via pores formed in the cuticle of the cap cell (Oross and Thomson, 1984). These pores were also observed in the salt glands of salt-treated *Z. matrella* cultivars. SEM studies showed that a large pore was present at the tip of glands that were secreting salt. This large pore could have been a result of rupturing of the cuticular chamber in response to salt accumulation in the chamber.

Based on the ultra structural observations made for *Z. matrella* salt glands, the following model can be proposed for salt excretion in this grass. Saline ions enter the basal cell from the mesophyll and epidermal cells via the symplast. Once inside the basal cell, the ions accumulate in the extracytoplasmic channels formed by invaginations of the plasma membrane from where these ions are transported via small vacuoles in order to avoid cytoplasmic damage to the cell by a hypertonic solution. This is necessary as the basal cells lacked the large central vacuole which is characteristic of most plant cells. Once inside these vacuoles, the ions are channeled towards the cap cell where these vacuoles fuse with the plasma membrane to release the ions into the extracytoplasmic space, from where the ions move into the cap cell via the symplast. Once inside the cap cell, the ions are again stored in vacuoles until they are delivered to the other end of the cap cell where the collecting chamber is located. Loading of ions in the extracytoplasmic space at the tip of the cap cell helps the ions diffuse through the cell wall and into the collecting chamber. From here, water and saline ions are excreted onto the leaf surface via cuticular pores where, after dehydration, salt crystals are formed.

The findings from this part of the project suggested that differences in morphology and ultrastructure of the salt glands possibly contribute towards the difference in salt tolerance between ‘Diamond’ and ‘Cavalier’. The next chapter aims to look for differences in salt gland density between ‘Diamond’ and ‘Cavalier’ as another possible factor responsible for the difference in salt tolerance between these cultivars.

CHAPTER III

HERITABILITY OF SALT GLANDS IN *Zoysia matrella*

INTRODUCTION

Based on their response to high salt (NaCl) concentrations in the environment, plants can be broadly classified into halophytes and glycophytes. Halophytes are native to saline soils and are capable of completing their life cycle in that environment while glycophytes have a lower level of tolerance to saline soils. After a threshold level of environmental salt concentration is crossed, glycophytes show signs of stress that include leaf discoloration, loss of dry weight, osmotic stress, ion toxicity, etc. Halophytes have evolved several mechanisms of coping with salinity stress. Based on their mechanism of controlling internal Na^+ and Cl^- levels, these halophytes can be classified into salt-excluders, salt-includers and salt-accumulators (Breckle, 2002). Salt-excluders restrict the uptake of saline ions in the shoot by controlling the amount of saline ion transport from the root to the shoot (Lauchli, 1986). Salt exclusion is commonly seen in several crop plants. While some monocotyledonous plants, including turf grasses, tend to restrict saline ion accumulation in the shoots (Marcum and Murdoch, 1994), dicotyledonous plants suffer from saline ion buildup in the shoots. Salt glands aid some halophytic plants to store and eventually excrete excess salts from their leaves; and have been reported in several families of dicotyledons and monocotyledons (Amarasinghe and Watson, 1988; Amarasinghe and Watson, 1989; Marcum and Pessarakli, 2006). Several grasses belonging to the subfamily Chloridoideae have since

been examined for salt tolerance, salt gland structure and density, etc. and include the genera *Zoysia* (Marcum, 1990; Marcum and Kopec, 1997; Marcum et al., 1998; Marcum, 1999; Marcum et al., 2003), *Spartina* (Skelding and Winterbotham, 1939; Levering and Thomson, 1971; Rozema and Gude, 1981), *Cynodon* (Oross and Thomson, 1982a; Oross and Thomson, 1982b; Oross and Thomson, 1984; Marcum and Kopec, 1997; Marcum, 1999; Marcum and Pessarakli, 2006), *Aeluropus* (Barhoumi et al., 2007; Barhoumi et al., 2008), *Distichlis* (Oross and Thomson, 1982b; Marcum and Kopec, 1997; Marcum, 1999), *Bouteloua* (Marcum and Kopec, 1997; Marcum, 1999), *Buchloe* (Marcum and Kopec, 1997; Marcum, 1999), and *Sporobolus* (Marcum and Kopec, 1997; Marcum, 1999).

In a previous study of Zoysiagrasses (Marcum, 1990), *Z. matrella* was reported to be the more salt-tolerant species when compared with *Z. japonica* because it secreted more Na^+ from its leaves when challenged with 200 mM NaCl, as determined by tissue washing experiments. When the salt gland density was examined, density of glands in *Z. matrella* was three times higher than *Z. japonica*, suggesting a possible correlation between salt gland density and salt tolerance in these species (Marcum, 1990). However, cultivars within each species were not examined. There was also no comparison of salt gland density between control and salt-treated plants for either species, which is essential for determining whether salt gland density in either species increases in response to salt treatment.

Marcum et al. (1998) later initiated a study to determine the role of salt gland secretion efficiency in the salinity tolerance of several turfgrasses. Their studies

involving 57 Zoysiagrass accessions from five *Zoysia* species showed a positive correlation between salt gland Na^+ secretion rate and salt gland density, as well as between salinity tolerance and the two aforementioned parameters (Marcum et al., 1998). The five species were *Z. matrella*, *Z. japonica*, *Z. tenuifolia*, *Z. sinica*, and *Z. macrostachya*. Among these species, *Z. macrostachya* had the highest salt gland density, while the density was lowest in *Z. japonica* (Marcum et al., 1998). Salinity tolerance of plants involved in Marcum's study was assessed in terms of percent leaf firing relative to control plants. Leaf firing, a commonly used parameter for assessing relative salinity tolerance in turf grasses, involves chlorosis and ultimately necrosis of the leaves. Leaf firing is inversely related to salinity tolerance. The two cultivars of *Z. matrella* used for the study in this dissertation, 'Diamond' and 'Cavalier', were included in the study by Marcum et al. 'Diamond' was reported to be the most salt-tolerant cultivar and relative percent leaf firing was higher for 'Cavalier' as compared to 'Diamond' (Marcum et al., 1998). In this study, plants within the same species did not show an increase in salt gland density in response to NaCl treatment suggesting that it is a genetically stable trait (Marcum et al., 1998).

Although salt gland density might be a genetically stable trait in several *Zoysia* species, this is not true of some other grasses in the subfamily Chloridoideae such as *Odyssea paucinervis* and *Aeluropus littoralis*. *Odyssea paucinervis* is a perennial, salt-excreting grass found commonly in saline or alkaline soils along the coastal regions of South Africa (Clayton and Renvoize, 1986; Somaru et al., 2002). Salinity treatment of *O. paucinervis* led to an induction of salt gland density in the treated plants (Somaru et

al., 2002). Plants treated with 80% sea water (equivalent to 450 mM NaCl) had slightly more than double (4200 cm^{-2}) the number of adaxial salt glands found in plants of the same species treated with 0.2% sea water (2000 cm^{-2}) i.e. 1 mM NaCl (Somaru et al., 2002). In *A. littoralis*, another salt-excreting halophytic grass, salt gland density was increased following treatment with 400 mM NaCl (Barhoumi et al., 2007). In this species, the salt treated plants had two and a half-fold more salt glands (6880 cm^{-2}) than the control plants (3810 cm^{-2}) on the adaxial leaf surface (Barhoumi et al., 2007; Barhoumi et al., 2008). In *O. paucinervis* as well as in *A. littoralis*, salinity treatment significantly increased salt gland density on both leaf surfaces although for *O. paucinervis* the increase was greater on the adaxial side.

In the current study, salt gland density was measured in two cultivars of *Z. matrella*, 'Diamond' and 'Cavalier' before and after salt treatment. This was done to (1) determine if there is a correlation between salt gland density and salt tolerance in these two cultivars, and (2) to examine whether or not salt gland density is increased by salt treatment in *Z. matrella* cultivars. In addition to the comparison of two cultivars, salt gland density was also determined for a population of 'Diamond' x 'Cavalier' hybrids in order to observe how salt gland density segregates in this population. *Z. matrella* (2n=4x=40) is an interspecific hybrid, being intermediate between the definitive forms of *Z. matrella*, *Z. pacifica* Goudsw., and *Z. japonica* Steud. (Engelke et al., 2002a; Engelke et al., 2002b). 'Diamond' and 'Cavalier' are both self-infertile and are propagated vegetatively (Engelke et al., 2002a; Engelke et al., 2002b). 'Cavalier' is resistant to the fall armyworm (a serious pest of turfgrasses) while 'Diamond' is

moderately tolerant; however, ‘Diamond’ is a more salt-tolerant cultivar than ‘Cavalier’ (Engelke et al., 2002; Engelke et al., 2002).

A mapping population was developed at the Texas AgriLife Research Center at Dallas, TX by crossing ‘Diamond’ (as the male parent) with ‘Cavalier’ (female parent). Of the 250 progeny that were obtained from multiple crosses involving the above two cultivars, a subset of 94 were chosen for this study based on their previous selection for resistance to the fall army worm. ‘Diamond’ and ‘Cavalier’ are highly heterozygous; therefore, considerable segregation would be expected in the F1 hybrids for a variety of traits including salt gland density and salt tolerance. Preliminary studies confirmed that the hybrid population exhibited a range of tolerance to salinity (M. Binzel, personal communication). Thus, these 94 lines were chosen as the population for our heritability study. The aim of this part of the study was to determine heritability of salt glands in this population and based on knowledge from previous studies, it was hypothesized that salt gland density is a heritable trait, but that it is not affected by exposure to salt.

The total phenotypic variance (V_T) seen in a population is due to a combination of genetic (V_g) and environmental factors (V_e) i.e. $V_T = V_g + V_e$ (Griffiths et al., 2008). A character is said to be heritable only if there is genetic variation in that character (Griffiths et al., 2008). Heritability can be defined as the variance for a given trait within a population that can be attributed to the genotypes of the individuals within that population. Heritability can be of two types, broad-sense heritability (H^2) and narrow-sense heritability (h^2). An H^2 value indicates the proportion of the variation in a population that is due to genotypic variation in that population, and ranges from 0 to 1.0.

An H^2 value of 0 indicates that none of the phenotypic variation seen in the population is due to genetic differences, while an H^2 value of 1.0 suggests that the phenotypic variation seen in the population is entirely due to differences in genotype i.e. there is a strong correlation between the phenotype observed and its genotype (Snustad and Simmons, 2008). H^2 is calculated as:

$$H^2 = \frac{Vg}{V_T}$$

Where, V_T = Total phenotypic variance of the quantitative trait being examined (salt gland density in this study)

Vg = Genetic variance (i.e. variance due to genotypic differences)

H^2 thus calculated represents total genetic variation including variation due to additive effects of individual alleles, dominance relationships between alleles, as well as the epistatic interactions between alleles of different genes. For any given trait, H^2 values will vary for each population being examined, depending on the degree of genetic variability in the different populations as well as based on environmental influence.

Since all the 96 lines (94 hybrid lines and the two parents) within each of the two treatments, control and salt-treated, were grown under the same closely controlled environmental conditions, there is theoretically no environmental variance within each group. Hence the total variance (V_T) estimated for each of these two independent groups will be an estimate of the genetic variance (V_g) in that group (i.e. variance due to differences in genotype). If H^2 = approaching 1, it will indicate that the salt gland density is governed largely by the genotypic differences in these lines. On the other hand, if the

value of H^2 shows a trend of being much less than 1, it will indicate that salt gland density varies even within experimental replicates and that selection of lines based on this trait is less reliable under conditions of salt treatment. In addition to this, in order to determine if salt gland density is induced in these lines following salt treatment, the means of salt gland density of the two groups (control and salt-treated) will be compared.

The genetic basis for salt gland density has not yet been determined for *Zoysia* or other turf grasses. It is not clear whether the density of salt glands is a genetically stable trait or is influenced by environmental factors, although one previous study has reported that salt gland density in five different *Zoysia* species is not increased in response to salt (NaCl) treatment (Marcum et al., 1998). The results from this study will be a good representation of this species in terms of how salt gland density is inherited and influenced by salt treatment. The degree of heritability of salt glands will be determined by comparing the salt gland density in 'Diamond' and 'Cavalier', as well as in the segregating population of 'Diamond' x 'Cavalier'. The hypothesis of this part of the research is that salt gland density is a key determinant of salt tolerance in *Z. matrella*. If salt gland density is a heritable trait in *Z. matrella* then this trait can serve as an important tool for plant breeders while selecting for salt tolerant cultivars of *Z.matrella*. If the results of this study show that the density of salt glands in *Zoysia* is highly heritable with H^2 = approaching 1.0, then it suggests that salt gland density in this population is genetically stable (i.e. does not vary in response to environmental change) and may offer a good selection criterion for highly salt-tolerant genotypes. The number

of salt glands in a cultivar could be treated as a simple, inexpensive and reliable morphological marker for this population by turf breeders.

MATERIALS AND METHODS

Plant material and salinity treatment

The parental lines as well as each of the 94 hybrid lines were propagated in plastic Cone-tainers (Stuewe & Sons, Tangent, OR). Each set of 94 lines along with the two parental lines ('Diamond' and 'Cavalier') were placed in a 96 cell rack. The Cone-tainers were plugged with fiber-fil at the bottom to prevent the clay from falling out, while allowing good drainage, and then filled with fritted clay before placing the plant material in it. The starting material for each line consisted of a portion of a stolon or a rhizome containing 1-2 nodes removed from a stock plant and propagated in the fritted clay. These Cone-tainers were then placed in the misting chamber for 6-8 weeks (until rooting occurred). Once rooting had occurred, the Cone-tainers were watered with a weak Peter's solution and moved to a greenhouse. Plants were fertilized weekly with Peter's 20-20-20 and allowed to develop until they filled out the surface area of the Cone-tainer.

One set of 96 lines served as a control group that did not receive any salt treatment. Three sets (trays) of 96 lines were used as experimental replicates for the salt-treated group and placed in sub-irrigation tubs, as was the control group. The irrigation solutions were supplied to each of the trays via an aquarium pump. Salt treatment was initiated by supplying the plants with a 50 mM NaCl solution, and increasing it to 300

mM in increments of 50 mM per consecutive day. The plants were then watered once a week with a solution containing either 0 mM or 300 mM NaCl (and Peter's 20-20-20) for at least six weeks before examining the leaves. The irrigation solution used to treat the plants was replaced every two weeks.

Salt gland density

The density of salt glands per unit area of leaf was determined using clear nail enamel to obtain epidermal imprints (Fisher, 1985). The imprint of the adaxial leaf surface was observed under a Olympus BX-51 microscope (Olympus, Hamburg, Germany) at 10X magnification for determining the distribution of functional salt glands. Images were captured using a CCD camera, Cool Snap HQ^2 (Photometrics, Tucson, AZ) attached to the microscope. The second youngest leaves from 4-5 shoots were used for density measurements and thirty microscopic fields (each representing a constant area) were counted for each genotype using a digital image editing software (Photoshop CS3-version 10.0, Adobe, San Jose, CA). Salt gland density was calculated as the number of salt glands per unit leaf area (cm^{-2}).

Statistical analysis

Measurements involved three replicates for salt-treated plants. Out of the 94 hybrid lines included in this study, six lines did not survive the long-term salt treatment and were hence not included in the analysis. For the comparison of control versus the combined data from three replicates of salt treated plants, the data was transformed to obtain square root values for salt gland density. This was done so that the data would be

normally distributed. The transformed values were used to build a model from which variance components could be estimated reliably. Tukey's test was used for pairwise comparison between four different sets (trays) of plants (one control, and three experimental replicates for salt treatment). Since this analysis did not detect any significant difference between the three salt trays, the data from these were combined and used for the comparison of lines in the two environments (water and salt, where salt = salt rep. 1 + salt rep. 2 + salt rep. 3). The statistical model used for this comparison was $Y_{ijkl} = Env_i + Line_j + Line*Env_{i,j} + Leaf\ (Line*Env)_{k(ij)} + Area\ (Leaf, Line, Env)_{l(kji)}$; where i = 1, 2 (water or salt); j = 1, 2, 3, ……..88 (the different 'Diamond' x 'Cavalier' hybrid lines); k = 1, 2, 3, ……..n_{ij} (number of leaves sampled); l = 1, 2, 3…….....r_{ijk} (different areas of leaves sampled depending on the environment, line and leaf number).

Random effects ANOVA and SAS (version 9.2) were used for the estimation of heritability in the salt treated population of 'Diamond' x 'Cavalier' hybrids, where the effects of the following parameters were considered – the lines/genotypes (i), tray within each line (j), variation in leaf measurements in each tray*line combination, multiple leaf areas observed within the different combinations of leaf + line + tray. The salt gland density (Y) was calculated as $Y_{ijkl} = line_i + tray\ (line)_{j(i)} + leaf\ (tray, line)_{k(j,i)} + area\ (leaf, tray, line)_{l(k, j, i)}$; where i = 1, 2, 3, ……..88; j = 1, 2, 3; k = 1, 2, 3, ……..n_{ij}; l = 1, 2, 3…….....r_{ijk}.

RESULTS

Effect of salt treatment on *Z. matrella* cultivars

The density of salt glands on both leaf surfaces was determined for the two *Z. matrella* cultivars using epidermal imprints (Table 3.1). Salt glands on the leaves were more abundant on the adaxial side compared to the abaxial side for both cultivars. The number of salt glands found in 'Diamond' (5222 glands cm^{-2}) was higher than the number reported for most halophytes (Waisel, 1972). The adaxial salt gland density for 'Diamond' was significantly higher than 'Cavalier', and was induced by salt treatment (Table 3.1). However, salt treatment did not have a significant effect on the salt gland density of 'Cavalier'. Abaxial salt gland density was not significantly different between the two cultivars however salt-treated 'Diamond' had fewer abaxial salt glands.

Table 3.1 – Comparison of salt gland density in 'Diamond' and 'Cavalier' after 6 weeks of treatment with 0 mM and 300 mM NaCl.

Treatment	**Gland density (glands/cm^2) (Adaxial)[1]**		**Gland density (glands/cm^2) (Abaxial)[1]**	
	'Diamond'	**'Cavalier'**	**'Diamond'**	**'Cavalier'**
0 mM NaCl	5222^a	4173^c	2621^a	2465^a
300 mM NaCl	6261^b	4411^c	1510^b	2643^a
LSD $_{0.05}$	398		453	

[1]Means followed by the same letter for a given trait are not significantly different at $\alpha = 0.05$ according to Fisher's LSD.

Salt gland density segregation in the hybrids

Salt gland density was determined for 'Diamond' x 'Cavalier' hybrids, before and after salt treatment with 300 mM NaCl. The hybrids exhibited a wide range of salt gland density. The average density in the control lines ranged from 4382 to 11,752 salt glands per cm^2 (Figure 3.1, Table 3.2). Salt treatment with 300 mM NaCl did affect the salt gland density in some lines and the average of the three experimental replicates ranged from 5106 to 11, 915 salt glands per cm^2 (Figure 3.2, Table 3.2).

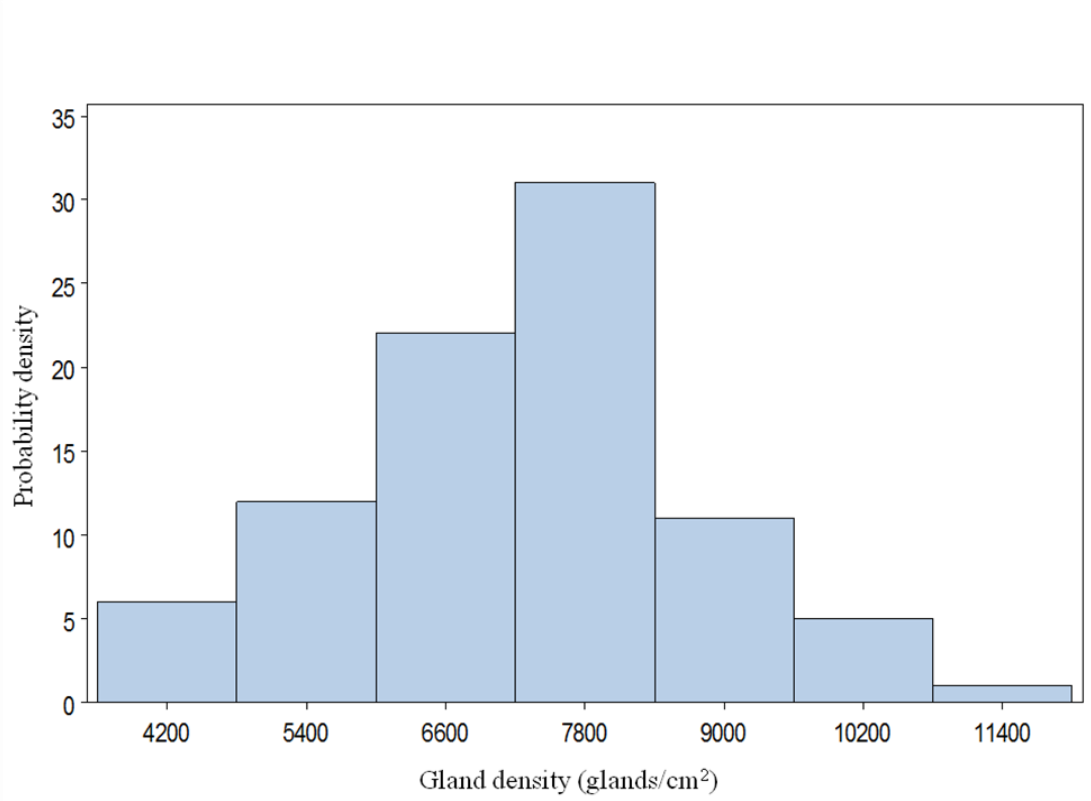

Figure 3.1 – Distribution of salt gland density in the 'Diamond' x 'Cavalier' hybrid lines treated with 0 mM NaCl.

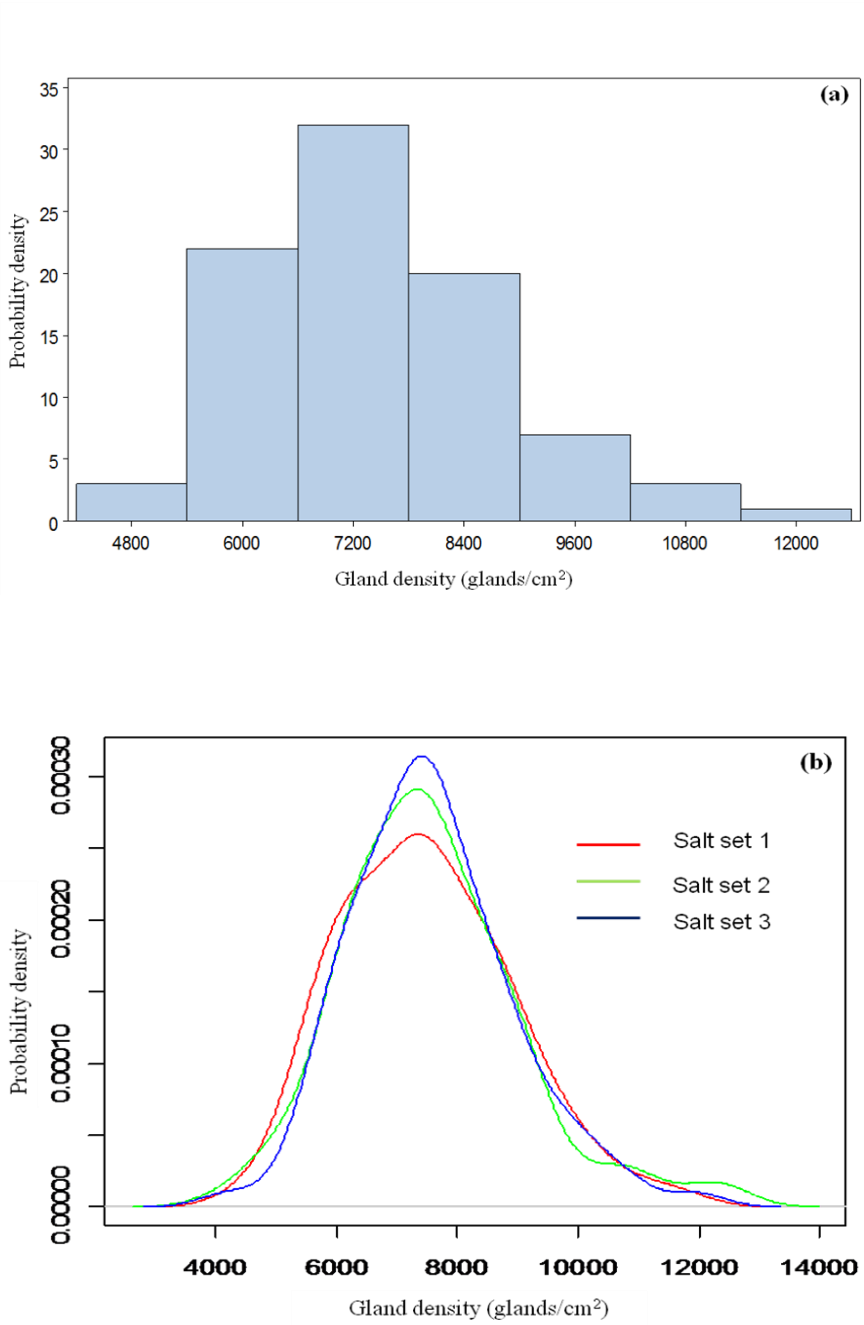

Figure 3.2 - Distribution of salt gland density in the 'Diamond' x 'Cavalier' hybrid lines treated with 300 mM NaCl.

Table 3.2 – Means of salt gland density for the 'Diamond' x 'Cavalier' hybrids treated with 0 mM NaCl (control) and 300 mM NaCl (salt).

Line	Control SG cm^{-2}	Salt Set 1 SG cm^{-2}	Salt Set 2 SG cm^{-2}	Salt Set 3 SG cm^{-2}
4680	8029	8817	7085	7080
4681*	5804	8633	8789	8952
4687	7151	7416	7482	7528
4689*	8600	9993	12349	10097
4690	8994	10015	9211	9607
4691	7560	7763	7736	7555
4692	7298	7555	7493	7708
4694	7447	7711	7857	7770
4696	6046	6179	6293	6534
4697	8163	8095	8547	8685
4698	7041	7627	7530	6953
4699	5550	5468	5583	5725
4701	7328	7564	7256	7235
4702	9909	10412	10740	9936
4704	8663	8935	8568	8490
4708	6891	6431	6946	7155
4709	6722	6917	6886	6897
4711	6526	7004	6873	7044
4712	7353	8544	7776	7991
4715	4382	5231	4892	5196
4719	7314	7804	7440	7565
4720	6657	6492	6623	6978
4721	7044	7324	7271	7188
4727	8029	8239	8170	8372
4729	8117	8159	8479	8136
4735*	4458	6315	6179	6873
4740	7899	7716	7943	7496
4741	6131	6319	6177	6273
4749	7114	7332	6933	7362
4750	5312	5978	6193	6567
4753*	4901	6897	6480	5975
4754	8071	7117	7594	7900
4757*	5149	6357	6901	6492
4764	8357	8329	8568	8467
4768	7536	8838	8394	8560
4779	10768	10571	10975	10645
4780	6287	6008	6304	6402
4784	5554	5774	6534	6179
4785	5300	5690	5029	6037
4789	8438	8502	8017	8686
4790	6006	6088	6222	6495
4796	6688	6344	6585	6411
4803	8410	8646	8831	8279
4804	4899	5323	5059	5666

Line	Control SG cm^{-2}	Salt Set 1 SG cm^{-2}	Salt Set 2 SG cm^{-2}	Salt Set 3 SG cm^{-2}
4830	4608	6723	6221	5350
4831	6959	7106	7044	6585
4833	8527	8596	8686	8734
4835	8061	7153	7351	7734
4836	8461	7854	8529	8648
4837	9375	9544	9221	9635
4845	6059	5828	6273	5799
4879	4975	5669	6508	6711
4881	7384	7056	7629	7363
4891	6077	5992	5737	5907
4892*	7691	5694	6231	6965
4893	6822	7044	6965	7315
4894	9288	8684	8926	8252
4895	8810	8956	8981	9002
4905	7151	6962	7263	6933
4938	7301	7787	7664	7738
4943	7896	8607	7380	8289
4944	8572	7429	7841	7640
4945*	6349	8654	8474	8289
4948	8529	7410	7008	7830
4949	5915	6116	5870	6064
4950	8122	8228	8044	8210
4951	7830	8249	8226	8082
4958	8266	9216	9462	9080
4960	7538	7504	7750	7491
4986	9168	9287	9322	9218
4991	7292	7449	7324	7561
4992	7586	7989	7708	7657
4995	7298	7563	7414	7591
4996	6481	6987	7590	7071
4999*	4533	6192	6023	6228
5001	11752	11700	12120	11925
5011	9932	10186	10031	9974
5012	6370	7198	6872	7054
5019	5524	6049	7427	7192
5023	6038	5945	6333	6155
5025	6672	6258	6405	6677
5026	6156	6330	6225	6350
5028	7266	8020	8137	7992
5030	10237	10996	10753	10679
5031	8772	9094	8940	9178
5033	7261	7647	7447	7334
5039	6509	6611	6333	6404

*Means are significantly higher in salt-treated plants based on p-values obtained after Bonferroni correction.

In order to determine if salt treatment had a significant effect on salt gland density in this population, the combined salt gland density from the three replicates of salt-treated hybrid lines was compared to the means from control plants of the same lines (refer to Methods for details). Data values obtained after square root transformation were normally distributed (Figure 3.3). Variances estimated for this comparison are shown in Table 3.3. The estimated means of salt gland density were significantly different between the two treatments (control versus salt), with the means of the salt-treated lines being higher than the control (Table 3.4).

The means of salt gland density obtained from the three replicates of salt-treated plants were compared to the plants grown under control conditions using Tukey's test. Pair-wise comparisons were performed using Tukey's test to determine if significant differences existed between the control and the salt-treated groups. In this test, the statistical measure of significant difference is the *P*-value; if the *P*-value is greater than 0.05 for a given pair of treatments, then the mean salt gland density between the two treatments is not significantly different. On the other hand, if *P*-value is less than 0.05, then the mean salt gland density between the two treatments is significantly different. In light of this, the results of this analysis showed that the mean salt gland density of each of the salt-treated groups was significantly different than the control group (Table 3.5). However, the difference between the mean salt gland densities seen across the three replications for salt-treated plants was not significantly different (Table 3.6).

Table 3.3 – Estimates of variance components for salt gland density for the population of 'Diamond' x 'Cavalier' hybrids in response to the two treatments - 0 mM NaCl and 300 mM NaCl.

Parameter	Estimate	Std. Error	Z value	Pr > Z
Variance between lines	57.9448	9.4606	6.12	< 0.0001*
[1]Environment*Line	5.9281	1.5815	3.75	< 0.0001*
Leaf (Env*Line)	14.3151	1.1527	12.42	< 0.0001*
Residual	29.2717	0.4183	69.97	< 0.0001*

[1]Data represents a comparison of the control set with means of the three salt sets.
*Values that are significant at $\alpha = 0.05$

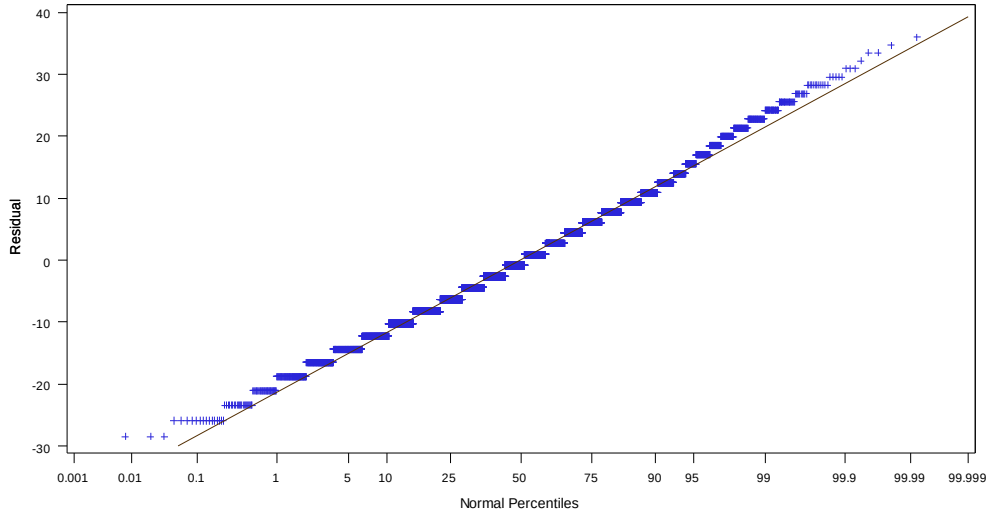

Figure 3.3 – Normal probability plot of residuals for square root transformed salt gland density.

Table 3.4 – Comparison of estimated means of salt gland densities for the population of 'Diamond' x 'Cavalier' hybrids in response to 0 mM NaCl and 300 mM NaCl.

Environment	Estimated means[1]	Std. Error	DF	t value	Pr > |t|
300 mM NaCl	**87**	0.8671	87	100.00	< 0.0001
0 mM NaCl	**85**	0.8695	87	97.33	< 0.0001

Parameter	Treatment DF	Line DF	F value	Pr > F
Environment	1	87	18.54	< 0.0001*

[1]Data represents means of square-root transformed data values for salt gland densities from both treatments.
*Salt gland density means are significantly different at $\alpha = 0.05$.

Table 3.5 – Tukey's pairwise comparison for mean salt gland density between the control (0 mM NaCl) and each of the replicates for the 'Diamond' x 'Cavalier' hybrids treated with 300 mM NaCl.

Treatment	Treatment	Std. Error	DF	p value
Control	Salt 1	0.4244	258	0.0001*
Control	Salt 2	0.4462	258	<0.0001*
Control	Salt 3	0.4247	258	<0.0001*

*Salt gland density means are significantly different at $\alpha = 0.05$.

Table 3.6 - Tukey's pairwise comparison for mean salt gland density between the three experimental replicates for 'Diamond' x 'Cavalier' hybrids treated with 300 mM NaCl.

Treatment	Treatment	Std. Error	DF	p value[1]
Salt 1	Salt 2	0.4478	258	0.7732[a]
Salt 1	Salt 3	0.4266	258	0.5988 [a]
Salt 2	Salt 3	0.4471	258	0.9958 [a]

[1]Means followed by the same letter are not significantly different at $\alpha = 0.05$

Heritability (H^2) of salt glands was calculated using the density data from three replicates of salt-treated 'Diamond' x 'Cavalier' hybrids. The H^2 value was calculated as the ratio of variance between the different lines due to differences in genotype (V_g) and the total phenotypic variance ($V_T = V_g + V_e$; where V_e was the variation between the three experimental replicates for each line). With reference to the values listed in Table 3.7, $H^2 = 56.7150 / (56.7150 + 2.1543)$. H^2 value thus estimated was 0.9634, which indicates that variance due to experimental replication across the three groups of salt-treated plants was very low i.e. the density of salt glands was a fairly stable trait in salt-treated 'Diamond' x 'Cavalier' hybrids, and was not significantly affected by the environmental conditions (Table 3.7).

Table 3.7 - Estimates of variance components for salt gland density across the three replicates for 300 mM NaCl-treated 'Diamond' x 'Cavalier' hybrids.

Parameter	Estimate	Std. Error	Z value	Pr > Z
Variance between lines = V_g	56.7150	8.8172	6.43	< 0.0001*
Variance within each line; Tray (Line) = V_e	2.1543	0.4378	4.92	< 0.0001*
Leaf (Tray*Line)	3.4346	0.3550	9.68	< 0.0001*
Residual	22.9600	0.3883	59.13	< 0.0001*

*Sources of variation that had a significant effect on the measurements of salt gland density.

Total variance (V_T) was calculated as $V_T = V_g + V_e$. Thus, $V_T = 56.7150 + 2.1543 = 58.8693$.

DISCUSSION

Several factors could account for salt tolerance in plants and these factors may vary with species. Factors responsible for salt tolerance may include density of salt glands and salt secretion efficiency of salt glands in addition to several other factors. This chapter focuses on the relationship between salt gland density and the salt tolerance for two *Z. matrella* cultivars, 'Diamond' and 'Cavalier'; as well as the heritability of salt gland density in the population of 'Diamond' x 'Cavalier' hybrids.

According to Waisel (1972), the salt gland density in halophytes ranges between 650 x 10^4 and 4800 x 10^4 glands m^{-2} of leaf area (i.e. 650-4800 glands cm^{-2}). In two separate studies done by Marcum et al. (Marcum and Murdoch, 1990; Marcum et al., 1998), salt gland density in salt-treated *Z. matrella* was found to be in the range of 76-99 glands mm^{-2} (i.e. 7600-9900 cm^{-2}), which is higher than what is seen in other halophytes. There is no information regarding which cultivar of *Z. matrella* was used for this study. 'Diamond' used in the current study had an adaxial salt gland density of 5222 cm^{-2}, which was significantly higher than the density for 'Cavalier', 4173 cm^{-2} (Table 3.1). Interestingly, salt treatment led to an increase (20%) in adaxial salt gland density only in 'Diamond', suggesting that the difference in salt gland density between these two cultivars could be one of the factors responsible for the difference in salt tolerance between them. Also, the increase in salt gland density of 'Diamond' following salt

treatment could be a mechanism by which 'Diamond' can exhibit a higher level of salt tolerance than 'Cavalier'. Although such a response has not been reported previously for any other Zoysiagrasses including *Z. matrella*, it has certainly been observed for some other Chloridoid grasses like *O. paucinervis* and *A. littoralis* where the increase in gland density after salt treatment was around two-fold (Somaru et al., 2002; Barhoumi et al., 2007). Such an increase in salt gland density in these halophytes can be attributed to the nature of the saline environment these species are exposed to in their natural habitat; *O. paucinervis* and *A. littoralis* are both halophytic in nature (Somaru et al., 2002; Barhoumi et al., 2007), while *Z. matrella* is not. Our results in conjunction with previous studies suggest that salt gland density for any given species can vary with the cultivar being studied and that the response of this trait to salt treatment cannot be generalized for all genotypes within a given species.

For both 'Diamond' and 'Cavalier', only the adaxial salt glands were functional in salt secretion (discussed in Chapter II), unlike *Cynodon dactylon* (Bermuda grass) and *Sporobolus virginicus* where salt secretion via salt glands occurs on both leaf surfaces (Marcum and Murdoch, 1990; Marcum and Pessarakli, 2006). In previous studies involving salt tolerance, there were comparisons of *Z. japonica* with *C. dactylon* and *S. virginicus*, although there have been no reports so far of a comparison of *Z. matrella* with either of the above mentioned species (Marcum, 1999; Marcum and Pessarakli, 2006). *Zoysia japonica*, like *Z. matrella*, has salt glands on both leaf surfaces but can secrete salt only from the glands on the adaxial side (Marcum and Murdoch, 1990). In a study involving comparison of seven Chloridoid grasses, the relative salinity tolerance as

well as leaf salt gland Cl^- and Na^+ secretion rates of *Z. japonica* were reported to be similar to *C. dactylon*; while the same two parameters for *S. virginicus* were higher than both *Z. japonica* and *C. dactylon* (Marcum, 1999; Marcum and Pessarakli, 2006). At the same time, it has been reported that *Z. matrella* is a more tolerant zoysiagrass than *Z. japonica* as determined by relative percent leaf firing (Marcum et al., 1998). Also, *Z. matrella* has a significantly greater number of salt glands (three times more) than *Z. japonica* (Marcum and Murdoch, 1990). These observations suggest that salt tolerance for a given plant species is not solely governed by salt gland density, but is also affected by some other factors including the salt secretion efficiency of the salt glands.

Heritability (H^2) estimates in our study were made using the salt-treated population of 'Diamond' x 'Cavalier' hybrids. Based on the results obtained from the examination of salt-treated hybrids in three replicates, H^2 was computed to be very high (0.9634). Such a high value of H^2 suggested that there was minimal environmental variation between the clones for each line separated by the three salt trays, and that any variation seen in this experiment was largely due to the genetic variation between the different lines. Hence, the salt gland density in the salt-treated plants can be considered to be a highly stable trait for the entire population of 'Diamond' x 'Cavalier' hybrids under the conditions employed in this study.

As previously reported (Marcum et al., 1998), salt gland density is a highly heritable trait in Zoysiagrasses. These studies involved the grasses *Z. japonica*, *Z. matrella*, *Z. tenuifolia*, *Z. macrostachya*, and *Z. sinica,* where none of these species showed an increase in salt gland density in response to salt (NaCl) treatment (Marcum et

al., 1998). However, the plants were treated with 400 mM NaCl for a relatively short time period of one week compared to the eight weeks salt treatment (300 mM NaCl) adopted in our current study. It is extremely important to screen for salt gland density after long term treatment because this provides the plants with more time for new leaves to form in the treated plants. It would be expected that increased salt gland density could only be observed in leaves that developed after exposure to salt, since new salt glands cannot form in mature leaves where cell differentiation is complete. In our study, in addition to screening for salt glands after long term salt treatment, the tips of existing leaves were also clipped at the beginning of the experiment, to distinguish them from the newly formed leaves which were chosen for the estimation of salt gland density at the end of the experiment. As is evident from the previous and current studies, the duration of salt treatment can have a meaningful effect on the salt gland density.

In our studies, in addition to the increase in salt gland density seen for 'Diamond', a similar induction response was also seen for some individuals in the population of 'Diamond' x 'Cavalier' hybrids (Tables 3.2, 3.4 & 3.5). A comparison of the means of salt gland densities under control and salt-treated conditions showed that salt gland density was increased in response to salt treatment and that this increase was significantly different (Table 3.2 & 3.4). These results provide breeders the information that if salt gland density is to be used as a morphological marker, then the selection for these lines should be done after salt-treatment; although caution should be exercised while deciding the duration of salt treatment. Identification of individual lines that responded to salt treatment with a statistically significant increase in salt gland density

would serve as good candidates for identifying specific genes expressed in response to salt treatment that could be responsible for salt gland induction in *Z. matrella*.

Apart from salt gland density, some other factors that can influence salt tolerance of a plant include ion transporters that are involved in Na^+ and Cl^- uptake in plants, as well as those that help avoid excess accumulation of Na^+ in the cytoplasm. The role of some of these ion transporters is discussed in Chapter IV.

CHAPTER IV

LOCALIZATION OF ION TRANSPORTERS IN *Zoysia matrella* LEAVES

INTRODUCTION

Salt glands contribute towards controlling the internal plant salt concentration by regulating salt excretion. While some ions are transported to the salt glands, some ions may be compartmentalized in the leaf or translocated back to the roots via the activity of ion transporters which function in ion uptake, ion redistribution and ion sequestration. Membrane transporters involved in the movement of ions in plants are classified as pumps, ion channels or carriers depending on the mechanism of transport. Pumps are active transport proteins that facilitate the movement of substrates against their electrochemical gradient, thus generating a gradient for secondary transport. The transport rate of pumps is a few hundred ions per second. Ion channels are passive transporters that move substrates down their electrochemical gradient. The transport capacity of ion channels is much larger than that of pumps i.e. several million ions per second. Carriers may function as active or passive transporters.

Ions present in saline soils include the cations Na^+, Mg^{2+}, Ca^{2+}, and the anions Cl^-, SO_4^{2-}, and CO_3^{2-}. Of these ions, Na^+ and Cl^- are the most abundant ones in saline soils. Although there are several transporters associated with the uptake of Na^+ and Cl^- in plants, most of the research done so far has focused mainly on Na^+ transporters because most plants do not require Na^+ as an essential nutrient, and excess Na^+ can cause toxic effects in plants. Plants resort to diverse mechanisms to avoid Na^+ toxicity at the cellular

level. These include restricted Na^+ uptake at the root; Na^+ exclusion to limit the amount of Na^+ transported from the roots to the shoots; and Na^+ compartmentation in the vacuole via the activity of Na^+/H^+ antiporters (Zhang and Blumwald, 2001; Zhu, 2003; Shabala and Cuin, 2008). Na^+/H^+ antiporters exchange Na^+ for H^+ using a proton gradient established by H^+ pumps localized in the plasma membrane and in the tonoplast.

There are several genes that encode proteins that participate in Na^+ transport. These include the *HKT* (high affinity K^+ transporter) gene family, *SOS1* (salt overly sensitive), and *NHX* (Na^+/H^+ antiporter) gene family (Mahajan et al., 2008). The role of each of these transporters is discussed below.

HKT (for High-affinity K^+ Transporter)

As the roots absorb water from the soil, the plasma membrane poses a selective barrier for the ions present in the vicinity. Ion transporters localized in the plasma membrane of the root epidermal cells play a key role in uptake of ions from the soil (Apse and Blumwald, 2007). HKT proteins include a family of plasma membrane-localized cation transporters (Schachtman and Liu, 1999). In plants, *HKT* was first isolated and characterized in wheat, *Triticum aestivum* and shown to exist as a single copy gene in both wheat, as *HKT1*, and in *A. thaliana*, as *AtHKT1* (Schachtman and Schroeder, 1994). *HKT1*, which was isolated from wheat roots derived from plants grown on a K^+-free medium, consists of an open reading frame of 1602 bp, which encodes a predicted protein of 534 amino acids (Schachtman and Schroeder, 1994). Heterologous studies done with HKT1-expressing *Xenopus* oocytes showed that this transporter was more selective for K^+ than Na^+, and mRNA expression analysis by *in*

situ hybridization showed *HKT1* localized in the root cortical cells as well as in the cells adjacent to the vascular tissue (Schachtman and Schroeder, 1994). A subsequent study showed that this transporter functions in high-affinity Na^+- K^+ co-transport and low-affinity Na^+ uptake in yeast or *Xenopus* oocytes depending upon the extracellular Na^+ and K^+ concentrations (Rubio et al., 1995). HKT1 however lost its ability to transport K^+, thus mediating low affinity Na^+ uptake, when the external environment had significantly higher Na^+ than K^+, as a consequence of Na^+ competing with K^+ binding sites on the transporter (Rubio et al., 1995; Gassmann et al., 1996).

HKT transporters have been divided into two distinct groups based on the specificity of their transport. Some members of this family that mediate Na^+ specific transport are classified under subfamily 1, while others that mediate Na^+-K^+ co-transport belong to subfamily 2 (Platten et al., 2006). Members of Subfamily 1 have a serine (Ser) residue in the first P-loop of the protein, while those in Subfamily 2 have a glycine (Gly) in this position. From studies done in *A. thaliana* and wheat, it has been demonstrated that the conserved Glycine residue in the first pore (P) loop of the HKT protein is responsible for K^+ uptake and selectivity (Mäser et al. 2002). AtHKT1;1 (previously AtHKT1) and OsHKT2;1 (previously OsHKT1) have a Ser at this position, while TaHKT2;1 (previously HKT1) and OsHKT2;2 (previously OsHKT2) have Gly. This single amino acid substitution from Gly to Ser was predicted to affect the transport properties of HKT transporters from being able to transport both Na^+ and K^+ (if Gly), to functioning as a Na^+-specific transporter (if Ser). This was confirmed by K^+ uptake studies done with mutated AtHKT1;1 (bearing a substitution of Ser to Gly) in *Xenopus*

oocytes where this mutation conferred K^+ uptake capacity to a normally Na^+-selective AtHKT1;1 (Mäser et al., 2002). Based on the identity of this amino acid residue (Ser or Gly), members of the plant HKT proteins from *A. thaliana* (AtHKT1;1), ice plant (McHKT1;1 and McHKT1;2), and rice (OsHKT1;1, OsHKT1;2 and OsHKT1;3) are some of the members classified under Subfamily 1; while Subfamily 2 includes *Phragmites australis* (PaHKT2;1), wheat (TaHKT2;1), rice (OsHKT2;1, OsHKT2;2, OsHKT2;3, and OsHKT2;4), and HvHKT2;1 from barley (Platten et al., 2006).

Only one isoform of *HKT* has been found in *A. thaliana* (Uozumi et al., 2000), while rice has nine *HKT* genes of which seven encode functional transporters and two are pseudogenes (Horie et al., 2001; Garciadeblás et al., 2003). HKT has been reported to function as a low affinity Na^+ transporter at the plasma membrane in these two species. AtHKT1;1, a Na^+-specific transporter, has been reported to be localized at the plasma membrane of xylem parenchyma cells in *A. thaliana* leaves (Sunarpi et al., 2005). Studies involving immunolocalization of AtHKT1;1 and examination of *athkt1* loss-of-function mutants, have proposed a role for AtHKT1;1 in unloading of excess leaf Na^+ from the xylem vessels into the xylem parenchyma and phloem, in order to reduce the Na^+ content of the shoots (Sunarpi et al., 2005). A parallel study with *SKC1* (*OsHKT8/OsHKT1;5*) in rice demonstrated that SKC1, which is localized in the xylem parenchyma cells of roots and leaves, transports Na^+ more actively resulting in more recirculation of Na^+ from the shoots to the roots in the salt-tolerant variety of rice (Ren et al., 2005). This difference in activity has been attributed to four amino acid changes arising from six nucleotide substitutions in the *SKC1* allele from the salt-sensitive rice

variety (Ren et al., 2005). These studies from *A. thaliana* and rice suggest a role for some *HKT* isoforms in the recirculation of Na^+ from the leaf to the roots as a means for achieving a certain level of salt tolerance.

Several studies involving RNA *in situ* localization of *HKT* transporters have been performed, but most of these studies have focused on rice (*OsHKT*s). In a study involving *in situ* localization of *OsHKT2;1* in two cultivars of Indica rice differing in salt tolerance, it was found that although the expression of *OsHKT2;1* in both the cultivars was similar, *OsHKT2;1* signal in the leaf phloem was stronger in the salt-sensitive cultivar (IR29) after 24 h of NaCl treatment (Golldack et al., 2002). In a subsequent study involving *OsHKT2;1*, Kader et al. (2006) reported that *OsHKT2;1* signals were stronger in the mesophyll of the salt-sensitive cultivar (BRRI Dhan 29). A more recent study involving Japonica rice showed *OsHKT2;1* transcripts localized in the xylem, phloem, and bulliform cells of leaves from salt-treated plants (Jabnoune et al., 2009). Although the presence of *HKT* transcripts in different cell types is not indicative of transporter activity, these observations in rice clearly indicate that the expression of a given *HKT* transporter can vary with cultivars within a species depending on its role in that species.

In the case of *Phragmites australis* (reed plants), an evolutionarily close relative of *Z. matrella* (Bouchenak-Khelladi et al., 2008), two to three copies of the *HKT* gene were predicted for the salt-tolerant cultivar based on Southern blot analysis while the salt-sensitive cultivar had one to two copies of the same, all of which function as a Na^+-K^+ co-transporter (Takahashi et al., 2007). The *PhaHKT1* sequence in the two cultivars

differed in the salt-sensitive cultivar's retention of two introns, resulting in a truncated PhaHKT1 protein. A similar observation has been made for *OsHKT2;1* in rice (Golldack et al., 2002), although the significance of alternative splicing of HKT genes in salt-tolerant plants has not yet been established.

Physiological studies with *P. australis*, have shown that this species avoids the toxic effects of Na^+ in the leaves by recirculation of the absorbed Na^+ back to the roots via the phloem (Matoh et al., 1988; Matsushita and Matoh, 1991). A comparative study of reed plants and rice plants confirmed that following salt (50 mM NaCl) treatment, the amount of Na^+ accumulated in the shoots of reed plants was ~3-4 times less than the rice plants, as a consequence of Na^+ recirculation to the roots contributing towards the salt tolerance of the reed plants. In this study it was reported that the salt-tolerant cultivar preferentially accumulated more Na^+ in the roots, while high levels of Na^+ were found in the shoots of the salt-sensitive cultivar. *Spartina alterniflora*, a Chloridoid grass like *Z. matrella*, is more salt-tolerant than reed plants, but the mechanism by which *S. alterniflora* achieves salt tolerance relies on Na^+ accumulation in the leaves followed by excretion of more than half of this Na^+ via salt glands (Vasquez et al., 2006).

To date, *HKT* homologs have not been cloned from or characterized in a species bearing salt glands, which is important because the presence of functional salt glands provides plants with an efficient way of eliminating excess Na^+ from the leaves. However, a *HKT1* homolog *McHKT1;1* has been cloned from *Mesembryanthemum crystallinum* (ice plant) and immunolocalization studies with polyclonal antibodies generated against an McHKT1 peptide showed that this protein was detected in the

epidermal bladder cells (modified trichomes) of salt-treated plants where Na^+ is sequestered (Su et al., 2003). In our study, cloning of an *HKT* homolog from *Z. matrella*, followed by RNA *in situ* localization studies will help determine if *Z. matrella* has *HKT* isoforms that could play a role in the transport of excess leaf Na^+ towards and into the salt glands.

Apart from *HKT* genes, the other Na^+ transporters that have been studied in detail include *SOS1* and *NHX*. *SOS1* functions as a plasma membrane Na^+/H^+ antiporter; while *NHX* is involved in Na^+/H^+ exchange at the tonoplast (Tuteja et al., 2007). Both, *SOS1* and *NHX* alleviate cytosolic Na^+ toxicity by pumping Na^+ into the apoplast or the vacuole, respectively.

SOS1 (Salt Overly Sensitive 1)

SOS1 was first identified in a screen for NaCl-hypersensitive mutants in *A. thaliana* and studies with *sos1* seedlings showed that *SOS1* plays an important role in the salt tolerance of the plant (Wu et al., 1996). Functional complementation of yeast mutants lacking Na^+ transporters with SOS1 established its function in lowering the cytosolic levels of Na^+ by functioning as a Na^+ efflux transporter (Shi et al., 2002). Based on sequence homology, subcellular localization of the SOS1-GFP fusion protein, and the phenotype of *sos1* knockout mutant cells, it was confirmed that SOS1 was a plasma membrane Na^+/H^+ antiporter (Shi et al., 2002). Comparison of the xylem sap of wild type and *sos1* mutant plants treated with 100 mM NaCl showed Na^+ accumulation in the mutants, thus suggesting a role for *SOS1* in excess Na^+ retrieval from the xylem to

avoid its toxic effects in the shoot. Studies with *SOS1* have since been done in many plant species comparing the role of *SOS1* in cultivars differing in salt tolerance.

A study of protoplasts from two Indica rice cultivars, employing plasma membrane and tonoplast H^+-ATPase inhibitors, showed that the salt tolerant cultivar relied on Na^+ sequestration into the vacuole, while the salt sensitive cultivar sequestered more Na^+ into the apoplast than the vacuole, for reducing cytosolic Na^+ levels (Kader and Lindberg, 2005). Also, the protoplasts isolated from leaves of the salt-tolerant rice cultivar had less cytosolic Na^+ than the roots from the same plants, as well as the leaves and roots of the salt-sensitive cultivar, in response to treatment with 100 mM NaCl. In a subsequent study with Na^+/H^+ antiporters from two cultivars of reed plants differing in salt tolerance, yeast cells expressing *PhaNHA1* from the salt tolerant cultivar grew better on media supplemented with NaCl and had a lower cellular Na^+ content than the ones expressing *PhaNHA1* from the salt-sensitive cultivar (Takahashi et al., 2009). Shoot Na^+ in the salt-tolerant cultivar was less compared to its roots, while the shoot Na^+ was two-fold higher in the salt-sensitive cultivar. For reed plants, *PhaNHA1* transcript levels were similar in both cultivars at the end of the salt treatment, although the levels were higher in the salt-tolerant cultivar at the intermediate time points. Both of these studies (rice and reed plants) suggest that greater salt tolerance was achieved by regulating the shoot cytosolic Na^+ content.

Although there have been no studies to date involving RNA *in situ* localization of *SOS1* in plants, the expression of GUS driven by the *AtSOS1* promoter was visualized in the parenchyma cells bordering the vascular tissue of the root, stem, and leaves; as well

as at the root tip (Shi et al., 2002). A recent study adopted SEM-EDX analysis for measurement of Na^+ in *Thellungiella salsuginea* leaf cells and found Na^+ accumulation in the mesophyll and palisade cells of *T. salsuginea ThSOS1*-RNAi lines (Oh et al., 2009). This suggests the role of *SOS1* in excluding Na^+ from the photosynthetic cells of the wild type plants.

Two transporters with Na^+/ H^+ antiporter activity have been studied in detail in plants, *SOS1* and *NHX1*. SOS1 as discussed above functions at the plasma membrane, while NHX1 is localized in the tonoplast (discussed in the next section), both of which assist with efflux of Na^+, to reduce the toxic effect of excess Na^+ in the cytosol.

***NHX* (Na^+/H^+ antiporter)**

The first plant NHX was cloned from *A. thaliana*, functionally characterized in yeast (Gaxiola et al., 1999), and shown to localize in the vacuolar membrane (Gaxiola et al., 1999; Yokoi et al., 2002). *NHX* transporters have since been cloned from several other plant species including rice (Fukuda et al., 1999), *T. aestivum* (Brini et al., 2005), *Zea mays* L. (Zorb et al., 2005), *Aeluropus littoralis* (Zhang et al., 2008), *Chenopodium glaucum* (Li et al., 2008) and *Zoysia japonica* (Du et al., 2010). An induction in *AtNHX1* and *OsNHX1* mRNA levels was seen in response to short-term NaCl treatments (Fukuda et al., 1999; Gaxiola et al., 1999). Studies involving reconstitution of AtNHX1 protein in liposomes have shown that AtNHX1 is capable of transporting Na^+ and K^+ with equal affinity (Venema et al., 2002). Later, five more NHX genes were identified from *A. thaliana* (Yokoi et al., 2002). It was shown that *AtNHX3* was a root-specific Na^+/H^+ antiporter, while the rest of the members were expressed in roots as well as shoots of *A.*

thaliana. Similarly, out of the six *ZmNHX* isoforms present in maize, three were root-specific while the remaining were shoot-specific (Zorb et al., 2005). For the six *NHX* isoforms studied in *A. thaliana* and rice, it was reported that each of the isoforms was expressed in a tissue and NaCl-specific pattern (Yokoi et al., 2002).

AtNHX1 promoter-GUS analysis suggested that *AtNHX1* is expressed in all tissues of *A. thaliana* seedlings except the root tip, with an increased GUS activity in the leaf mesophyll cells following salt treatment (Shi and Zhu, 2002). RNA *in situ* localization studies showed strong hybridization signals around the leaf vascular tissue, and weaker signals in the epidermal cells and leaf parenchyma (Apse et al., 2003). Apart from leaves, *AtNHX1* transcripts were also detected in siliques, flowers (petals, anthers), and in the phloem of stems. Attempts to localize *OsNHX1* using the RNA *in situ* technique were unsuccessful, probably due to the low level of these transcripts in rice. However, promoter-GUS expression in the shoots was detected in the vascular bundles and trichomes for *OsNHX1*, and in the vascular bundles and pollen grains for *OsNHX5* suggesting different roles for these two *NHX* isoforms in rice (Fukuda et al., 2011). Recently, *NHX* homologs were cloned from two grass species belonging to sub-family Chloridoideae – *Z. japonica* (Du et al., 2010) and *A. littoralis* (Zhang et al., 2008). Since the *Zoysia* genome has not yet been sequenced, the *NHX* sequences of these above mentioned grasses served as a reference to design primers for cloning a *NHX* homolog from *Z. matrella*.

Studies involving salinity stress have focused on the proteins – HKT, SOS, and NHX, as they are involved in the cross membrane transport of Na^+ at the whole plant

level. However, no studies to date have been done regarding the role of these transporters in a plant species with salt glands. Also, although these transporters have been cloned from several plant species including *A. thaliana*, wheat, rice, etc., no sequence information is available for *Z. matrella*. This part of the project was initiated with an objective of studying the localization of the transcripts of three Na^+ transporters - *HKT, SOS* and *NHX* from *Z. matrella*. In order to achieve this goal, *Z. matrella* sequence for each of the transporters was obtained by partial cloning of cDNA. Following cloning of these transporters, RNA *in situ* expression studies were performed to localize these transporters in *Z. matrella* leaves.

METHODS

Plant material and salinity treatment

'Diamond' and 'Cavalier' lines were obtained from the Texas AgriLife Research Center at Dallas, Texas. Salt treatment was applied by irrigating the plants with a 50 mM NaCl solution, and increasing it to 300 mM in increments of 50 mM per consecutive day to avoid the plants experiencing an osmotic shock. The plants were then watered once a week with 0 mM (control) or 300 mM NaCl (containing Peter's 20-20-20 fertilizer) for at least four weeks before harvesting the leaves for total RNA isolation.

Isolation and cloning of transporters from *Z. matrella*

***ZmatHKT* –** Total RNA was isolated from salt-treated 'Diamond' leaves using Trizol reagent (Invitrogen, Carlsbad, CA). RT-PCR primers were designed based on the sequence of *PhaHKT1*. Using the primer pair 5'-

TCGTGTTTGTCTACCGATTCGTTGCA-3' and 5'-ATAGCACTAGAACGGCAGGGGAGA-3', and Blue-Print One-Step RT-PCR kit (Takara Bio Inc., Madison, WI), a partial cDNA clone of *ZmatHKT1* was amplified from salt-treated 'Diamond' leaves. Amplified cDNA fragments were sub-cloned into a pGEM T-Easy vector (Promega, Madison, WI) and amplified using Big Dye (Gene Technologies Lab, Texas A&M University, College Station, TX) and the primers (above) that were used to amplify *ZmatHKT1*. The PCR products were then sequenced at the IPGB sequencing facility (Texas A&M University, College Station, TX).

ZmatSOS - Total RNA was isolated from salt-treated 'Diamond' leaves using Trizol reagent. First-strand cDNA was synthesized using Oligo (dT) and MMLV RT (Clontech Laboratories, Inc., Mountain View, CA) by incubating the reaction for 10 min at 25 °C, 30 min at 40 °C, and 5 min at 85 °C. The cDNA's were amplified by RT-PCR using degenerate primers corresponding to the coding sequences of rice (AY785147) and wheat (EU552490) plasma membrane Na^+/H^+ antiporters. The primer pair used to amplify the *Z. matrella SOS1* homolog were ZmSOS-F1, 5'–TGCTTACTGGGGAATGCTTG-3' and ZmSOS-R1, 5'-AGAAAATCATGTAGYTGTCKCC-3'. The amplified cDNA fragments were sub-cloned into a pGEM T-Easy vector and sequenced as described for *HKT1*.

ZmatNHX - Total RNA was isolated from 'Diamond' leaves treated with 300 mM NaCl for six weeks using Trizol. First-strand cDNA was synthesized using Oligo (dT) and MMLV RT by incubating for 10 min at 25 °C, 30 min at 40 °C, and 5 min at 85 °C. The cDNA's were amplified using heterologous primers 5'-

TGCTTTTGCAACTTTGTCCTT-3' and 5'-GTTGTCTCCAGGTTATTTTTTCAG-3', that were designed based on the conserved regions of *NHX* from other grasses. The PCR products were sub-cloned into pGEM T-Easy vector, sequenced as described for *HKT1*, and used for designing *Z. matrella*-specific primers for 5' and 3' RACE.

Random amplification of cDNA ends (RACE) for cloning full-length *ZmatNHX* cDNA

Poly $(A)^+$ RNA was purified from total RNA obtained above using the Nucleotrap mRNA mini kit (Clontech Laboratories, Inc., Mountain View, CA). 5' and 3' RACE-Ready cDNA was synthesized using Smart II Oligo A primer and MMLV-RT following user instructions listed in the SMART RACE kit (Clontech Laboratories, Inc., Mountain View, CA). These cDNA's were used as the template for all subsequent RACE PCR reactions.

Using the partial cDNA obtained by RT-PCR, *Z. matrella* specific primers were designed for 5' and 3' RACE. The full-length *NHX* cDNA was amplified from both cultivars using the primers 5'-AGCCATTGCGACGTACTAACAGTTC-3' and 5'-GTTCAACTGTCCATCAACCTGAACC-3'. The cDNA's containing the open reading frame were sub cloned into the pGEM T-Easy vector (Promega, Madison, WI) and multiple colonies were sequenced to screen for *ZmatNHX* isoforms.

ClustalW (version 2.1) was used for multiple sequence alignment and phylogenetic tree construction. The Kyte-Doolittle method and TMpred program was used for generating a hydropathy plot for ZmatNHX1. Prosite was used for the detection of conserved motifs.

Southern blot analysis

Leaves collected from 'Diamond' and 'Cavalier' were harvested and stored in a freezer at -80 °C until ready to use. The leaf tissue was ground in liquid nitrogen and genomic DNA was isolated from the leaves of each cultivar using CTAB (Stewart and Via, 1993). Genomic DNA thus isolated was quantified using a Nanodrop (Thermoscientific, Wilmington, DE). Ten µg of DNA was digested either with *Bam*HI, *Eco*RI, or *Hind*III. The digests were separated on a 1% (w/v) agarose gel, and blotted onto a charged nylon membrane. The membrane was prehybridized for 4 hours at 65 °C in a buffer containing 0.5 M (w/v) $NaHPO_4$ (pH 7.2), 1 mM (w/v) EDTA, 7% (v/v) SDS and 1% (v/v) BSA. Fifty ng of template was labeled with [α-^{32}P] dGTP using the random labeling method. Klenow was used for probe synthesis and the reaction was incubated at 37 °C for 1 h. The membrane was hybridized overnight in hybridization buffer containing ^{32}P-labeled partial cDNA of *Z. matrella NHX, SOS* or *HKT*. The membrane was washed twice for 5 min each at room temperature with buffer 1 (2X SSPE, 0.1% SDS) followed by two washes at 65 °C for 15 min each with buffer 2 (0.2X SSPE, 0.1% SDS). The membrane was then exposed to a Phosphor imaging plate (Fujifilm) for 6-12h depending on the intensity of the hybridization signal, and the image was analyzed using a Fujifilm BAS-5000 Phosphoimager (Functional Genomics Lab, Texas A&M University, College Station, TX).

In situ hybridization

Zoysia matrella leaf sections fixed in FAA were dehydrated and embedded in Paraplast Plus (Fisher Scientific, Pittsburgh, PA) according to the protocol described by Krizek (1999). Microtome sections, 8 µm thick, were mounted on Poly-L-lysine-coated microscopic slides (Fisher, Pittsburgh, PA) and baked overnight at 45-50 °C. The leaf sections were deparaffinized and rehydrated, followed by treatment with Proteinase K.

Plasmids (pGEM T-Easy) containing partial cDNA fragments of *ZmatHKT1*, *ZmatSOS1* or *ZmatNHX1* were linearized with ScaI, and *in vitro* transcribed using the Riboprobe *in vitro* transcription kit (Promega, Madison, WI). Synthesis of Digoxigenin (DIG)-labeled sense and antisense probes, and hybridization were performed at 45 °C according to the protocol described by Krizek (1999) with a few modifications. Anti-DIG antibodies conjugated with alkaline phosphatase (Roche, Mannheim, Germany) were used for the detection of DIG-labeled probes and NBT/BCIP substrate was used for signal detection.

RESULTS

Cloning of *Z. matrella* transporters

ZmatHKT1 - Using RT-PCR, a partial cDNA clone (1022 nucleotides) containing a portion of the open reading frame of *ZmatHKT1* was isolated from 'Diamond'. Alignment of the predicted protein sequence with other plant HKT transporters suggested that ZmatHKT1 is more closely related to members of HKT subfamily 2 (Figure 4.1). The deduced amino acid sequence of ZmatHKT1 contained a

glycine residue in the region corresponding to the first P loop of plant HKTs (Figure 4.2). The presence of this glycine residue also supports the conclusion that ZmatHKT1 belongs to the HKT subfamily 2, the members of which function as a Na^+-K^+ co-transporters (Mäser et al., 2002). Also included in the same HKT family are genes from other monocotyledonous plants like rice (*OsHKT2*), wheat and reed plant. This suggests that ZmatHKT1 may be functioning as a Na^+- K^+ co-transporter in *Z. matrella*.

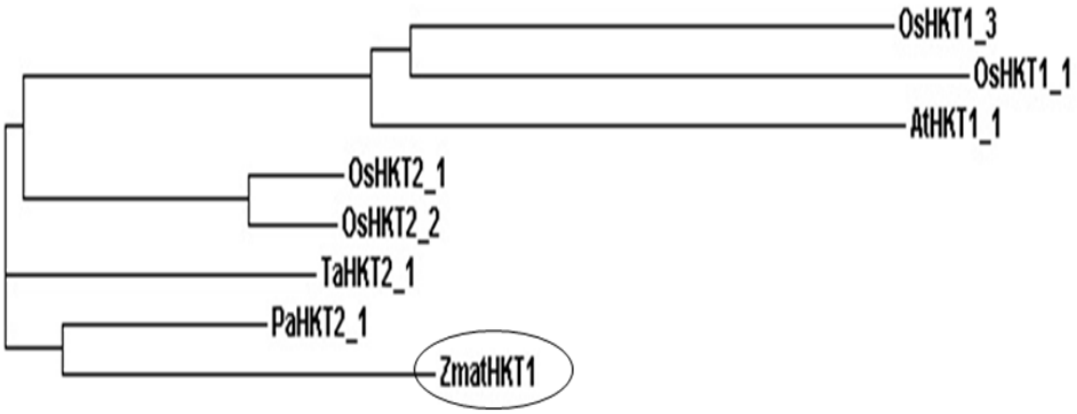

Figure 4.1 - Phylogenetic relationship between deduced protein sequence of ZmatHKT1 and other plant HKTs.

The accession numbers for the proteins sequences are – OsHKT1;3 (CAD37185); OsHKT1;1 (CAD37183); AtHKT1;1 (AAF68393); OsHKT2;1 (BAB61789); OsHKT2;2 (BAB61791); TaHKT2;1 (AAA52749) and PaHKT2;1 (BAE44385).

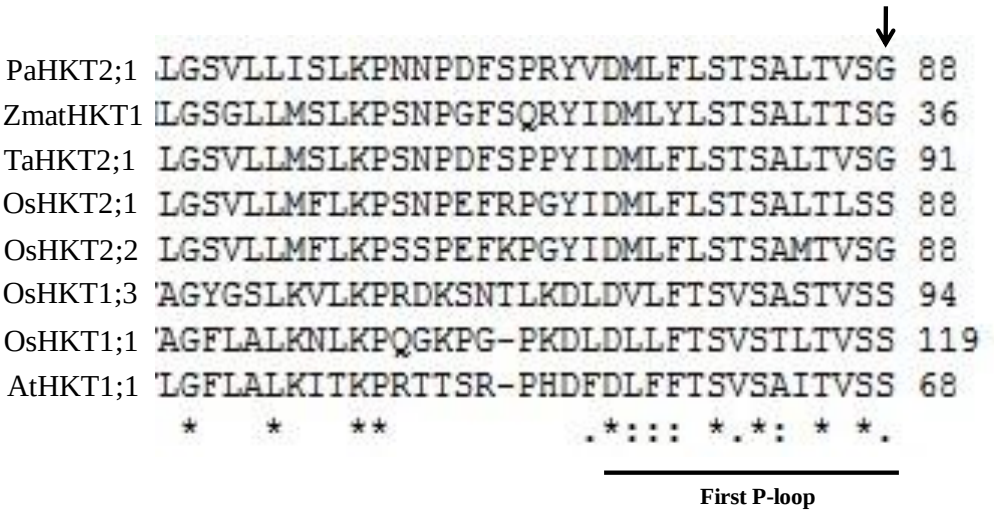

Figure 4.2 - Multiple sequence alignment of ZmatHKT1 with HKT proteins from other plant species.

Rice (OsHKT2;1, OsHKT2;2, OsHKT1;1, OsHKT1;3), *P. australis* (PhaHKT2;1), *Z. matrella* (ZmatHKT1), wheat (TaHKT2;1), and *A. thaliana* (AtHKT1;1). The black bar indicates the region corresponding to the first P-loop of the HKT protein and the conserved glycine residue in this loop is shown by the arrow.

The partial cDNA fragment of *ZmatHKT1* was used as a probe for performing genomic blot analysis. Different band patterns were seen for the two cultivars. Two bands were detected in 'Diamond' after *Bam*HI and *Hind*III digestion suggesting the presence of two copies of the *ZmatHKT1* gene in this cultivar (Figure 4.3). On the other hand, in 'Cavalier', *Bam*HI digest detected three bands and *Hind*III digest detected four

bands, suggesting that the 'Cavalier' genome has at least three copies of the *ZmatHKT* gene.

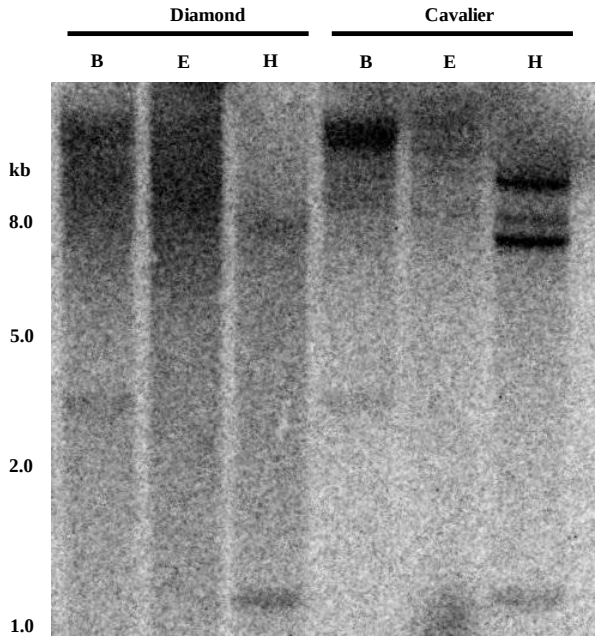

Figure 4.3 - Genomic Southern blot analysis of *ZmatHKT1*.

'Diamond' or 'Cavalier' genomic DNA (10 μg) was digested with *Bam*HI (B), *Eco*RI (E) or *Hind*III (H), and hybridized with ^{32}P-labelled coding sequence of *ZmatHKT1*.

ZmatSOS1 - Using RT-PCR and degenerate primers, a partial cDNA homologue (1.5 kb) of *ZmatSOS1* was isolated from salt-treated 'Diamond' plants. This partial cDNA was used as a probe for performing genomic blot analysis. One band was detected for 'Diamond' after *Bam*HI digestion, while digestion with *Eco*RI and *Hind*III showed two bands each (Figure 4.4). For 'Cavalier', three bands were detected after DNA was digested with *Bam*HI and *Hind*III, while only two bands were seen after *Eco*RI

digestion. This hybridization pattern suggests the presence of one to two copies of *ZmatSOS1* in 'Diamond', and two to three copies for 'Cavalier'.

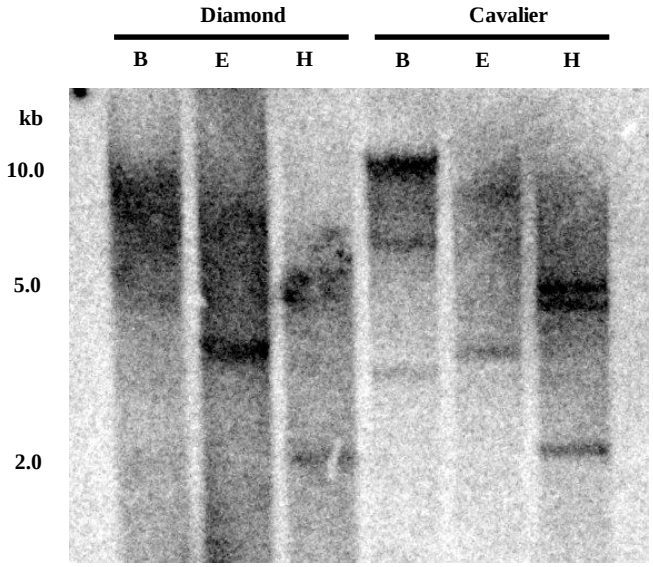

Figure 4.4 - Genomic Southern blot analysis of *ZmatSOS1*.

'Diamond' or 'Cavalier' genomic DNA (10 µg) was digested with *Bam*HI (B), *Eco*RI (E) or *Hind*III (H), and hybridized with ^{32}P-labelled coding sequence of *ZmatSOS1*.

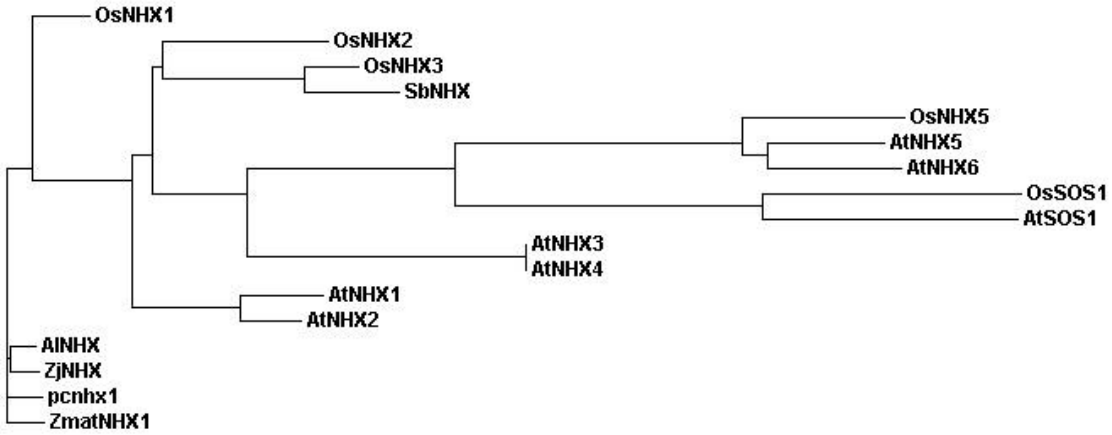

Figure 4.5 - Phylogenetic analysis of ZmatNHX1 with Na^+/H^+ antiporters from other plant species.

The accession numbers are - *Z. japonica*, ZjNHX (ABY19311); *A. littoralis*, AlNHX (AAV80466); *P. australis*, pcnhx1 (BAD95562); *S. bicolor*, SbNHX (ACD64982); *O. sativa*, OsNHX1 (BAA83337); *A. thaliana*, AtNHX1 (NP_198067); *A. thaliana*, AtSOS1 (NP_178307); and *O. sativa*, OsSOS1 (AAW33875).

ZmatNHX1 - The *ZmatNHX1* full-length cDNA sequence was 2482 bp and included a 5'-UTR of 536 bp, an open reading frame of 1622 bp, and a 3'-UTR of 324 bp. The open reading frame is predicted to encode a protein with 540 amino acids. A phylogenetic analysis of plant NHX proteins including ZmatNHX1 showed that there was a high homology for ZmatNHX1 with other plant tonoplast Na^+/H^+ antiporters, but the homology with plasma membrane Na^+/H^+ antiporter (AtSOS1) was very low (Figure 4.5). ZmatNHX was clustered together with AlNHX from *A. littoralis,* ZjNHX from *Z. japonica*, and pcnhx1 from *P. australis*, all of which belong to the same sub-family (Chloridoideae) as *Z. matrella*; and thus, are more closely related in terms of evolution. ZmatNHX1 was distantly related to the plasma membrane Na^+/H^+ antiporters, AtSOS1 and OsSOS1. Hydropathy analysis of ZmatNHX1, using the Kyte and Doolittle method (Kyte and Doolittle, 1982), predicted the presence of 12 transmembrane domains (Figure 4.6). An amiloride binding domain (LFFIYLLPPI), conserved in all plant NHX proteins, was present in ZmatNHX1 (shown in Figure 4.7).

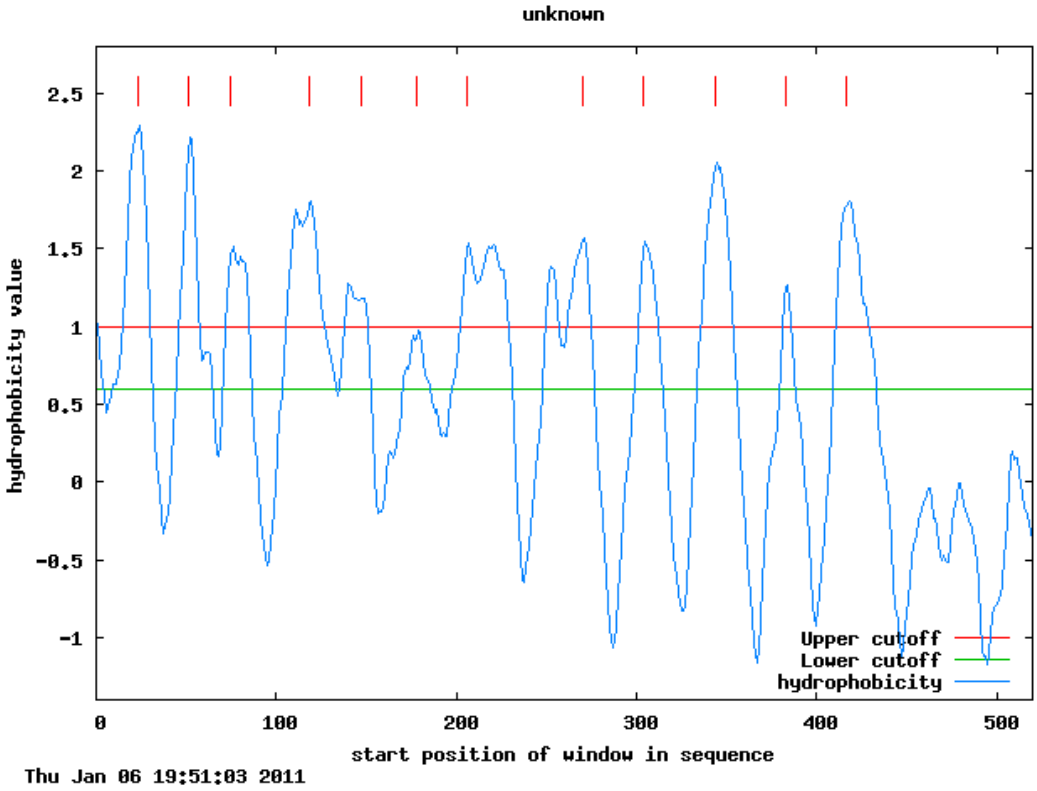

Figure 4.6 - Hydropathy plot of ZmatNHX1.

The plots were performed according to the method of Kyte and Doolittle (1982). Positive values denote hydrophobic amino acids.

Figure 4.7 - Multiple sequence alignment of the deduced amino acid sequence of ZmatNHX1;1 with NHX from other plant species.

A. littoralis (AlNHX, AAV80466), *Z. japonica* (ZjNHX, ABY19311), *P. australis* (pcnhx1, BAD95562), Rice (OsNHX1, BAA83337), *A. thaliana* (AtNHX1, NP_198067), and Sorghum (SbNHX, ACD64982). The conserved amiloride binding domain is indicated by a black bar.

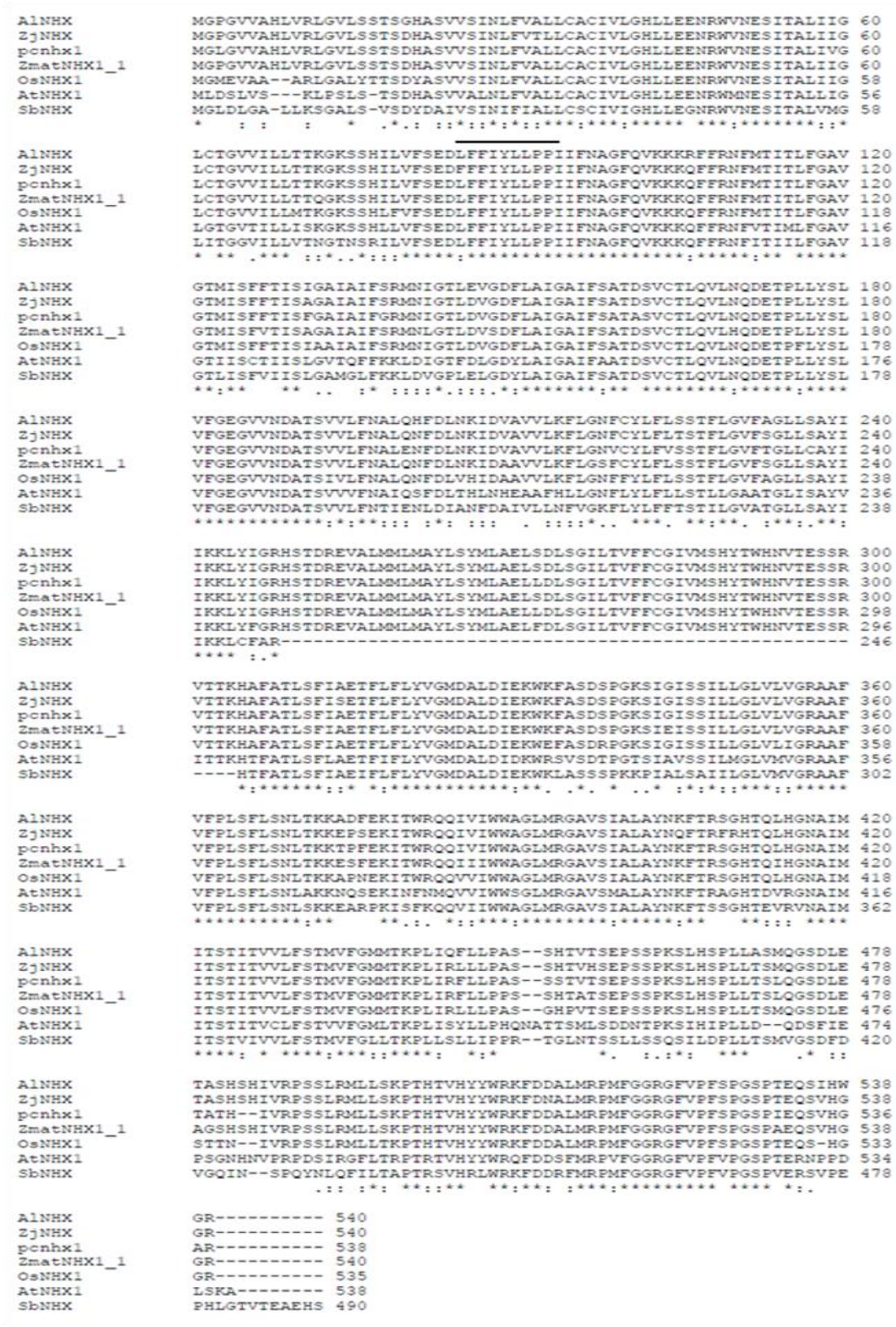
AlNHX MGPGVVAHLVRLGVLSSTSGHASVVSINLFVALLCACIVLGHLLEENRWVNESITALIIG 60
ZjNHX MGPGVVAHLVRLGVLSSTSDHASVVSINLFVTLLCACIVLGHLLEENRWVNESITALIIG 60
pcnhx1 MGLGVVAHLVRLGVLSSTSDHASVVSINLFVALLCACIVLGHLLEENRWVNESITALIVG 60
ZmatNHX1_1 MGPGVVAHLVRLGVLSSTSDHASVVSINLFVALLCACIVLGHLLEENRWVNESITALIIG 60
OsNHX1 MGMEVAA--ARLGALYTTSDYASVVSINLFVALLCACIVLGHLLEENRWVNESITALIIG 58
AtNHX1 MLDSLVS---KLPSLS-TSDHASVVALNLFVALLCACIVLGHLLEENRWMNESITALLIG 56
SbNHX MGLDLGA-LLKSGALS-VSDYDAIVSINIFIALLCSCIVIGHLLEGNRWVNESITALVMG 58
AlNHX LCTGVVILLTTKGKSSHILVFSEDLFFIYLLPPIIFNAGFQVKKKRFFRNFMTITLFGAV 120
ZjNHX LCTGVVILLTTKGKSSHILVFSEDFFFIYLLPPIIFNAGFQVKKKQFFRNFMTITLFGAV 120
pcnhx1 LCTGVVILLTTKGKSSHILVFSEDLFFIYLLPPIIFNAGFQVKKKQFFRNFMTITLFGAV 120
ZmatNHX1_1 LCTGVVILLTTQGKSSHILVFSEDLFFIYLLPPIIFNAGFQVKKKQFFRNFMTITLFGAV 120
OsNHX1 LCTGVVILLMTKGKSSHLFVFSEDLFFIYLLPPIIFNAGFQVKKKQFFRNFMTITLFGAV 118
AtNHX1 LGTGVTILLISKGKSSHLLVFSEDLFFIYLLPPIIFNAGFQVKKKQFFRNFVTIMLFGAV 116
SbNHX LITGGVILLVTNGTNSRILVFSEDLFFIYLLPPIIFNAGFQVKKKQFFRNFITIILFGAV 118
AlNHX GTMISFFTISIGAIAIFSRMNIGTLEVGDFLAIGAIFSATDSVCTLQVLNQDETPLLYSL 180
ZjNHX GTMISFFTISAGAIAIFSRMNIGTLDVGDFLAIGAIFSATDSVCTLQVLNQDETPLLYSL 180
pcnhx1 GTMISFFTISFGAIAIFGRMNIGTLDVGDFLAIGAIFSATASVCTLQVLNQDETPLLYSL 180
ZmatNHX1_1 GTMISFVTISAGAIAIFSRMNLGTLDVSDFLAIGAIFSATDSVCTLQVLHQDETPLLYSL 180
OsNHX1 GTMISFFTISIAAIAIFSRMNIGTLDVGDFLAIGAIFSATDSVCTLQVLNQDETPFLYSL 178
AtNHX1 GTIISCTIISLGVTQFFKKLDIGTFDLGDYLAIGAIFAATDSVCTLQVLNQDETPLLYSL 176
SbNHX GTLISFVIISLGAMGLFKKLDVGPLELGDYLAIGAIFSATDSVCTLQVLNQDETPLLYSL 178
AlNHX VFGEGVVNDATSVVLFNALQHFDLNKIDVAVVLKFLGNFCYLFLSSTFLGVFAGLLSAYI 240
ZjNHX VFGEGVVNDATSVVLFNALQNFDLNKIDVAVVLKFLGNFCYLFLTSTFLGVFSGLLSAYI 240
pcnhx1 VFGEGVVNDATSVVLFNALENFDLNKIDVAVVLKFLGNVCYLFVSSTFLGVFTGLLCAYI 240
ZmatNHX1_1 VFGEGVVNDATSVVLFNALQNFDLNKIDAAVVLKFLGSFCYLFLSSTFLGVFSGLLSAYI 240
OsNHX1 VFGEGVVNDATSIVLFNALQNFDLVHIDAAVVLKFLGNFFYLFLSSTFLGVFAGLLSAYI 238
AtNHX1 VFGEGVVNDATSVVVFNAIQSFDLTHLNHEAAFHLLGNFLYLFLLSTLLGAATGLISAYV 236
SbNHX VFGEGVVNDATSVVLFNTIENLDIANFDAIVLLNFVGKFLYLFFTSTILGVATGLLSAYI 238
AlNHX IKKLYIGRHSTDREVALMMLMAYLSYMLAELSDLSGILTVFFCGIVMSHYTWHNVTESSR 300
ZjNHX IKKLYIGRHSTDREVALMMLMAYLSYMLAELSDLSGILTVFFCGIVMSHYTWHNVTESSR 300
pcnhx1 IKKLYIGRHSTDREVALMMLMAYLSYMLAELLDLSGILTVFFCGIVMSHYTWHNVTESSR 300
ZmatNHX1_1 IKKLYIGRHSTDREVALMMLMAYLSYMLAELSDLSGILTVFFCGIVMSHYTWHNVTESSR 300
OsNHX1 IKKLYIGRHSTDREVALMMLMAYLSYMLAELLDLSGILTVFFCGIVMSHYTWHNVTESSR 298
AtNHX1 IKKLYFGRHSTDREVALMMLMAYLSYMLAELFDLSGILTVFFCGIVMSHYTWHNVTESSR 296
SbNHX IKKLCFAR---------- 246
AlNHX VTTKHAFATLSFIAETFLFLYVGMDALDIEKWKFASDSPGKSIGISSILLGLVLVGRAAF 360
ZjNHX VTTKHAFATLSFISETFLFLYVGMDALDIEKWKFASDSPGKSIGISSILLGLVLVGRAAF 360
pcnhx1 VTTKHAFATLSFIAETFLFLYVGMDALDIEKWKFASDSPGKSIGISSILLGLVLVGRAAF 360
ZmatNHX1_1 VTTKHAFATLSFIAETFLFLYVGMDALDIEKWKFASDSPGKSIEISSILLGLVLVGRAAF 360
OsNHX1 VTTKHAFATLSFIAETFLFLYVGMDALDIEKWEFASDRPGKSIGISSILLGLVLIGRAAF 358
AtNHX1 ITTKHTFATLSFLAETFIFLYVGMDALDIDKWRSVSDTPGTSIAVSSILMGLVMVGRAAF 356
SbNHX ----HTFATLSFIAEIFLFLYVGMDALDIEKWKLASSSPKKPIALSAIILGLVMVGRAAF 302
AlNHX VFPLSFLSNLTKKADFEKITWRQQIVIWWAGLMRGAVSIALAYNKFTRSGHTQLHGNAIM 420
ZjNHX VFPLSFLSNLTKKEPSEKITWRQQIVIWWAGLMRGAVSIALAYNQFTRFRHTQLHGNAIM 420
pcnhx1 VFPLSFLSNLTKKTPFEKITWRQQIVIWWAGLMRGAVSIALAYNKFTRSGHTQLHGNAIM 420
ZmatNHX1_1 VFPLSFLSNLTKKESFEKITWRQQIIIWWAGLMRGAVSIALAYNKFTRSGHTQIHGNAIM 420
OsNHX1 VFPLSFLSNLTKKAPNEKITWRQQVVIWWAGLMRGAVSIALAYNKFTRSGHTQLHGNAIM 418
AtNHX1 VFPLSFLSNLAKKNQSEKINFNMQVVIWWSGLMRGAVSMALAYNKFTRAGHTDVRGNAIM 416
SbNHX VFPLSFLSNLSKKEARPKISFKQQVIIWWAGLMRGAVSIALAYNKFTSSGHTEVRVNAIM 362
AlNHX ITSTITVVLFSTMVFGMMTKPLIQFLLPAS--SHTVTSEPSSPKSLHSPLLASMQGSDLE 478
ZjNHX ITSTITVVLFSTMVFGMMTKPLIRLLLPAS--SHTVHSEPSSPKSLHSPLLTSMQGSDLE 478
pcnhx1 ITSTITVVLFSTMVFGMMTKPLIRFLLPAS--SSTVTSEPSSPKSLHSPLLTSLQGSDLE 478
ZmatNHX1_1 ITSTITVVLFSTMVFGMMTKPLIRFLLPPS--SHTATSEPSSPKSLHSPLLTSLQGSDLE 478
OsNHX1 ITSTITVVLFSTMVFGMMTKPLIRLLLPAS--GHPVTSEPSSPKSLHSPLLTSMQGSDLE 476
AtNHX1 ITSTITVCLFSTVVFGMLTKPLISYLLPHQNATTSMLSDDNTPKSIHIPLLD--QDSFIE 474
SbNHX ITSTVIVVLFSTMVFGLLTKPLLSLLIPPR--TGLNTSSLLSSQSILDPLLTSMVGSDFD 420
AlNHX TASHSHIVRPSSLRMLLSKPTHTVHYYWRKFDDALMRPMFGGRGFVPFSPGSPTEQSIHW 538
ZjNHX TASHSHIVRPSSLRMLLSKPTHTVHYYWRKFDNALMRPMFGGRGFVPFSPGSPTEQSVHG 538
pcnhx1 TATH--IVRPSSLRMLLSKPTHTVHYYWRKFDDALMRPMFGGRGFVPFSPGSPIEQSVHG 536
ZmatNHX1_1 AGSHSHIVRPSSLRMLLSKPTHTVHYYWRKFDDALMRPMFGGRGFVPFSPGSPAEQSVHG 538
OsNHX1 STTN--IVRPSSLRMLLTKPTHTVHYYWRKFDDALMRPMFGGRGFVPFSPGSPTEQS-HG 533
AtNHX1 PSGNHNVPRPDSIRGFLTRPTRTVHYYWRQFDDSFMRPVFGGRGFVPFVPGSPTERNPPD 534
SbNHX VGQIN--SPQYNLQFILTAPTRSVHRLWRKFDDRFMRPMFGGRGFVPFVPGSPVERSVPE 478
AlNHX GR---------- 540
ZjNHX GR---------- 540
pcnhx1 AR---------- 538
ZmatNHX1_1 GR---------- 540
OsNHX1 GR---------- 535
AtNHX1 LSKA-------- 538
SbNHX PHLGTVTEAEHS 490

For ‘Diamond’, the hybridization pattern from Southern blot analysis showed two bands after *Eco*RI digestion and three bands after *Hind*III digestion, suggesting the presence of two to three copies of the *ZmatNHX1* gene in the ‘Diamond’ genome (Figure 4.8). For ‘Cavalier’, three bands each were detected on the blot after *Eco*RI and *Hind*III digestion, suggesting that the ‘Cavalier’ genome has three copies of the *ZmatNHX1* gene.

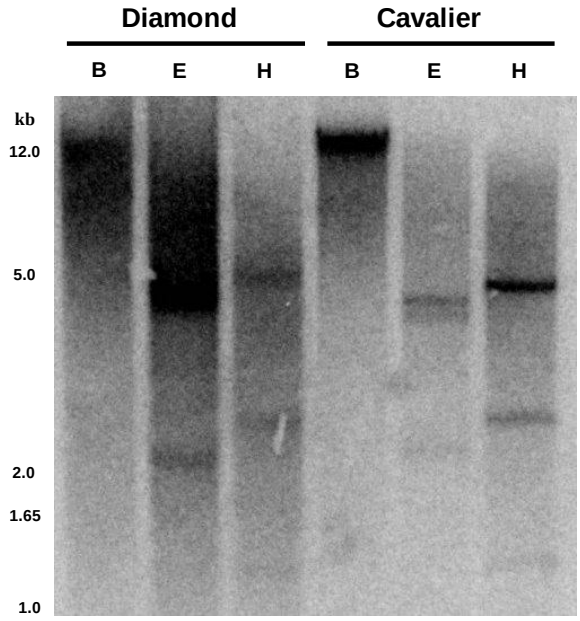

Figure 4.8 - Genomic Southern blot analysis of *ZmatNHX1*.

‘Diamond’ or ‘Cavalier’ genomic DNA (10 µg) was digested with *Bam*HI (B), *Eco*RI (E) or *Hind*III (H), and hybridized with ^{32}P-labelled coding sequence of *ZmatNHX1*.

To screen for the existence of multiple *NHX* isoforms in *Z. matrella*, ten clones each containing full-length *NHX* cDNAs from 'Diamond' or 'Cavalier' were sequenced in both directions. Although a few nucleotide differences were present within the several clones sequenced, they had identical 5'- and 3'-UTR regions, which suggested that they originated from the same genomic location of *Z. matrella*. This isoform was named *ZmatNHX1* and the variation seen among the different clones was presumed to be due to allelic variation of *ZmatNHX1*. *Z. matrella* is an allotetraploid; hence, the existence of allelic variants in *ZmatNHX1* is not surprising. Multiple sequence alignment of the clones encoding a full-length ZmatNHX protein showed the existence of three different alleles, denoted as *ZmatNHX1;1*, *ZmatNHX1;2*, and *ZmatNHX1;3*. At the nucleotide level *ZmatNHX1;2* was 99% identical to *ZmatNHX1;1* and *ZmatNHX1;3;* while, *ZmatNHX1;3* was 96% identical to *ZmatNHX1;1*. Comparison of the predicted amino acid sequences showed that these alleles were 99 % identical to each other with two to three amino acid differences in ZmatNHX1;3 and ZmatNHX1;2, respectively (Figure 4.9). Of these three alleles, *ZmatNHX1;1* transcripts were present in the leaves of both cultivars, but only in the leaves of salt-treated 'Diamond'. *ZmatNHX1;2* transcripts were isolated only from salt-treated 'Diamond' leaves while *ZmatNHX1;3* transcripts were present only in the leaves of salt-treated 'Cavalier'. Table 4.1 shows the percent identity of ZmatNHX alleles with other plant *NHX* transporters.

Figure 4.9 - Multiple sequence alignment of the deduced amino acid sequences of the ZmatNHX1 alleles.

Arrows show the regions of amino acid substitutions in the three alleles.

Table 4.1 - Amino acid percent identity of ZmatNHX alleles with NHX and SOS homologs of different plant species.

	ZmatNHX1;1	ZmatNHX1;2	ZmatNHX1;3
ZjNHX	**94**	**94**	**95**
AlNHX1	**94**	**94**	**94**
pcnhx1	**94**	**93**	**94**
SbNHX	**67**	**67**	**67**
OsNHX1	**90**	**89**	**90**
AtNHX1	**71**	**71**	**72**
AtSOS1	**18**	**18**	**18**
OsSOS1	**18**	**18**	**18**

ZjNHX (ABY19311) *Z. japonica*; AlNHX (AAV80466) *A. littoralis*; pcnhx1 (BAD95562) *P. australis*; SbNHX (ACD64982) Sorghum; OsNHX1 (BAA83337) rice; AtNHX1 (NP_198067) *A. thaliana*; AtSOS1 (NP_178307) *A. thaliana*; OsSOS1 (AAW33875) rice.

Expression of *Z. matrella* transporters

***ZmatHKT1*-** RNA *in situ* studies were used for spatial localization of *ZmatHKT1* expression in *Z. matrella* leaves. The hybridization pattern of the *ZmatHKT1* antisense probe indicated the preferential localization of *ZmatHKT1* transcripts in the leaf bundle sheath cells, as well as, in the mesophyll cells around them (Figure 4.10). Expression was also detected in the functional salt glands located on the adaxial leaf surface (Figure 4.10). The *ZmatHKT1* mRNA expression pattern we observed was similar for both 'Diamond' and 'Cavalier'. No signal was detected in the vascular tissue, mestome sheath cells, abaxial salt glands, or in the prickles; or with the sense probe (negative control).

***ZmatSOS1*-** *ZmatSOS1* transcripts were localized in the leaves of salt-treated 'Diamond' and 'Cavalier' using *in situ* hybridization with *ZmatSOS1*-specific RNA probes. The hybridization signals were detected in both cultivars; however, the expression pattern of *ZmatSOS1* mRNA varied between salt-treated 'Diamond' and 'Cavalier'. In the leaves from both cultivars, *ZmatSOS1* mRNA expression was localized to xylem parenchyma cells (Figure 4.11).

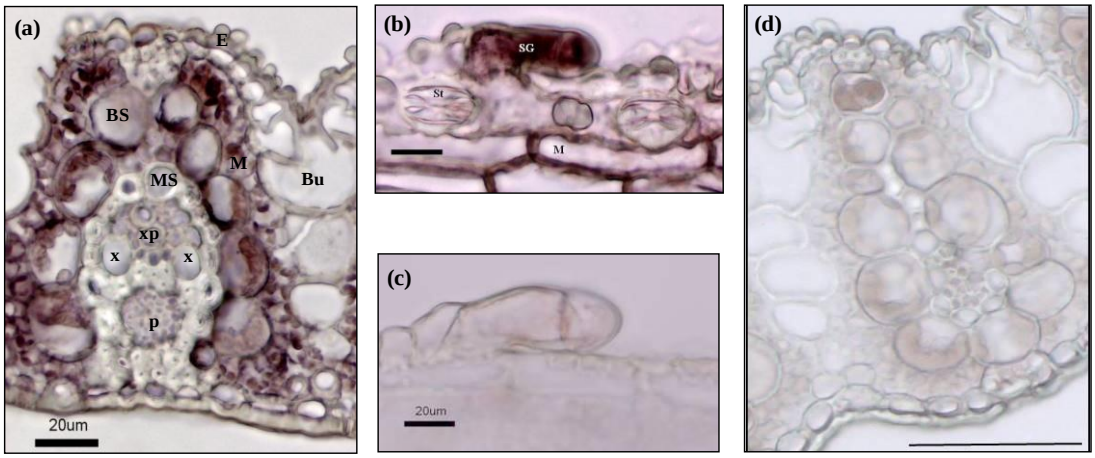

Figure 4.10 - *In situ* hybridization of *ZmatHKT1* in a leaf from 'Diamond' treated with 300 mM NaCl.

(a) Cross-section of a leaf from 'Diamond' showing *ZmatHKT1* transcripts localized in the bundle-sheath and mesophyll.

(b) Longitudinal-section of a leaf from 'Diamond' showing *ZmatHKT1* transcripts localized in the adaxial salt gland.

(c) Longitudinal-section of a leaf from 'Diamond' showing the absence of hybridization signal in the *ZmatHKT1* sense control.

(d) Cross-section of a leaf from 'Diamond' showing the absence of hybridization signal in the *ZmatHKT1* sense control.

M, mesophyll; BS, bundle sheath; MS, mestome sheath; SG, salt gland; E, adaxial epidermis; x, xylem; xp, xylem parenchyma; p, phloem; Bu, bulliform cells.

Scale bar = 20 µm (Figure b), 50 µm (Figure d).

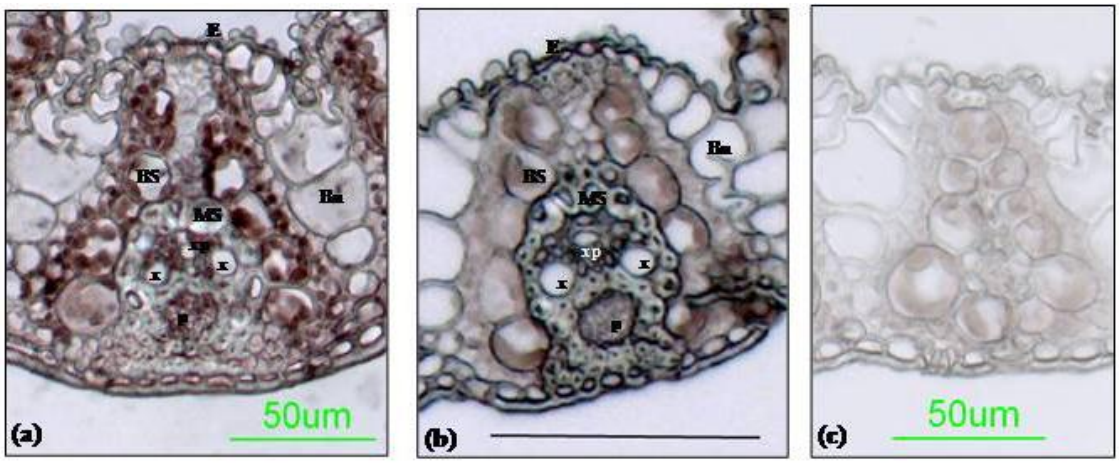

Figure 4.11 - *In situ* hybridization of *ZmatSOS1* in the leaves of 'Diamond' and 'Cavalier' treated with 300 mM NaCl.

(a) Cross-section of a leaf from 'Diamond' showing *ZmatSOS1* transcripts localized in the bundle-sheath, xylem parenchyma, and phloem.

(b) Cross-section of a leaf from 'Cavalier' showing *ZmatSOS1* transcripts localized in the mestome sheath, xylem parenchyma, and cells bordering the phloem.

(c) Cross-section of a leaf from 'Diamond' showing the absence of hybridization signal in the *ZmatSOS1* sense control.

M, mesophyll; BS, bundle sheath; MS, mestome sheath cells; SG, salt gland; E, adaxial epidermis; x, xylem; xp, xylem parenchyma; p, phloem; Bu, bulliform cells.

Scale bar = 100 μm (Figure b).

In the leaves of ‘Diamond’, stronger signals were detected in the bundle sheath cells (Figure 4.11), while in ‘Cavalier’ the signal was strongest in the mestome sheath cells located between the vascular tissue and the bundle sheath cells (Figure 4.11). Although *ZmatSOS1* transcripts were detected in the mestome sheath cells of both cultivars, the hybridization signal was stronger in ‘Cavalier’.

Inside the vascular tissue, *ZmatSOS1* expression was evident in the phloem for ‘Diamond’ (Figure 4.11) while in ‘Cavalier’ expression was detected only in the cells bordering the phloem (Figure 4.11). Expression of *ZmatSOS1* was not detected in the salt glands of either cultivar when the longitudinal sections of leaves were examined.

ZmatNHX1- *In situ* localization studies done with *ZmatNHX1* antisense probes showed a very low hybridization signal in the leaves, as compared to the signals seen with *ZmatHKT1* and *ZmatSOS1*. The signal for *ZmatNHX1* mRNA was observed in the epidermal cells located in the vicinity of the salt glands for both cultivars, although the signal in ‘Cavalier’ was stronger than ‘Diamond’ (Figure 4.12). Low levels of *ZmatNHX1* transcripts were also detected in the salt glands and mesophyll cells.

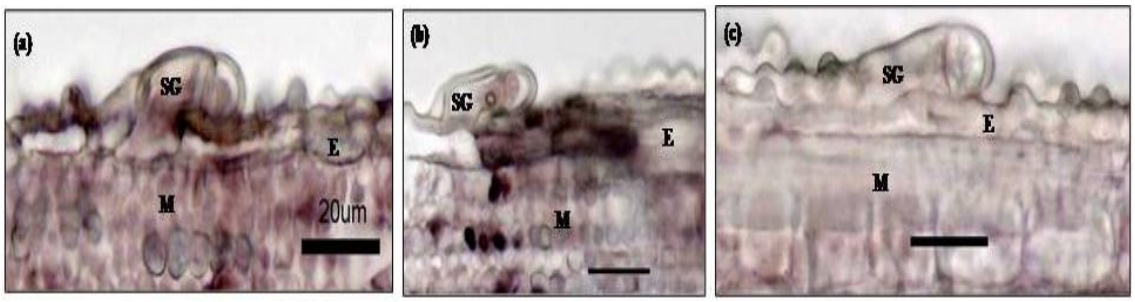

Figure 4.12 – *In situ* hybridization of *ZmatNHX1* in the leaves of 'Diamond' and 'Cavalier' treated with 300 mM NaCl.

(a) Longitudinal-section of a leaf from 'Diamond' showing *ZmatNHX1* transcripts localized in the epidermal cells adjacent to an adaxial salt gland.

(b) Longitudinal-section of a leaf from 'Cavalier' showing a stronger signal for *ZmatNHX1* transcript localization in the epidermal cells next to an adaxial salt gland, than Diamond **(a)**.

(c) Longitudinal-section of a leaf from 'Diamond' showing the absence of hybridization signal in the *ZmatNHX1* sense control.

M, mesophyll; SG, salt gland; E, adaxial epidermis. Scale bar = 20 μm

DISCUSSION

This part of the project was initiated with an objective of determining tissue-specific localization of three *Z. matrella* Na^+ transporters– *HKT1*, *SOS1* and *NHX1*, in the leaves of *Z. matrella* by means of RNA *in situ* hybridization. Using the *Z. matrella* cDNA sequence obtained in our study, RNA probes were synthesized for *in situ* hybridization studies in order to visualize the spatial expression pattern of *HKT1*, *SOS1* and *NHX1* transporters in salt-treated *Z. matrella* leaves.

Comparison of the predicted amino acid sequence of ZmatHKT1 with HKT family members from other plants and phylogenetic analysis showed that ZmatHKT1 was clustered along with HKT members in subfamily 2, that have a glycine residue in the first pore loop of the protein and function as Na^+-K^+ co-transporters (Platten et al., 2006). This suggests that ZmatHKT1 may serve a similar function in *Z. matrella*, although functional analysis including ion uptake assays will be required to confirm the activity and ion specificity of ZmatHKT1 after the full-length cDNA of *ZmatHKT1* is obtained. Future studies could involve 5' and 3' RACE for extending the partial cDNA of *ZmatHKT1* in both directions to obtain the full-length cDNA of this transporter. Once the full-length sequence is obtained, additional studies involving heterologous expression in yeast, coupled with ion uptake assays, could be performed to verify the ion uptake characteristics of ZmatHKT1.

The expression pattern of *ZmatHKT1* in *Z. matrella* differed to some extent from the expression of other *HKT1* homologs in the HKT subfamily 2 (namely *TaHKT2;1*, *OsHKT2;1*, and *OsHKT2;2*). Based on RNA *in situ* localization studies, the expression

of *OsHKT2;1* was detected in the leaf phloem (Golldack et al., 2002) and mesophyll (Kader et al., 2006) of salt-sensitive cultivars of rice, while a promoter-GUS fusion showed preferential expression of GUS in the region of the vascular bundles (Horie et al., 2007). The expression of *OsHKT2;2* has been reported in the leaf mesophyll, phloem, and in the region between the mesophyll and phloem (Kader et al., 2006). On the other hand, the expression of *TaHKT2;1* in wheat was specific to the cells surrounding the leaf vascular tissue (Schachtman and Schroeder, 1994). All these observations led to the theory that monocots like rice and wheat adopt the strategy of excluding Na^+ from the xylem, by recirculation to the roots via the phloem (Hauser and Horie, 2010).

Our RNA *in situ* studies with *ZmatHKT1* showed that the mRNA was localized in the bundle sheath cells and the surrounding mesophyll cells, in the leaves from salt-treated plants of both 'Diamond' and 'Cavalier' (Figure 4.10). A strong hybridization signal was also seen in the adaxial salt glands that are functional in salt secretion (Figure 4.10 & Chapter II). A similar observation has been made in ice plant where McHKT1 was immunolocalized in the leaf epidermal bladder cells, where it is proposed to sequester excess Na^+ (Su et al., 2003). *Zoysia matrella* has salt glands for excretion of excess Na^+ arriving into the leaves from the transpiration stream in the xylem (Chapter II); while, species like rice and *A. thaliana* that have no such structural adaptations for excess Na^+ removal adopt a mechanism of Na^+ recirculation via the phloem (Ren et al., 2005; Sunarpi et al., 2005). Based on the observation made in *Z. matrella* and previous studies with other species including ice plant (Su et al., 2003), *S. alterniflora* (Vasquez

et al., 2006), rice (Ren et al., 2005) and *A. thaliana* (Sunarpi et al., 2005), we hypothesize that *ZmatHKT1* plays an important role in channeling Na^+ transport from the xylem to the adaxial salt glands via symplastic transport through the bundle sheath and mesophyll cells located in between them. This theory is partly supported by the lack of *ZmatHKT1* mRNA signal in the abaxial glands which do not secrete salt in *Z. matrella* (Chapter II). The similar expression patterns seen for 'Diamond' and 'Cavalier' suggest that the spatial localization of *ZmatHKT1* may not be a factor contributing to the differential salt tolerance between these cultivars.

In order to determine the role of the other two Na^+ transporters in the salt tolerance of 'Diamond' and 'Cavalier', similar expression studies were done with *ZmatSOS1* and *ZmatNHX1*. In our studies with *Z. matrella*, *ZmatSOS1* transcripts were detected by RNA *in situ* hybridization in the xylem parenchyma cells of leaves from both cultivars (Figure 4.11). Differences in *ZmatSOS1* expression between the cultivars was seen in the area around the vascular tissue. In 'Diamond', *ZmatSOS1* transcripts were localized in the bundle sheath cells and the phloem (Figure 4.11); while in 'Cavalier', they were localized in the mestome sheath cells and the cells bordering the phloem (Figure 4.11). The strong hybridization signal seen for *ZmatSOS1* mRNA in the bundle sheath cells suggests a role for *ZmatSOS1* in efflux of excess Na^+ from these cells into the apoplast, in order to avoid cytosolic toxicity of these photosynthetically active cells; while, also allowing symplastic or apoplastic flow of Na^+ into the mesophyll. Na^+ that has entered the apoplast, could arrive to the salt glands via the symplast or apoplast, although our studies involving Cl^- localization showed a preference for the symplastic

route (Chapter II); and localization of *ZmatHKT1* mRNA in the leaf area between the bundle sheath and mesophyll suggested that Na^+ transport in this area of *Z. matrella* leaves may be via the symplast.

On the other hand, for 'Cavalier' a strong signal for *ZmatSOS1* was observed in the mestome sheath cells. These cells are photosynthetically inactive, and have suberized lamellae in their walls, which can limit the amount of ion transport via the apoplast around this region of the leaf (Eastman et al., 1988; Leegood, 2008). Higher expression of *ZmatSOS1* in these cells suggests that if the activity of this transporter is high in these cells, it would lead to Na^+ efflux into the apoplast of the mestome sheath cells, thus limiting the amount of leaf Na^+ that will be transported to the salt glands. This would result in less Na^+ excreted by 'Cavalier' as a consequence of a greater Na^+ retention inside the leaves.

Most plant species that retain Na^+ in their leaves resort to Na^+ compartmentalization in the vacuole via the activity of NHX. In this study, we identified one isoform of *NHX* in *Z. matrella*, *ZmatNHX1*. However, different alleles of this isoform are predicted to exist in 'Diamond' and 'Cavalier' due to the allotetraploid nature of *Z. matrella*, hence the existence of allelic variants in *ZmatNHX1* is not surprising. The allele *ZmatNHX1;1* was present in both cultivars, while the alleles *ZmatNHX1;2* and *ZmatNHX1;3* were genotype specific. *ZmatNHX1;2* was present in 'Diamond' while *ZmatNHX1;3* was present in 'Cavalier'. Each of these three alleles had a unique expression pattern. *ZmatNHX1;3* transcripts were detected only in the leaves of salt-treated 'Cavalier', and *ZmatNHX1;2* transcripts in the leaves of salt-treated

'Diamond'. *ZmatNHX1;1* on the other hand was expressed in both cultivars but was not detected in the leaves of salt-treated 'Cavalier'.

Apart from the full-length cDNAs that were found to code for the three ZmatNHX1 alleles, several other full-length cDNAs containing the open reading frame were isolated and found to code for prematurely truncated proteins of varying sizes. Sequence alignment of these with the cDNA sequences of *ZmatNHX1* alleles indicated the presence of several nucleotide and amino acid substitutions. Insertions and deletions were also present in some of these clones. Using the *OsNHX1* genomic sequence as a reference, it was evident that each of the insertions was similar to an intron in rice. Based on their similarity with the three *ZmatNHX1* alleles, these sequences were hypothesized to be alternatively spliced forms of *ZmatNHX1*.

Three alternatively spliced forms of *ZmatNHX1;1* were identified and denoted as *ZmatNHX1;1-A* (expressed in 'Diamond' leaves treated with 0 mM NaCl), *ZmatNHX1;1-B* (expressed in salt-treated 'Diamond' leaves), and *ZmatNHX1;1-C* (expressed in 'Cavalier' leaves treated with 0 mM NaCl). Insertions within the coding sequence were seen in *ZmatNHX1;1-A* (80 bp & 92 bp); *ZmatNHX1;1-C* (92 bp, 123 bp & 490 bp); while 38 bp deletions in the coding sequence were seen in *ZmatNHX1;1-A* and *ZmatNHX1;1-B*. These insertions are predicted to encode truncated proteins with 270 aa (ZmatNHX1;1-A & ZmatNHX1;1-C) or 391 aa (ZmatNHX1;1-B). There were two alternatively spliced forms of *ZmatNHX1;3* that had insertions in their coding sequence, *ZmatNHX1;3-A* (92 bp) and *ZmatNHX1;3-B* (80 bp & 92 bp). The splice variants of *ZmatNHX1;3* were present only in the leaves of salt-treated 'Cavalier'.

ZmatNHX1;3-A had one insertion while *ZmatNHX1;3-B* had two insertions in the coding region, and both encoded truncated proteins of 270 and 160 amino acids, respectively. For *ZmatNHX1;2*, no alternatively-spliced forms were identified in this study.

In situ localization studies did not reveal a strong expression of *ZmatNHX1* mRNA in the leaf cells, although a relatively stronger signal was seen in epidermal cells near the salt gland (Figure 4.12). We hypothesize that these epidermal cells help in vacuolar sequestration of excess Na^+ until it is transported to the salt gland. Previous studies have reported that the expression of GUS driven by an *AtNHX1* promoter was found in all tissues of *A. thaliana* seedlings and a NaCl-dependant up-regulation of GUS activity was seen in the mesophyll cells, root hairs, and in guard cells (Shi and Zhu, 2002). A later study involving *in situ* localization of *AtNHX1* reported the presence of a strong signal for *AtNHX1* mRNA around the vascular tissue, with a weaker signal also seen in the epidermal and mesophyll cells (Apse et al., 2003). However, since these *in situ* localization results were obtained with wild-type plants, it is likely that the expression pattern may differ in salt-treated plants especially since *AtNHX1* mRNA has been found to be up-regulated by NaCl stress (Shi and Zhu, 2002; Jha et al., 2010). For studies done with rice, *OsNHX1* expression was undetectable by *in situ* studies, although *OsNHX* promoter-GUS analysis showed strong GUS staining in the guard cells and trichomes with the *OsNHX1* promoter; and in the pollen grains and at the root tip with the *OsNHX5* promoter (Fukuda et al., 2011).

We have identified three different alleles of *ZmatNHX1* that were expressed in a cultivar and NaCl-specific manner. Although the significance of multiple alleles or

alternatively-spliced forms of *ZmatNHX1* is unclear at this point, a recent study involving sulphate transporters in rice has shown that alternatively-spliced forms of some of these sulphate transporters displayed differential expression in response to a variety of abiotic stresses including drought, cold and salinity stress (Kumar et al., 2011). Similarly, in *A. thaliana* a strong correlation was found to exist between the degree of salt tolerance in different accessions and the strength of *AtHKT1;1* alleles expressed in each accession (Baxter et al., 2010). Likewise, in a comparative study of *A. thaliana* and its close relative *T. halophila* (which is salt tolerant), two splice variants of *SOS1* were found in *T. halophila* compared to the one variant seen in *A. thaliana* (Taji et al., 2010). In order to understand the role and significance of allelic variants as well as alternatively spliced forms of *ZmatNHX1* in *Z. matrella*, allele-specific temporal and spatial expression pattern needs to be studied. A tissue-specific expression pattern of *NHX* isoforms has been reported for other plant species including *A. thaliana* (Yokoi et al., 2002), maize (Zorb et al., 2005), and *A. littoralis* (Qiao et al., 2007).

The existence of additional *ZmatNHX* isoforms cannot be ruled out because the isoforms present in the root and stem were not investigated in this study. Based on the data from Southern blot analysis, *Z. matrella* is predicted to have at least two more isoforms of *ZmatNHX*. Phylogenetic analysis showed that *ZmatNHX1* is grouped with other plant vacuolar Na^+/H^+ antiporters; however, heterologous expression studies and localization studies are essential to confirm its function as a vacuolar Na^+/H^+ antiporter. At this point it is difficult to say if all the alleles of *ZmatNHX1* encode functional

transporters and further studies involving antiporter activity will be necessary to elucidate the role of these transporters.

To summarize, one isoform each for *HKT*, *SOS*, and *NHX* was identified in *Z. matrella* cultivars; and their spatial expression pattern in the leaves was studied using RNA *in situ* hybridization. Although these results can be used to propose a role for these transporters in 'Diamond' and 'Cavalier', additional studies are necessary to confirm the role of these transporters in the salt tolerance of 'Diamond' and 'Cavalier'. Some of the transporter-related factors that could possibly contribute the difference in salt-tolerance of the two cultivars, and need to be tested, include protein localization, transporter activity, and transport properties (ion specificity).

CHAPTER V

SUMMARY

In this study, the structure-function relationship of salt glands in *Z. matrella* was examined using two cultivars that differed in their degree of salt tolerance. Differences in salt gland-related factors were found that could play a key role in the salt tolerance of this species. A comparison of the two cultivars, 'Diamond' and 'Cavalier', revealed that 'Diamond', which was more salt-tolerant of the two cultivars, not only had a higher adaxial salt gland density than 'Cavalier' but also showed an increase in salt gland density following salt treatment. Interestingly, the adaxial salt glands in salt-treated 'Diamond' were bigger than the ones found in salt-treated 'Cavalier'; and, salt gland size was increased by salt only in 'Diamond'. In order to determine if these cultivars also exhibited any morphological differences, the ultrastructure of salt glands from both cultivars was examined. Although the basic structure of *Z. matrella* salt glands was similar to that seen in other Chloridoid grasses, a few unique ultrastructural modifications were observed in this species. One of these modifications was observed in the organization of plasma membrane invaginations in the basal cell of the salt gland, suggesting that the salt secretion mechanism in *Z. matrella* may be different from the other Chloridoid grasses studied so far. When the salt glands of 'Diamond' were compared with 'Cavalier', it was observed that there was an apoplastic barrier present between the salt gland of 'Cavalier' and the underlying mesophyll cells, perhaps preventing the backflow of salt that has arrived in the salt gland. In addition to this, in

'Cavalier', a symplastic connection was present between the salt gland and the neighboring epidermal cells suggesting a role for the epidermal cells as a reservoir for salt storage before it is transported to the salt glands. Neither of the above-mentioned features was observed in 'Diamond'.

In addition to the ultrastructural and morphological modifications observed in 'Diamond' and 'Cavalier', interesting differences were also seen when the expression of select ion transporters were examined. Three ion transporters involved in Na^+ transport were cloned from *Z. matrella* (*ZmatHKT1*, *ZmatSOS1*, and *ZmatNHX1*), and spatially localized in *Z. matrella* leaves using RNA *in situ* hybridization. Although no specific differences were observed in the expression pattern of *ZmatHKT1* between 'Diamond' and 'Cavalier', the cell-type specific localization of *ZmatHKT1* was different from the expression pattern observed in rice and wheat, both of which are weakly salt-tolerant crop species that lack salt glands. The localization of *ZmatHKT1* mRNA in both cultivars of *Z. matrella* was consistent with the path of salt transport (from the vascular tissue to the adaxial salt glands) that was proposed based on the observations made from the Cl^- localization studies in Chapter II. The deduced amino acid sequence of ZmatHKT1 suggested that this transporter may be involved in Na^+-K^+ co-transport, similar to the HKT transporters from other monocots including rice, barley, wheat, and *Phragmites*. Future studies with ZmatHKT1 could confirm the activity of this protein and also elucidate its transport properties.

The localization of *ZmatSOS1* in *Z. matrella* showed different patterns of expression for 'Diamond' and 'Cavalier'. Although the transcripts were detected around

the vascular tissue for both cultivars, *ZmatSOS1* transcripts were localized in different cell types between 'Diamond' and 'Cavalier' suggesting different roles for this transporter in the two cultivars. The most interesting finding with *ZmatSOS1* mRNA expression was its localization in the leaf mestome sheath cells for 'Cavalier', possibly presenting an apoplastic barrier for Na^+ transport from the vascular tissue to the salt glands, potentially resulting in Na^+ retention within the leaf apoplast. This suggests that less Na^+ secreted by 'Cavalier' leaves could be either a consequence of high expression of *ZmatSOS1* in the mestome sheath cells resulting in high leaf Na^+ content; or a cause of less Na^+ being delivered to the salt glands due to accumulation of Na^+ in the apoplast of mestome sheath cells. In conjunction with the findings from Chapter III where the salt gland density of 'Cavalier' was found to be less than 'Diamond' and unresponsive to salt treatment, it may seem like the latter might be the case in 'Cavalier'.

Comparison of *ZmatNHX1* mRNA localization in 'Diamond' and 'Cavalier' leaves did not reveal any striking differences between the two cultivars, however three different alleles of *ZmatNHX1* and three alternatively spliced forms of *ZmatNHX1* were identified that showed a cultivar-specific expression pattern. This data, coupled with other recent findings regarding the existence of multiple alleles and splice variants, suggest that differential expression and alternative splicing of Na^+ transporters may play a role in determining salt tolerance. Using the 'Diamond' x 'Cavalier' lines from our study that fall at the two extremes in terms of salt gland density, a study could be initiated to determine if there is a correlation between salt gland density and the degree of salt tolerance in these lines. If the results of this proposed study show a strong

correlation between the above-mentioned parameters, then transporter activity could be compared between the same lines to look for correlation between salt gland density and transporter activity.

Although *HKT*, *SOS1* and *NHX* transporters have been studied and characterized in several different plant species, our study presents a first report on localization of ion transporters in a plant species bearing salt glands. Since interesting differences in spatial expression of these transporters was seen in Diamond and Cavalier, future studies could be initiated to examine the transcriptomes of adaxial and abaxial salt glands to look for differential expression of transporter-related genes in the two cell types. The results from this study may yield some information regarding the selective secretion of salt by adaxial salt glands in *Z. matrella*.

The finding that salt gland density was induced in 'Diamond', as well as some of the 'Diamond' x 'Cavalier' lines, in response to salt treatment is unique because such an observation has not been made for several other Zoysiagrasses that have been studied in the past. Future studies could involve determining the correlation between increased salt gland density and Na^+ secretion rate. Identification of lines from the 'Diamond' x 'Cavalier' population that show an induction in salt gland density, and also show an increase in Na^+ secretion in response to salt, could be used as turf in areas like golf courses and lawns, where a lot of fresh water is being used for turf maintenance. The use of recycled water (especially high in Na^+) could be used for maintenance of this turf, thus serving as a means to conserving potable water. At the same time, these lines could also serve as potential lines for bioremediation of salt-affected soils. The results obtained

from this study could also be used for future studies aiming towards crop improvement. Diamond x Cavalier lines that showed an induction in salt gland density in response to salt could serve as potential lines for isolation of candidate genes involved in the induction of salt glands. These genes could be transformed into other commercial varieties of *Zoysia* that are tolerant to other abiotic stresses, making them also suitable for growth and maintenance under conditions involving low quality water.

REFERENCES

Aist, J.R. (1976). Papillae and related wound plugs of plant cells. Annu. Rev. Phytopathol. **14**: 145-163.

Amarasinghe, V. and Watson, L. (1988). Comparative ultrastructure of microhairs in grasses. Bot. J. Linn. Soc. **98**(4): 303-319.

Amarasinghe, V. and Watson, L. (1989). Variation in salt secretory activity of microhairs in grasses. Aust. J. Plant Physiol. **16**(2): 219-229.

Apse, M. P. and Blumwald, E. (2007). Na^+ transport in plants. FEBS Lett. **581**(12): 2247-2254.

Apse, M. P., Scottosanto, J. B., and Blumwald, E. (2003). Vacuolar cation/H^+ exchange, ion homeostasis, and leaf development are altered in a T-DNA insertional mutant of AtNHX1, the *A. thaliana* vacuolar Na^+/H^+ antiporter. Plant J. **36**(2): 229-239.

Barhoumi, Z., Djebali, W., Abdelly, C., Chaibi, W., and Smaoui, A. (2008). Ultrastructure of *Aeluropus littoralis* leaf salt glands under NaCl stress. Protoplasma **233**(3-4): 195-202.

Barhoumi, Z., Djebali, W., Smaoui, A., Chaibi, W., and Abdelly, C. (2007). Contribution of NaCl excretion to salt resistance of *Aeluropus littoralis* (Willd) Parl. J. Plant Physiol. **164**(7): 842-850.

Baxter, I., Brazelton, J. N., Yuu, D., Huang, Y.S., Lahner, B., Yakubova, E., Li, Y., Bergelson, J., Borevitz, J.O., Nordborg, M., Vitek, O., and Salt, D.E. (2010). A coastal cline in sodium accumulation in *A. thaliana thaliana* is driven by natural variation of the sodium transporter AtHKT1;1. PLoS Genet. **6**(11): 1-8.

Bennett, J. and Khush, G. (2003). Enhancing Salt Tolerance in Crops through Molecular Breeding : A New Strategy. (New York: Hayworth Press).

Bouchenak-Khelladi, Y., Salamin, N., Savolainen, V., Forest, F., Bank, M., Chase, M.W., and Hodkinson, T.R. (2008). Large multi-gene phylogenetic trees of the grasses (Poaceae): Progress towards complete tribal and generic level sampling. Mol. Phylogenet. Evol. **47**(2): 488-505.

Breckle, S.-W. (2002). Salinity, halophytes and salt affected natural ecosystems. In Salinity: Environment-Plants-Molecules. Lauchli, A. and Luttge, U.ed (The Netherlands: Kluwer Academic Publishers) pp. 53-77.

Brini, F., Gaxiola, R. A., Berkowitz, G.A., and Masmoudi, K. (2005). Cloning and characterization of a wheat vacuolar cation/proton antiporter and pyrophosphatase proton pump. Plant Physiol. Biochem. **43**(4): 347-354.

Campbell, N. and Thomson, W. W. (1975). Chloride localization in the leaf of Tamarix. Protoplasma **83**: 1-14.

Clayton, W. A. and Renvoize, S. A. (1986). *Genera Graminum* - Grasses of the World. (London: Lubrecht and Cramer Ltd).

Du, Y., Hei, Q., Liu, Y., Zhang, H., Xu, K., and Xia, T. (2010). Isolation and characterization of a putative vacuolar Na^+/H^+ antiporter gene from *Zoysia japonica* L. J. Plant Biol. **53**(4): 251-258.

Eastman, P. A. K., Dengler, N. G., and Peterson, C. A. (1988). Suberized bundle sheaths in grasses (*Poaceae*) of different photosynthetic types I: Anatomy, ultrastructure and histochemistry. Protoplasma **142**(2-3): 92-111.

Engelke, M. C., Colbaugh, P. F., Reinert, J. A., Marcum, K. B., White, R. H., Ruemmele, B., and Anderson, S.J. (2002a). Registration of 'Diamond' zoysiagrass. Crop Sci. **42**(1): 304-305.

Engelke, M. C., Reinert, J. A., Colbaugh, P. F., White, R. H., Ruemmele, B. A., Marcum, K. B., and Anderson, S. J. (2002b). Registration of 'Cavalier' zoysiagrass. Crop Sci. **42**(1): 302-303.

Fitzgerald, M. A., Orlovich, D. A., and Allaway, W. G. (1992). Evidence that abaxial leaf glands are the sites of salt secretion in leaves of the mangrove *Avicennia marina* (Forsk.) Vierh. New Phytol. **120**: 1-7.

Flowers, T. (1985). Physiology of halophytes. Plant and Soil. **89**(1): 41-56.

Fukuda, A., Nakamura, A., Hara, N., Toki, S., and Tanaka, Y. (2011). Molecular and functional analyses of rice NHX-type Na^+/H^+ antiporter genes. Planta. **233**(1): 175-188.

Fukuda, A., Nakamura, A., and Tanaka, Y. (1999). Molecular cloning and expression of the Na^+/H^+ exchanger gene in *Oryza sativa*. Biochim. Biophys. Acta. **1446**(1-2): 149-155.

Garciadeblás, B., Senn, M. E., Bañuelos, M.A., and Rodríguez-Navarro, A. (2003). Sodium transport and HKT transporters: The rice model. Plant J. **34**(6): 788-801.

Gassmann, W., Rubio, F., and Schroeder, J.I. (1996). Alkali cation selectivity of the wheat root high-affinity potassium transporter HKT1. Plant J. **10**(5): 869-882.

Gaxiola, R. A., Rao, R., Sherman, A., Grisafi, P., Alper, S. L., and FRink, G. R. (1999). The *A. thaliana thaliana* proton transporters, AtNhx1 and Avp1, can function in cation detoxification in yeast. Proc. Natl. Acad. Sci. USA **96**(4): 1480-1485.

Golldack, D., Su, H., Quigley, F., Kamasani, U. R., Muñoz-Garay, C., Balderas, E., Popova, O.V., Bennett, J., Bohnert, H.J., Pantoja, O. (2002). Characterization of a HKT-type transporter in rice as a general alkali cation transporter. Plant J. **31**(4): 529-542.

Greenway, H. and Munns, R. (1980). Mechanisms of salt tolerance in nonhalophytes. Ann. Rev. Plant Physiol. **31**: 149-190.

Griffiths, A. J. F., Miller, J. H., Suzuki, D.T., Lewontin, R. C., and Gelbart, W. M. (2008). Introduction To Genetic Analysis. 9th Ed. (New York: W. H. Freeman and Company).

Gunning, B. E. S. (1977). Transfer cells and their roles in transport of solutes in plant. Sci. Progr. London. **64**: 539-568.

Haberlandt, G. (1914). Physiological Plant Anatomy. (London U.K.: Macmillan and Co., Ltd).

Hasegawa, P.M., Bressan, R. A., Zhu, J.-K., and Bohnert, H. J. (2000). Plant cellular and molecular responses to high salinity. Ann. Rev. Plant Biol. **51**: 463-499.

Hauser, F. and Horie, T. (2010). A conserved primary salt tolerance mechanism mediated by HKT transporters: A mechanism for sodium exclusion and maintenance of high K^+/Na^+ ratio in leaves during salinity stress. Plant Cell Environ. **33**(4): 552-565.

Hill, A. E. (1967a). Ion and water transport in *Limonium*: I. Active transport by the leaf gland cells. Biochim Biophys Acta. **135**(3): 454-460.

Hill, A. E. (1967b). Ion and water transport in *Limonium*: II. Short-circuit analysis. Biochim Biophys Acta. **135**(3): 461-465.

Hill, A. E. (1970a). Ion and water transport in *Limonium*: III. Time constants of the transport system. Biochim Biophys Acta. **196**(1): 66-72.

Hill, A. E. (1970b). Ion and water transport in *Limonium*: IV. Delay effects in the transport process. Biochim Biophys Acta. **196**(1): 73-79.

Hodges, T. K., Leonard, R. T., Bracker, C. E., and Keenan, T. W. (1972). Purification of an ion-stimulated adenosine triphosphatase from plant roots : Association with plasma membranes. Proc. Natl. Acad. Sci. USA **69**(11): 3307-3311.

Horie, T., Costa, A., Kim, T. H., Han, M. J., Horie, R., Leung, H-Y., Miyao, A., Hirochika, H., An, G., and Schroeder, J. I. (2007). Rice OsHKT2;1 transporter mediates large Na^+ influx component into K^+-starved roots for growth. EMBO J **26**(12): 3003-3014.

Horie, T., Yoshida, K., Nakayama, H., Yamada, K., Oiki, S., and Shinmyo, A. (2001). Two types of HKT transporters with different properties of Na^+ and K^+ transport in *Oryza sativa*. Plant J. **27**(2): 129-138.

Jabnoune, M., Espeout, S., Mieulet, D., Fizames, C., Verdeil, J-C., Conéjéro, G., Rodríguez-Navarro, A., Sentenac, H., Guiderdoni, E., Abdelly, C. and Véry, A-A. (2009). Diversity in expression patterns and functional properties in the rice HKT transporter family. Plant Physiol. **150**(4): 1955-1971.

Jha, D., Shirley, N., Tester, M., and Ro, S. J. (2010). Variation in salinity tolerance and shoot sodium accumulation in *A. thaliana* ecotypes linked to differences in the natural expression levels of transporters involved in sodium transport. Plant Cell Environ. **33**(5): 793-804.

Kader, M. A. and Lindberg, S. (2005). Uptake of sodium in protoplasts of salt-sensitive and salt-tolerant cultivars of rice, *Oryza sativa* L. determined by the fluorescent dye SBFI. J. Exp. Bot. **56**(422): 3149-3158.

Kader, M. A., Seidel, T., Golldack, D., and Lindberg, S. (2006). Expressions of OsHKT1, OsHKT2, and OsVHA are differentially regulated under NaCl stress in salt-sensitive and salt-tolerant rice (*Oryza sativa* L.) cultivars. J. Exp. Bot. **57**(15): 4257-4268.

Khan, M. and Ungar, I. (1995). Biology of Salt Tolerant Plants. (Michigan: Book Crafters).

Koehler, D. E., Leonard, R. T., Van Der Woude, W. J., Linkins, A. E., and Lewis, L. N. (1976). Association of latent cellulase activity with plasma membranes from kidney bean abscission zones. Plant Physiol. **58**(3): 324-330.

Krizek, B. A. (1999). Ectopic expression of AINTEGUMENTA in *A. thaliana* plants results in increased growth of floral organs. Dev. Genet. **25**(3): 224-236.

Kumar, S., Asif, M. H., Chakrabarty, D., Tripathi, R. D., and Trivedi, P. K. (2011). Differential expression and alternative splicing of rice sulphate transporter family members regulate sulphur status during plant growth, development and stress conditions. Funct. Integr. Genomics (In Press).

Kyte, J. and Doolittle, R. F. (1982). A simple method for displaying the hydropathic character of a protein. J. Mol. Biol. **157**(1): 105-132.

Larkum, A. W. D. and Hill, A. E. (1970). Ion and water transport in Limonium. V. The ionic status of chloroplasts in the leaf of *Limonium vulgare* in relation to the activity of the salt glands. Biochim. Biophys. Acta **203**(1): 133-138.

Läuchli, A. (1986). Responses and adaptations of crops to salinity. Acta Hort. **190**: 243-246.

Leegood, R. C. (2008). Roles of the bundle sheath cells in leaves of C3 plants. J. Exp. Bot. **59**(7): 1663-1673.

Leonard, R. and Van Der Woude, W. (1976). Isolation of plasma membranes from corn roots by sucrose density gradient centrifugation. Plant Physiol. **57**(1): 105-114.

Lessani, H. and Marschner, H. (1978). Relation between salt tolerance and long-distance transport of sodium and chloride in various crop species. Aust. J. Plant Physiol. **5**: 27-37.

Levering, C. A. and Thomson, W. W. (1971). The ultrastructure of the salt gland of *Spartina foliosa*. Planta. **97**(3): 183-196.

Li, J.-Y., He, X.-W., Xu, L., Zhou, J., Wu, P., Shou, H.-X., and Zhang, F.-C. (2008). Molecular and functional comparisons of the vacuolar Na^+/H^+ exchangers originated from glycophytic and halophytic species. J Zhejiang Univ Sci B **9**(2): 132-140.

Liphschitz, N. and Waisel, Y. (1974). Existence of salt glands in various genera of the Gramineae. New Phytol. **73**(3): 507-513.

Luttge, U. (1971). Structure and function of plant glands. Annu. Rev. Plant Physiol. **22**(1): 23-44.

Ma, L., Zhou, E., Huo, N., Zhou, R., Wang, G., and Jia, J. (2007). Genetic analysis of salt tolerance in a recombinant inbred population of wheat (*Triticum aestivum* L.). Euphytica **153**(1-2): 109-117.

Mahajan, S., Pandey, G. K., and Tuteja, N. (2008). Calcium- and salt-stress signaling in plants: shedding light on SOS pathway. Arch. Biochem. Biophy. **471**(2): 146-158.

Marcum, K. B. (1999). Salinity tolerance mechanisms of grasses in the subfamily Chloridoideae. Crop Sci. **39**(4): 1153-1160.

Marcum, K. B., Anderson, S. J. and Engelke, M. C. (1998). Salt gland ion secretion: A salinity tolerance mechanism among five Zoysiagrass species. Crop Sci. **38**: 806-810.

Marcum, K. B. and Kopec, D. M. (1997). Salinity tolerance of turfgrasses and alternative species in the subfamily Chloridoideae (Poaceae). Inter. Turf. Soc. **8**: 735-742.

Marcum, K. B. and Murdoch, C. L. (1990a). Growth responses, ion relations, and osmotic adaptations of eleven C4 turfgrasses to salinity. Agron. J. **82**(5): 892-896.

Marcum, K. B. and Murdoch, C.L. (1990b). Salt glands in the Zoysieae. Ann. Bot. **66**: 1-7.

Marcum, K. B. and Murdoch, C. L. (1994). Salinity tolerance mechanisms of six C4 turfgrasses. J. Amer. Soc. Hort. Sci. **119**(4): 779-784.

Marcum, K. B. and Pessarakli, M. (2006). Salinity tolerance and salt gland excretion efficiency of bermudagrass turf cultivars. Crop Sci. **46**: 2571-2574.

Marcum, K. B., Wess, G., Ray, D. T., and Engelke, M. C. (2003). Zoysiagrasses, salt glands, and salt tolerance. USGA Turfgrass and Environmental Research Online **2**(14): 1-6 (http://turf.lib.msu.edu/2000s/2003/031120).

Mäser, P., Hosoo, Y., Goshima, S., Horie, T., Eckelman, B., Yamada, K., Yoshida, K., Bakker, E. P., Shinmyo, A., Oiki, S., Schroeder, J. I., and Uozumi, N. (2002). Glycine residues in potassium channel-like selectivity filters determine potassium selectivity in four-loop-per-subunit HKT transporters from plants. Proc. Nat. Acad. Sci. USA **99**(9): 6428-6433.

Matoh, T., Matsushita, N. and Takahashi, E. (1988). Salt tolerance of the reed plant *Phragmites communis*. Physiol. Plant. **72**(1): 8-14.

Matsushita, N. and Matoh, T. (1991). Characterization of Na^+ exclusion mechanisms of salt-tolerant reed plants in comparison with salt-sensitive rice plants. Physiol. Plant. **83**(1): 170-176.

Mayo, M. A. and Cocking, E. C. (1969). Detection of pinocytic activity using selective staining with phosphotungstic acid. Protoplasma **68**(1): 231-236.

McWhorter, C.G., Ouzts, C., and Paul, R.N. (1993). Micromorphology of Johnsongrass (*Sorghum halepense*) leaves. Weed Sci. 41: 583-589.

Munns, R. and Teermat, A. (1986). Whole-plant responses to salinity. Aust. J. Plant Physiol. **13**: 143-160.

Nagahashi, G., Leonard, R. T., and Thomson, W. W. (1978). Purification of plasma membranes from roots of barley : Specificity of the phosphotungstic acid-chromic acid stain. Plant Physiol. **61**(6): 993-999.

Naidoo, Y. and Naidoo, G. (1998). Salt glands of *Sporobolus virginicus*: Morphology and ultrastructure. S. Afr. J. Bot. **69**: 939-949.

Oh, D. H., Leidi, E., Zhang, Q., Hwang, S. M., Quintero, F. J., Jiang, X., D'Urzo, M. P., Lee, S. Y., Zhao, Y., Bahk, J. D., Bressan, R. A., Yun, D. J., Pardo, J. M., and Bohnert, H. J. (2009). Loss of halophytism by interference with SOS1 expression. Plant Physiol. **151**(1): 210-222.

Oross, J. W. and Thomson, W. W. (1982a). The ultrastructure of *Cynodon* salt glands: The apoplast. Eur. J. Cell Biol. **28**(2): 257-263.

Oross, J. W. and Thomson, W. W. (1982b). The ultrastructure of the salt glands of *Cynodon* and *Distichlis* (Poaceae). Am. J. Bot. **69**(6): 939-949.

Oross, J. and Thomson, W. W. (1984). The ultrastructure of *Cynodon* salt glands: secreting and nonsecreting. Eur. J. Cell Biol. **34**: 287-291.

Platt-Aloia, K. A., Bliss, R. D., and Thomson, W. W. (1983). Lipid-lipid interactions and membrane fusion in plant salt glands [*Tamarix aphylla*, structure]. In: Biosynthesis and function of plant lipids : Proceeedings of the Sixth Annual Symposium in Botany, January 13-15, 1983, University of California, Riverside edited by Thomson, W. W., Mudd, J. B., Gibbs, M., Rockville, MD: Amer Soc Plant Physio (1983): 160-15.

Platten, J. D., Cotsaftis, O., Berthomieu, P., Bohnert, H., Davenport, R. J., Fairbairn, D. J., Horie, T., Leigh, R. A., Lin, H. X., Luan, S., Maser, P., Pantoja, O., Rodríguez-Navarro, A., Schachtman, D. P., Schroeder, J. I., Sentenac, H., Uozumi, N., Véry, A.A., Zhu, J.K., Dennis, E.S., and Tester, M. (2006). Nomenclature for HKT transporters, key determinants of plant salinity tolerance. Trends Plant Sci. **11**(8): 372-374.

Pollack, G. and Waisel, Y. (1970). Salt secretion in *Aeluropus litoralis* (Willd.) Parl. Ann. Bot. **34**: 879-888.

Qiao, W., Zhao, X. Y., Li, W., Luo, Y., and Zhang, X. S. (2007). Overexpression of AeNHX1, a root-specific vacuolar Na^+/H^+ antiporter from *Agropyron elongatum*, confers salt tolerance to *A. thaliana* and Festuca plants. Plant Cell Rep. **26**: 1663-1672.

Rao, S., Pendleton, M., Binzel, M. L., and Ellis, E. A. (2008). Modified cryo-preparation for studying salt glands in the turf grass *Zoysia matrella*. Microscopy Today **16**(2): 44.

Ren, Z.-H., Gao, J.-P., Li, L.-G., Cai, X.-L., Huang, W., Chao, D.-Y., Zhu, M.-Z., Wang, Z.-Y., Luan, S., and Lin, H.-X. (2005). A rice quantitative trait locus for salt tolerance encodes a sodium transporter. Nat. Genet. **37**(10): 1141-1146.

Reynolds, R. (1963). The use of lead citrate at high pH as an electron-opaque stain in electron microscopy. J. Cell Biol. **17**: 208-213.

Roland, J. C., Lembi, C.A. and Morre, D.J. (1972). Phosphotungstic acid-chromic acid as a selective electron-dense stain for plasma membranes of plant cells. Stain Technology **47**: 195-200.

Rozema, J. and Gude, H. (1981). An ecophysiological study of the salt secretion of four halophytes. New Phytol. **89**(2): 201-217.

Rubio, F., Gassmann, W., and Schroeder, J. I. (1995). Sodium-driven potassium uptake by the plant potassium transporter HKT1 and mutations conferring salt tolerance. Science **270**: 1660-1663.

San Antonio Water System (SAWS), May 2006. (http://www.saws.org/our_water/recycling/handbook/recycled_water_hb_rev20080620.pdf).

Schachtman, D. P. and Liu, W. (1999). Molecular pieces to the puzzle of the interaction between potassium and sodium uptake in plants. Trends Plant Sci. **4**(7): 281-286.

Schachtman, D. P. and Schroeder, J. I. (1994). Structure and transport mechanism of a high-affinity potassium uptake transporter from higher plants. Nature **370**(6491): 655-658.

Sen, D. and Kasera, P. (2002). Biology and Physiology of Saline Plants. Handbook of Plant and Crop Physiology. M. Pessarakli (New York: Marcel Dekker), pp. 563-581.

Shabala, S. and Cuin, T. A. (2008). Potassium transport and plant salt tolerance. Physiol. Plant. **133**(4): 651-669.

Shachar-Hill, B. and Hill, A. E. (1970). Ion and water transport in Limonium. Biochim. Biophys. Acta **211**: 313-317.

Shi, H., Quintero, F. J., Pardo, J. M., and Zhu, J.-K. (2002). The putative plasma membrane Na^+/H^+ antiporter SOS1 controls long-distance Na^+ transport in plants. Plant Cell **14**(2): 465-477.

Shi, H. and Zhu, J.-K. (2002). Regulation of expression of the vacuolar Na^+/H^+ antiporter gene *AtNHX1* by salt stress and abscissic acid. Plant Mol. Biol. **50**: 543-550.

Skelding, A. and Winterbotham, J. (1939). The structure and development of hydathodes of *Spartina townsendii* Groves. New Phytol. **38**: 69-79.

Snustad, D. and Simmons, M. (2008). Principles of Genetics. (New Jersey: John Wiley & Sons, Inc.).

Solley, W., Pierce, R., and Perlman, H. (1998). Estimated use of water in the United States in 1995. (Reston, VA: United States Geological Survey), pp. 1-71.

Somaru, R., Naidoo, Y., and Naidoo, G. (2002). Morphology and ultrastructure of the leaf salt glands of *Odyssea paucinervis* (Stapf) (Poaceae). Flora **197**(1): 67-75.

Spurr, A. (1969). A low-viscosity epoxy resin embedding medium for electron microscopy. J. Ultrastruct. Res. **26**: 31-43.

Stewart, C. N., Jr. and Via, L. E. (1993). A rapid CTAB DNA isolation technique useful for RAPD fingerprinting and other PCR applications. Biotechniques **14**: 748-751.

Su, H., Balderas, E., Vera-Estrella, R., Golldack, D., Quigley, F., Zhao, C., Pantoja, O., and Bohnert, H. J. (2003). Expression of the cation transporter McHKT1 in a halophyte. Plant Mol. Biol. **52**(5): 967-980.

Sunarpi, Horie, T., Motoda, J., Kubo, M., Yang, H., Yoda, K., Horie, R., Chan, W. Y., Leung, H. Y., Hattori, K., Konomi, M., Osumi, M., Yamagami, M., Schroeder, J. I., and Uozumi, N. (2005). Enhanced salt tolerance mediated by AtHKT1 transporter-induced Na^+ unloading from xylem vessels to xylem parenchyma cells. Plant J. **44**(6): 928-938.

Sundberg, I. and Lembi, C. A. (1976). Phosphotungstic acid-chromic acid : A selective stain for algal plasma membranes. J. Phycology **12**(1): 48-54.

Sutherland, G. K. and Eastwood, A. (1916). The physiological anatomy of *Spartina townsendii*. Ann. Bot. **30**(2): 333-350.

Taiz, L. and Zeiger, E. (2010). Stress Physiology. (Sunderland, MA: Sinauer Associates, Inc.).

Taji, T., Komatsu, K., Katori, T., Kawasaki, Y., Sakata, Y., Tanaka, S., Kobayashi, M., Toyoda, A., Seki, M., and Shinozaki, K. (2010). Comparative genomic analysis of 1047 completely sequenced cDNAs from an Arabidopsis-related model halophyte, *Thellungiella halophila*. BMC Plant Biol. 10: 261.

Takahashi, R., Liu, S., and Takano, T. (2007). Cloning and functional comparison of a high-affinity K^+ transporter gene *PhaHKT1* of salt-tolerant and salt-sensitive reed plants. J. Exp. Bot. **58**(15-16): 4387-4395.

Takahashi, R., Liu, S., and Takano, T. (2009). Isolation and characterization of plasma membrane Na^+/H^+ antiporter genes from salt-sensitive and salt-tolerant reed plants. J. Plant Physiol. **166**(3): 301-309.

Tester, M. and Davenport, R. (2003). Na^+ tolerance and Na^+ transport in higher plants. Ann. Bot. **91**(5): 503-527.

Thomson, W. W. (1975). The structure and function of salt glands. In Plant in Saline Environments, A. Poljakoff-Mayber, ed. (Berlin: Springer-Verlag), pp. 118-146.

Tuteja, N. (2007). Mechanisms of high salinity tolerance in plants. Methods Enzymol. **428**: 419-438.

Uozumi, N., Kim, E. J., Rubio, F., Yamaguchi, T. Muto, S., Tsuboi, A., Bakker, E. P., Nakamura, T., and Schroeder, J. I. (2000). The *A. thaliana HKT1* Gene Homolog Mediates Inward Na^+ Currents in *Xenopus laevis* Oocytes and Na^+ Uptake in *Saccharomyces cerevisiae*. Plant Physiol. **122**(4): 1249-1260.

Van Der Woude, W. J., Lembi, C. A., and Morré, D. J. (1974). β-Glucan synthetases of plasma membrane and golgi apparatus from onion stem. Plant Physiol. **54**(3): 333-340.

Vasquez, E. A., Glenn, E. P., Guntenspergen, G. R., Brown, J. J., and Nelson, S. G. (2006). Salt tolerance and osmotic adjustment of *Spartina alterniflora* (Poaceae) and the invasive M haplotype of *Phragmites australis* (Poaceae) along a salinity gradient. Am. J. Bot. **93**(12): 1784-1790.

Venema, K., Quintero, F. J., Pardo, J. M., and Donaire, J. P. (2002). The *A. thaliana* Na^+/H^+ exchanger AtNHX1 catalyzes low affinity Na^+ and K^+ transport in reconstituted liposomes. J. Biol. Chem. **277**(4): 2413-2418.

Vickers, A. (2001). Handbook of Water Use and Conservation. (Amherst, MA: Water Plow Press).

Waisel, Y. (1961). Ecological studies on *Tamarix aphylla* (L.) Karst. III. The salt economy. Plant Soil **13**: 356-364.

Waisel, Y. (1972). Biology of Halophytes. (New York and London: Acadmic Press).

Water for Texas (2011), Population and Water Demand Projections, Texas Water Development Board (http://www.twdb.state.tx.us/wrpi/data/pop.asp).

Wu, S. J., Ding, L., and Zhu, J.K. (1996). SOS1, a genetic locus essential for salt tolerance and potassium acquisition. Plant Cell **8**(4): 617-627.

Yokoi, S., Quintero, F. J., Cubero, B., Ruiz, M. T., Bressan, R. A., Hasegawa, P.M., and Pardo, J. M. (2002). Differential expression and function of *A. thaliana thaliana* NHX Na^+/H^+ antiporters in the salt stress response. Plant J. **30**(5): 529-539.

Zhang, G.-H., Su, Q., and Wu, S. (2008). Characterization and expression of a vacuolar Na^+/H^+ antiporter gene from the monocot halophyte *Aeluropus littoralis*. Plant Physiol. Biochem. **46**: 117-126.

Zhang, H.-X. and Blumwald, E. (2001). Transgenic salt-tolerant tomato plants accumulate salt in foliage but not in fruit. Nature Biotech. **19**(8): 765.

Zhu, J.-K. (2003). Regulation of ion homeostasis under salt stress. Curr. Opin. Plant Biol. **6**(5): 441-445.

Zörb, C., Noll, A., Karl, S., Leib, K., Yan, F., and Schubert, S. (2005). Molecular characterization of Na^+/H^+ antiporters (*ZmNHX*) of maize (*Zea mays* L.) and their expression under salt stress. Plant Physiol. **162**: 55-66.

VITA

Name:	Sheetal Sadanand Rao
Address:	c/o Marla L. Binzel
	Texas AgriLife Research and Extension Center
	17360 Coit Road, Dallas, TX 75252
Email address:	s_rao1112@hotmail.com
Education:	B. S., Botany and Biotechnology, University of Mumbai, 2000
	M. S., Plant Biotechnology, University of Mumbai, 2002
	Ph.D., Molecular & Environmental Plant Sciences,
	Texas A&M University, 2011